NASA/TM-2007-214892

Revisiting and Extending Interface Penalties for Multi-Domain Summation-by-Parts Operators

Mark H. Carpenter
Langley Research Center, Hampton, Virginia

Jan Nordström
The Royal Institute of Technology, Stockholm, Sweden

David Gottlieb
Brown University, Providence, Rhode Island

August 2007

The NASA STI Program Office . . . in Profile

Since its founding, NASA has been dedicated to the advancement of aeronautics and space science. The NASA Scientific and Technical Information (STI) Program Office plays a key part in helping NASA maintain this important role.

The NASA STI Program Office is operated by Langley Research Center, the lead center for NASA's scientific and technical information. The NASA STI Program Office provides access to the NASA STI Database, the largest collection of aeronautical and space science STI in the world. The Program Office is also NASA's institutional mechanism for disseminating the results of its research and development activities. These results are published by NASA in the NASA STI Report Series, which includes the following report types:

- TECHNICAL PUBLICATION. Reports of completed research or a major significant phase of research that present the results of NASA programs and include extensive data or theoretical analysis. Includes compilations of significant scientific and technical data and information deemed to be of continuing reference value. NASA counterpart of peer-reviewed formal professional papers, but having less stringent limitations on manuscript length and extent of graphic presentations.

- TECHNICAL MEMORANDUM. Scientific and technical findings that are preliminary or of specialized interest, e.g., quick release reports, working papers, and bibliographies that contain minimal annotation. Does not contain extensive analysis.

- CONTRACTOR REPORT. Scientific and technical findings by NASA-sponsored contractors and grantees.

- CONFERENCE PUBLICATION. Collected papers from scientific and technical conferences, symposia, seminars, or other meetings sponsored or co-sponsored by NASA.

- SPECIAL PUBLICATION. Scientific, technical, or historical information from NASA programs, projects, and missions, often concerned with subjects having substantial public interest.

- TECHNICAL TRANSLATION. English-language translations of foreign scientific and technical material pertinent to NASA's mission.

Specialized services that complement the STI Program Office's diverse offerings include creating custom thesauri, building customized databases, organizing and publishing research results ... even providing videos.

For more information about the NASA STI Program Office, see the following:

- Access the NASA STI Program Home Page at ***http://www.sti.nasa.gov***

- E-mail your question via the Internet to help@sti.nasa.gov

- Fax your question to the NASA STI Help Desk at (301) 621-0134

- Phone the NASA STI Help Desk at (301) 621-0390

- Write to:
  NASA STI Help Desk
  NASA Center for AeroSpace Information
  7115 Standard Drive
  Hanover, MD 21076-1320

NASA/TM-2007-214892

Revisiting and Extending Interface Penalties for Multi-Domain Summation-by-Parts Operators

Mark H. Carpenter
Langley Research Center, Hampton, Virginia

Jan Nordström
The Royal Institute of Technology, Stockholm, Sweden

David Gottlieb
Brown University, Providence, Rhode Island

National Aeronautics and
Space Administration

Langley Research Center
Hampton, Virginia 23681-2199

August 2007

Available from:

NASA Center for AeroSpace Information (CASI)
7115 Standard Drive
Hanover, MD 21076-1320
(301) 621-0390

National Technical Information Service (NTIS)
5285 Port Royal Road
Springfield, VA 22161-2171
(703) 605-6000

REVISITING AND EXTENDING INTERFACE PENALTIES FOR MULTI-DOMAIN SUMMATION-BY-PARTS OPERATORS

Mark H. Carpenter, * Jan Nordström † David Gottlieb‡

Abstract

General interface coupling conditions are presented for multi-domain collocation methods, which satisfy the summation-by-parts (SBP) spatial discretization convention. The combined interior/interface operators are proven to be L_2 stable, pointwise stable, and conservative, while maintaining the underlying accuracy of the interior SBP operator. The new interface conditions resemble (and were motivated by) those used in the discontinuous Galerkin finite element community, and maintain many of the same properties. Extensive validation studies are presented using two classes of high-order SBP operators: 1) central finite difference, and 2) Legendre spectral collocation.

*Computational Aerosciences Branch, NASA Langley Research Center, Hampton, VA 23681-2199. Work performed in part while in residence at TU Delft, Delft, The Netherlands, technical monitor Prof. Dr. Ir. H. Bijl. E-mail: *m.h.carpenter@larc.nasa.gov.*

†Computational Aerodynamics Department, FOI SE-16490, Stockholm, Sweden; and the Department of Information Technology, Box 337, 751 05 Uppsala, Sweden; The Department of Aeronautical and Vehicle Engineering, KTH - The Royal Institute of Technology, SE-100 44, Stockholm, Sweden; E-mail: *nmj@foi.se.*

‡Division of Applied Mathematics, Brown University, Providence, RI 02912. Work supported by AFOSR grant F49620-96-1-0150 and by NSF grant DMS-9500814. E-mail: *dig@cfm.brown.edu.*

1 Introduction

High order finite difference methods (HOFDM) are ideally suited for simulations of complex physics requiring high fidelity solutions, and for a simple reason: efficiency. Low-order techniques (whether they be finite difference, finite volume, or finite element) lack sufficient accuracy for a given cost to make them competitive in this environment. HOFDM have for decades been used for direct numerical and large eddy simulations (DNS/LES) of fundamental problems in fluid mechanics. In recent years, they have begun to impact a wide variety of other aerodynamic applications, including 1) subsonic noise reduction, 2) air space utilization/safety, 3) uninhabited combat air vehicles (UCAV), 4) circulation control, 5) fluid/structure interactions, 6) turbomachinary, 7) aircraft in flight, 8) helicopters, 9) atmospheric chemistry, 10) windmill optimization. Other disciplines that HOFDM are making inroads into include 11) computational electromagnetics, 12) ocean models, 13) meteorology, 14) magnetohydrodynamics, 15) weather forecasting, 16) oil recovery simulation, 17) modeling of shallow waters, 18) transport of contaminant in porous media, 19) viscoelastic flows, 20) semiconductor device simulation, to name a few.

The basis of the argument used to advocate the use of HOFDM is not new, and in fact dates back to early 1970's work by Kriess and Oliger [25]. They showed that the efficiency of HOFDM increased with each consecutive order up to approximately 5th-order for time-dependent hyperbolic problems. In spite of their theoretical advantage, however, two significant impediments continue to face HOFDM. They are: 1) stable boundary closure formulae maintaining the formal accuracy of the interior scheme, and 2) extension to complex geometries.

Many theoretical (and ad hoc) boundary closures for HOFDM have been proposed over the past three decades. Most, however, still rely on low-order boundary closures to achieve stability and robustness. Unfortunately, even one low-order point can have a detrimental effect on asymptotic solution accuracy. Specifically, Gustafsson [18] showed that for hyperbolic equations, boundary stencil accuracy can differ from interior stencil accuracy by one order at most, if design order is to be maintained (e.g. $(p)^{th}$-order interior with $(p-1)^{th}$-order boundaries maintains $(p)^{th}$-order asymptotic accuracy). Svärd and Nordström [38] recently showed how to relax this constraint to allow $(p-2)^{th}$-order boundary closures for strictly parabolic problems. Nevertheless, numerical schemes for hyperbolic, incompletely parabolic (Navier Stokes: NS) or parabolic equations all suffer the potential consequence of low-order closures; and thus, boundary closures must be carefully designed.

High-order biased stencils near boundaries (on uniform grids) are susceptible to Runge-type oscillations/instabilities that frequently compromise the stability of the simulation. A simple remedy to the problem of boundary closure stencils originates in the early work of Kriess and Scherer[26]. They realized that stability issues could be controlled by simply constructing semi-discrete finite difference operators that satisfy a semi-discrete energy estimate. That is, the semi-discrete operator "mimics" the discrete operator in terms of the energy of the system. The critical element that enables the existence of the continuous energy estimate is the integration-by-parts property of the differential operator. Thus, semi-discrete operators that mimic this property are said to satisfy a summation-by-parts (SBP) condition. Although Kriess and Scherer focused exclusively on low-order methods, Strand [36, 37] in his Ph.D. thesis and Olsson [32, 33] extended these ideas to HOFDM, and the field of summation-by-parts (SBP) high-order schemes was born.

In principle, SBP operators can be derived for virtually every conceivable operator type. By construction, weak form FEM operators automatically satisfy the SBP property. Additionally, operators that satisfy the SBP property exist for 2^{nd}-, 4^{th}-, 6^{th}- and 8^{th}-order central schemes [36, 10], Padé schemes [10, 1], upwind schemes [27], dispersion preserving schemes [29], and strong form nodal "spectral element" schemes [11, 15, 12, 20, 21, 22, 23]. Operators that satisfy the SBP form need not only be applied to hyperbolic systems. Indeed, parabolic equations are amenable to SBP forms, either by the action of two first order SBP operators or by constructing operators specific to the second derivative [10, 27]. Special considerations must be accounted for when dealing with these equations, but no great difficulties are encountered[28].

An implementation detail related to SBP operators emerged in the work of Carpenter et al. [10], dealing with the imposition of the physical boundary data. Specifically, they noted that if the physical data were "injected" in the conventional manner, then the energy of the semi-discrete system could become unbounded. Borrowing ideas from the interior penalty approaches used in Finite-Elements (IPFEM) [16, 4, 39] and those used in pseudospectral collocation [17], they devised a means of imposing the data, [which was designated SAT Simultaneous Approximation Term (SAT)], that guaranteed bounded energy while maintaining formal accuracy. The SAT procedure solves a linear combination of the boundary conditions and the differential equations near the boundary. A similar alternative was developed by Olsson [32, 33] based on orthogonal projection techniques, that also guaranteed stability and accuracy of the discretized system, including physical boundary data.

The extension of HOFDM to complex domains proves more difficult to accomplish. Multi-domain HOFDM are a natural candidate for extension, but are fraught with the complexity of interface coupling procedures. Specifically, they must address the interface accuracy constraints, as well as contend with coupled stability conditions and interface conservation issues. Many ad hoc procedures have been developed to accommodate multi-domain methods, including conforming, nonconforming, and overset/overlapping procedures. Once again, the key to success for these procedures seems to be reduction of the order of accuracy at the interface region and the subsequent loss of solution accuracy throughout the entire domain.

A simple solution to the multi-domain problem for HOFDM was provided in the work of Carpenter, Nordström, Gottlieb[13] (henceforth referred to as CNG). Motivated by the recent popularity/success of Discontinuous Galerkin Finite Element methods (DGFEM), and the internal penalty approaches, they proposed combining the SBP operators within each domain, with a penalty technique at the interfaces. The formulation requires only weak grid continuity at the interface (C_0: matching but not necessarily smooth), and is applicable to any operator that satisfies a SBP property. Furthermore, the operators need not be the same in adjoining domains. It maintains formal accuracy through the interface, is conservative and maintains a bounded semi-discrete energy estimate consistent with the underlying SBP operators. Although originally developed for the linear, constant coefficient, scalar, advection-diffusion operator on multiple domains, the CNG interface formulation was subsequently generalized to systems of equations with constant coefficients by Nordström et al.[30], and finally to the linearized Navier-Stokes equations.[31] Similar developments within the nodal spectral element community were reported by Hesthaven et al. [22, 23, 24].

In summary, the CNG formulation, patterned after the IPFEM/DGFEM methods, attempted to provide a "general" technique to couple multiple SBP domains. Conventional penalties were constructed at interfaces based on Dirichlet and Neumann data from either side. After accuracy, stability and conservation were enforced, two free parameters remained, one for convection and one for diffusion. Significant maturation has occurred within the DGFEM community over the past 6 years, especially in the treatment of diffusion terms. Recent work by Arnold et al. [3] provides a clean unifying description of all the approaches typically used in IPFEM and DGFEM, and has tied up many of the loose ends. These, and other recent developments for the treatment of the DG diffusive terms, make it apparent that the CNG formulation is (although correct) not a general procedure. In fact, additional penalty terms could have been included in the original formulation!

The objective of this paper, is to present a "general" treatment of multi-block interfaces, connecting adjoining domains discretized with SBP operators. The strong (nodal) form of the governing equations is the primary focus of this work, although an elementary discussion of FEM methods is presented to motivate the new interface treatments. Two equivalent formulations are presented for the new interface conditions, similar in spirit to the flux and primal forms used in the FEM literature. Both new formulations are valid for the linear, constant coefficient, scalar advection diffusion system, and are accurate, stable and conservative, just as was the previous CNG [13] formulation. Five free parameters remain unspecified at interfaces in the new formulations, and can be chosen quite arbitrarily (only mild stability constraints). Furthermore, judicious choices for the parameters yield commonly used schemes from the FEM literature.

The rest of this paper proceeds as follows. In section 2, we present the unified DGFEM approach to the interface treatment, written in the weak form. This formulation is then reformulated in terms of the strong form of the equations. In section 3, the new approach is presented for the strong form of the equations, including proofs of stability and conservation. This approach incorporates penalties on the solution and first derivative that are more general than the original CNG formulation. In section 4, a general penalty procedure is introduced that includes penalties on the second derivatives. Section 5 presents a derivation of the theoretical accuracy of the new penalties, in the context of HOFDM. Section 6 identifies several commonly used schemes in terms of the new penalty parameters. In section 7, numerical examples are presented for a variety of SBP operators. A discussion followed by conclusions are presented in sections 8 and 9, respectively. Finally, several appendices include related theoretical derivations.

2 Discontinuous Galerkin FEM

Our goal is to develop accurate, stable and conservative interface treatments applicable to multi-block HOFDM and other general collocation approaches; methods formulated in terms of *derivatives* of the *strong form* of the equations. Given the close similarity between *strong form* HOFDM and *weak form* DGFEM approaches, an elementary discussion of discontinuous finite elements for parabolic equations is presented. The derivation will in turn motivate a new penalty

treatment for the strong form of the equations.

2.1 Nomenclature and definitions

Parallel development of two distinct methodologies and nomenclatures exists in the discontinuous finite element literature, devoted to solving elliptic and parabolic equations. The biharmonic equations are the genesis for Interior Penalty (IP) methods, which date back as early as the middle 70's. The IP methods (and others based on the biharmonic equations) are often described as using the *primal formulation*, and they are primarily used for solving elliptic equations. Interest in parabolic equations with a strong hyperbolic component has recently motivated the development of *flux formulation* methods, named for their utilization/reliance on inter-element flux reconstruction techniques such as exact or approximate Reimann solvers. Arnold et al. [2, 3] present an extensive review that unifies nearly all the DG schemes that appear in the literature. They study both flux and primal formulations, establishing the precise relationship between the two approaches.

A brief derivation of the *primal formulation* and *flux formulation* is now presented. The objective is to establish the relationship between these two approaches, and a third methodology; the *strong formulation*, which will be the exclusive focus this work. We begin by discussing the flux formulation, and then, derive the primal form and strong form as a special cases of the flux formulation.

Consider the scalar, 1-D, parabolic equation,

$$\mathsf{u}_t \;=\; \mathsf{u}_{xx},\; |x| \le 1, t \ge 0. \tag{1}$$

with suitable initial data and boundary conditions. (For ease of presentation, but without loss of generality, we study the 1-D, linear, strictly parabolic equation.) An example of a flux formulation FEM is the one proposed by Cockburn and Shu [14], denoted the local discontinuous Galerkin (LDG) method. Their approach (modeled after that of Bassi and Rebay [5]) begins by transforming the second-order equation to a "system" of first-order equations

$$\mathsf{u}_t \;=\; \mathsf{q}_x, \quad \mathsf{q} \;=\; \mathsf{u}_x, \quad |x| \le 1, t \ge 0. \tag{2}$$

Multiplying equation (2) by test functions, and integrating by parts, the LDG method is then defined as: "find $u,\, q \in V_{\Delta x}$ such that for all test functions $v,\, w \in V_{\Delta x}$, the following relations hold"

$$\begin{array}{rcrcrcl} \int_{I_j} u_t\, v\, dx & = & -\int_{I_j} q\, v_x dx & + & \hat{q}_{j+\frac{1}{2}} v^-_{j+\frac{1}{2}} & - & \hat{q}_{j-\frac{1}{2}} v^+_{j-\frac{1}{2}} \\ \int_{I_j} q\; w\, dx & = & -\int_{I_j} u\, w_x dx & + & \hat{u}_{j+\frac{1}{2}} w^-_{j+\frac{1}{2}} & - & \hat{u}_{j-\frac{1}{2}} w^+_{j-\frac{1}{2}}\,. \end{array} \tag{3}$$

with $\hat{q}$ and $\hat{u}$ being suitably chosen interface fluxes. Figure 1 provides a schematic of the nomenclature for the discretization. Here, the intervals $I_j \;=\; [x_{j-\frac{1}{2}}, x_{j+\frac{1}{2}}]$ is defined for $j \;=\; 1, ..., N$, on the periodic domain $\Omega \;=\; [0, 2\pi]$. The points x_j are defined by $x_j \;=\; \frac{1}{2}(x_{j-\frac{1}{2}} + x_{j+\frac{1}{2}})$ and the element spacing by $\Delta x_j \;=\; x_{j+\frac{1}{2}} - x_{j-\frac{1}{2}}$. The test functions v, w are piecewise polynomials of at most degree k such that $v, w \;\in V_{\Delta x}$, where

$$V_{\Delta x} \;=\; \{v : v \text{ is a polynomial of degree at most } k \text{ for } x \in I_j, j \;=\; 1, ..., N\}. \tag{4}$$

Define e_j to be the edge between elements j and $j+1$, and the union of all edges to be $\sum_j e_j \;=\; \Gamma$. Further define the vectors $n1_j$ and $n2_j$ on e_j, pointing exterior to each element adjoining e_j, and the superscripts $^-$ and $^+$ to be the limiting interface value approaching from the left and right, respectively.

Next, note that both the solutions u, q and the test functions v, w are discontinuous at the element interfaces. To facilitate manipulation of equation (3), we define average and jump operators on the edges. Written in terms of an arbitrary variable ζ these operators are defined as

$$\{\zeta_j\} \;=\; \frac{1}{2}(\zeta_j^- + \zeta_j^+); \quad [[\zeta_j]] \;=\; (\zeta_j^- n1_j + \zeta_j^+ n2_j) \qquad \forall e_j \tag{5}$$

where $\zeta_j^{\mp}$ are the left and right values of the double valued function ζ_j on the interface j. Summing equation (3) over all elements defines the method on the entire domain Ω.

$$\begin{array}{rcrcrcl} \int_{\Omega} u_t\, v\, dx & = & -\int_{\Omega} q\, v_x dx & + & \sum_{\Gamma} [[\hat{q} v]] \\ \int_{\Omega} q\; w\, dx & = & -\int_{\Omega} u\, w_x dx & + & \sum_{\Gamma} [[\hat{u} w]] \end{array} \tag{6}$$

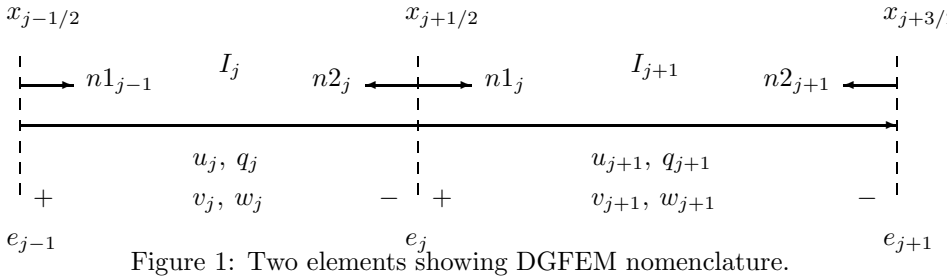

Figure 1: Two elements showing DGFEM nomenclature.

The primal formulation can be obtained from the flux formulation as follows. Allowing the test function w in equation (3.b) to satisfy $w = v_x$ (assuming $v \neq c_0$, with c_0 a constant) produces the equation

$$\int_\Omega\ q\ v_x\, dx \quad = \quad -\int_\Omega\ u\, v_{xx} dx \quad + \quad \sum_\Gamma\ [[\hat{u} v_x]] \tag{7}$$

which when substituted back into equation (3.a) yields

$$\int_\Omega\ u_t\, v\, dx \quad = \quad \int_\Omega\ u\, v_{xx} dx \quad - \quad \sum_\Gamma (\ [[\hat{u} v_x]] \quad - \quad [[\hat{q} v]]) \tag{8}$$

Integrating equation (8) by parts once more, produces the primal formulation

$$\int_\Omega\ u_t\, v\, dx \quad = \quad -\int_\Omega\ u_x\, v_x dx \quad - \quad \sum_\Gamma (\ [[(\hat{u} - u) v_x]] \quad - \quad [[\hat{q} v]])\ . \tag{9}$$

The exact form of interface fluxes $\hat{u}$ or $\hat{q}$ is immaterial, for the purpose of the previous derivation of the flux and primal formulations. In practice, however, these fluxes can not be chosen arbitrarily. Additional constraints (such as global stability and conservation), establish admissible relationships between the $\hat{u}$ or $\hat{q}$. See Appendix A for a brief discussion on admissible fluxes satisfying global stability, as well as a listing of several popular schemes.

2.2 Strong Form

The previously discussed methods, are defined based on *integrals* of the *weak form* of the governing equations. Specifically, equation (1) is multiplied by an arbitrary test function, and then formally integrated once or twice. We now derive a strong form equation suitable for developing collocation approaches.

Starting with equation (9), an auxiliary primal form can be obtained by once more integrating the term $u_x\, v_x$, resulting in the expression

$$\int_\Omega\ u_t\, v\, dx \quad = \quad \int_\Omega\ u_{xx}\, v \quad - \quad \sum_\Gamma (\ [[(\hat{u} - u) v_x]] \quad - \quad [[(\hat{q} - u_x) v]])\ . \tag{10}$$

Reverse engineering strong form methods is most easily accomplished at the element level. Reformulating equation (10) for a single element yields

$$\begin{aligned} \int_{I_j}\ u_t\, v\, dx\ = \ \int_{I_j}\ u_{xx}\, v\, dx \quad + \quad & [(\hat{u} - u)^-_{j+\frac{1}{2}} v_x{}^-_{j+\frac{1}{2}} \ - \ (\hat{u} - u)^+_{j-\frac{1}{2}} v_x{}^+_{j-\frac{1}{2}}] \\ - \quad & [(\hat{q} - u_x)^-_{j+\frac{1}{2}} v^-_{j+\frac{1}{2}} \ - \ (\hat{q} - u_x)^+_{j-\frac{1}{2}} v^+_{j-\frac{1}{2}}] \end{aligned} \tag{11}$$

which upon substitution of the primal flux form given in equation (153) (and reversing the order of multiplication), yields

$$\begin{aligned} \int_{I_j}\ v\, u_t\, dx\ = \ \int_{I_j}\ v\, u_{xx}\, dx \quad + \quad & v_x{}^-_{j+\frac{1}{2}} (c_1\, [[u]] \ + \ c_2\, [[u_x]])^-_{j+\frac{1}{2}} \\ - \quad & v_x{}^+_{j-\frac{1}{2}} (c_1\, [[u]] \ + \ c_2\, [[u_x]])^+_{j-\frac{1}{2}} \\ - \quad & v^-_{j+\frac{1}{2}} (c_3\, [[u]] \ + \ c_4\, [[u_x]])^-_{j+\frac{1}{2}} \\ + \quad & v^+_{j-\frac{1}{2}} (c_3\, [[u]] \ + \ c_4\, [[u_x]])^+_{j-\frac{1}{2}} \end{aligned} \tag{12}$$

The inverse transformation from weak to strong form involves replacing all polynomial integrals and derivatives, with discrete matrix vector operations on collocated data. The only subtle aspect of this task is representing the interface data in collocation form. To accomplish this, we define the discrete boundary operators

$$\mathbf{e}^+_j \ = \ [0, 0, ..., 0, 1]^T \ ; \ \mathbf{e}^-_j \ = \ [1, 0, ..., 0, 0]^T. \tag{13}$$

The action of these vectors isolates data at the left ($-$) and right ($+$) edges of the element.

Next, assume that discrete derivative and integration operations are defined by

$$\zeta_x \;=\; \mathcal{D}\zeta \;+\; O(h^r); \quad \int_{I_j} \eta\,\zeta\,dx \;=\; \eta^T\,\mathcal{P}\zeta \;+\; O(h^r) \tag{14}$$

where $\mathcal{D}$ and $\mathcal{P}$ are discrete nodal differentiation and integration operators, respectively.

Expressing equation (12) in terms of these definitions (13), (14) and the element identity matrix $\mathcal{I}_j$, yields

$$\begin{aligned} \mathbf{V_j}^T\{ \quad \mathcal{P}\mathbf{U}_t \;=\; \mathcal{P}\mathcal{D}\mathcal{D}\mathbf{U} \quad &+ \quad \mathcal{D}^T\mathbf{e}_j^+(c_1\,[[\mathbf{U}]] \;+\; c_2\,[[\mathcal{D}\,\mathbf{U}]])_{j+\frac{1}{2}} \\ &- \quad \mathcal{D}^T\mathbf{e}_j^-(c_1\,[[\mathbf{U}]] \;+\; c_2\,[[\mathcal{D}\,\mathbf{U}]])_{j-\frac{1}{2}} \\ &- \quad \mathcal{I}^T\mathbf{e}_j^+(c_3\,[[\mathbf{U}]] \;+\; c_4\,[[\mathcal{D}\,\mathbf{U}]])_{j+\frac{1}{2}} \\ &+ \quad \mathcal{I}^T\mathbf{e}_j^-(c_3\,[[\mathbf{U}]] \;+\; c_4\,[[\mathcal{D}\,\mathbf{U}]])_{j-\frac{1}{2}} \quad \} \end{aligned} \tag{15}$$

Equation (15) is satisfied for an arbitrary test function $\mathbf{V}^T$. A sufficient condition to satisfy the equation is for the bracketed terms to be identically zero. Dropping the premultiplication by the test function $\mathbf{V}^T$ results in the strong form representation of the Discontinuous Galerkin FEM.

The HOFDM and the nodal spectral element communities are accustomed to formulations (and stability proofs) involving two adjoining elements and the included interface. Rewriting equation (15) in this form yields the desired result

$$\begin{aligned} \mathcal{P}\mathbf{U}_t^j \;=\; \mathcal{P}\mathcal{D}\mathcal{D}\mathbf{U}^j \quad &+ \quad \mathcal{D}^T\mathbf{e}_j^+(c_1\,[[\mathbf{U}]] \;+\; c_2\,[[\mathcal{D}\,\mathbf{U}]])_{j+\frac{1}{2}} \\ &- \quad \mathcal{I}^T\mathbf{e}_j^+(c_3\,[[\mathbf{U}]] \;+\; c_4\,[[\mathcal{D}\,\mathbf{U}]])_{j+\frac{1}{2}} \\ \mathcal{P}\mathbf{U}_t^{j+1} \;=\; \mathcal{P}\mathcal{D}\mathcal{D}\mathbf{U}^{j+1} \quad &- \quad \mathcal{D}^T\mathbf{e}_{j+1}^-(c_1\,[[\mathbf{U}]] \;+\; c_2\,[[\mathcal{D}\,\mathbf{U}]])_{j+\frac{1}{2}} \\ &+ \quad \mathcal{I}^T\mathbf{e}_{j+1}^-(c_3\,[[\mathbf{U}]] \;+\; c_4\,[[\mathcal{D}\,\mathbf{U}]])_{j+\frac{1}{2}} \;. \end{aligned} \tag{16}$$

Note that the derivative and integration operators $\mathcal{D}$ and $\mathcal{P}$ remain undefined in equation (16), so that this method could be applied to a wide variety of difference operators. Clearly, the method defined in equation (16) mimics the properties of the DGFEM method defined in equation (10). It is, however, legitimate to question whether the two forms are equivalent.

Consider an arbitrary set of collocation points on the interval $[x_0 \;=\; x_{j-\frac{1}{2}},\, x_1,\, x_2,\, ...,\, x_{N-1},\, x_N \;=\; x_{j+\frac{1}{2}}]$, and let $f(x)$ be defined everywhere on the interval. The interpolation polynomial $f_N(x)$ that collocates $f(x)$ at the points x_j is given by

$$f_N(x) \;=\; J_N\,f \;=\; \sum_{j=0}^{N} f(x_j)\,L_j(x) \;, \tag{17}$$

where $L_j(x)$ are the Lagrange polynomials defined on the discrete set of points. It is well known (see Carpenter and Gottlieb [12]) that for this case,

$$\mathbf{f}_x \;=\; \mathcal{D}\mathbf{f} \tag{18}$$

where the differentiation matrix $\mathcal{D}$ is given by

$$\mathcal{D} \;=\; \mathcal{P}^{-1}\mathcal{Q} \;=\; \frac{\partial}{\partial x}\,L_k(x_j) \tag{19}$$

with

$$p_{kl} \;=\; \int_{j-\frac{1}{2}}^{j+\frac{1}{2}} L_l(x)\,L_k(x)\,dx \quad ; \quad q_{kl} \;=\; \int_{j-\frac{1}{2}}^{j+\frac{1}{2}} \frac{\partial}{\partial x}L_l(x)\,L_k(x)\,dx \tag{20}$$

Substituting these definitions back into the strong form given by equation (16), and comparing the resulting expression with that of equation (10) (using the Lagrange polynomials as test functions), we achieve term by term agreement with the original weak form method. Thus, the strong and weak forms of the linear, constant coefficient heat equation, result in identical solutions.

Remark. One has only to include a variable coefficient in the equation for the two formulations to produce different results. In this case, the collocation approach would have a truncation error associated with the inexactness of the differentiation operation. The DGFEM would, however, integrate exactly the polynomial of higher degree.

Closing Remark.
The principle result of this brief review of DGFEM is equation (16), which expresses the "strong form equivalent" of the underlying FEM method. In this expression, it is clear that the $\mathcal{D}^T$ matrix plays a critical role in the collocation approach, in determining accuracy, stability and conservation at the interface. The previous derivation of "general" multi-domain interface conditions for HOFDM, (see Carpenter et al. [13]), although correct, **lacked the generality necessary to include the $\mathcal{D}^T$ interface contribution**! Armed with the $\mathcal{D}^T$ matrix in our arsenal of mathematical tricks, we now derive the general interface coupling conditions for arbitrary collocation approaches, including HOFDM and nodal spectral collocation methods.

3 The semi-discrete problem

Our goal is to derive stable, conservative and accurate semi-discrete interface coupling operators. As we shall see, these operators closely relate to (mimic) the corresponding properties of the continuous operators. In the discussion to follow, we shall introduce each step with a discussion at the continuous level, followed by the derivation of the semi-discrete mimetic operators.

3.1 Definitions

Consider the linear initial boundary value problem

$$\begin{array}{rcll} w_t & = & Pw + \delta F(x,t) & ,x \in \Omega \quad ,t \geq 0, \\ w & = & \delta f(x) & ,x \in \Omega \quad ,t = 0, \\ L_C w & = & \delta g(t) & ,x \in \Gamma \quad ,t \geq 0, \end{array} \tag{21}$$

where P is the differential operator and L_C is the boundary operator. The initial function δf, the forcing function δF, and the boundary data δg are the data of the problem; w denotes the difference between a solution with data f,F,g and one with data $f+\delta f$,$F+\delta f$,$g+\delta g$. There are many concepts of wellposedness, see [19]. Here we consider the following definition.

Definition 1 *The problem (21) is strongly wellposed if the solution w exists, is unique, and satisfies*

$$\|w\|_\Omega^2 + \int_0^t \|w\|_\Gamma^2 dt \leq K_c e^{\eta_c t}\{\|\delta f\|_\Omega^2 + \int_0^t (\|\delta F\|_\Omega^2 + \|\delta g\|_\Gamma^2)dt\}, \tag{22}$$

where K_c and η_c may not depend on δF, δf,δg. $\|\cdot\|_\Omega$ and $\|\cdot\|_\Gamma$ are suitable continuous norms, such as

$$\|uv\|_\Omega = \int_{-1}^{+1} uv dx, \quad \|u\|_\Omega^2 = \int_{-1}^{+1} uu dx, \quad \|u\|_\Gamma^2 = |u|_{x=-1}^2 + |u|_{x=+1}^2$$

The semidiscrete version of (21) is

$$\begin{array}{rcll} (w_j)_t & = & Qw_j + \delta F_j(t) & ,x_j \in \Omega \quad ,t \geq 0, \\ w_j & = & \delta f_j & ,x_j \in \Omega \quad ,t = 0,, \\ L_D w_j & = & \delta g(t) & ,x_j \in \Gamma \quad ,t \geq 0, \end{array} \tag{23}$$

where Q is the difference operator approximating the differential operator P, δF_j is the forcing function, δf_j the initial function, L_D the discrete boundary operator where numerical boundary conditions are included, and δg the boundary data. It is assumed that (23) is a consistent approximation of (21).

Closely related to the concept of wellposedness is the concept of stability.

Definition 2 *The problem (23) is strongly stable, if for a sufficiently fine mesh, the solution w_j satisfies*

$$\|w\|_\mathcal{P}^2 + \int_0^t \|w\|_\Gamma^2 dt \leq K_d e^{\eta_d t}\{\|\delta f\|_\mathcal{P}^2 + \int_0^t (\|\delta F\|_\mathcal{P}^2 + \|\delta g\|_\Gamma^2)dt\}, \tag{24}$$

where K_d and η_d may not depend on δF_j, δf_j,δg. $\|\cdot\|_\mathcal{P}$ and $\|\cdot\|_\Gamma$ are suitable discrete norms, such as

$$\|vw\|_\mathcal{P} = v^T \mathcal{P} w, \quad \|u\|_\mathcal{P}^2 = u^T \mathcal{P} u, \quad \|u\|_\Gamma^2 = |u|_{x=-1}^2 + |u|_{x=+1}^2$$

Here, $\|vw\|_\mathcal{P}$, $\|u\|_\mathcal{P}^2$, and $\|u\|_\Gamma^2$ denote the L_2 scalar product, the L_2 norm, and the boundary norm, respectively.

3.2 Discrete Spatial Operators

Let U and $\mathcal{D}\mathbf{U}$ be the discrete approximations of the scalar quantities u and u_x. The approximation $\mathcal{D}\mathbf{U}$ of the first derivative

$$\mathcal{D}\mathbf{U} \;=\; \mathcal{P}^{-1}\,\mathcal{Q}\mathbf{U}, \quad \mathcal{P}\mathbf{u_x} \,-\, \mathcal{Q}\mathbf{u} \;=\; \mathcal{P}T_{e1}, \quad |T_{e1}| \;=\; \mathcal{O}(\Delta x^i, \Delta x^b) \tag{25}$$

satisfies the SBP rule

$$(\mathbf{U}, \mathcal{D}\mathbf{V})_{\mathcal{P}} \;=\; U_N V_N - U_0 V_0 - (\mathcal{D}\mathbf{U}, \mathbf{V})_{\mathcal{P}} \tag{26}$$

$$(\mathbf{U}, \mathbf{V})_{\mathcal{P}} = \mathbf{U}^T \mathcal{P} \mathbf{V}, \quad \mathcal{P} \;=\; \mathcal{P}^T, \quad \mathcal{Q} + \mathcal{Q}^T = \mathcal{B}, \quad \mathcal{B} = diag[-1, 0, .., 0, 1], \tag{27}$$

$0 < p_{min}\Delta x\|\mathcal{I}\| \leq \|\mathcal{P}\| \leq p_{max}\Delta x\|\mathcal{I}\|$. The matrix $\mathcal{P}$ is symmetric positive definite, the matrix $\mathcal{Q}$ is skew-symmetric with the exception of boundary points.

A second derivative operator can be obtained by applying any two first derivative operators, or by constructing the operator directly. Both techniques are suitable for spectral collocation. In HOFDM, using two consecutive non-dissipative first derivatives, results in a second derivative operator that is unnecessarily wide and inaccurate and can lead to odd-even mode decoupling. The operator, however, often leads to stability if varying coefficients are considered. Forming the HOFDM second derivative directly requires an operator with the following properties,

$$\mathcal{D}^2\mathbf{U} = \mathcal{P}^{-1}\mathcal{R}_2\mathbf{U}, \quad \mathcal{P}\mathbf{u_{xx}} - \mathcal{R}_2\mathbf{u} = \mathcal{P}\mathbf{T_{e2}}, \quad \mathbf{T_{e2}} = \mathcal{O}(\Delta x^i, \Delta x^b), \tag{28}$$

$$\mathcal{R}_2 = (-\mathcal{S}^T\mathcal{M} + \mathcal{B})\mathcal{S}, \tag{29}$$

as suggested in reference [13] (see also [28]). The matrix $\mathcal{B}$ is given in (27); $\mathcal{M}$ is positive definite, i.e., $\mathbf{U}^T\mathcal{M}\mathbf{U} > 0$ and $0 < m_{min}\Delta x\|\mathcal{I}\| \leq \|\mathcal{M}\| \leq m_{max}\Delta x\|\mathcal{I}\|$.

The matrix $\mathcal{S}$ is nearly diagonal with a discrete representation of the first derivative on the first and last rows,

$$\{\mathcal{S}u\}_0 = \{\mathcal{D}u\}_0 = u_x(x_0, t) + T_{e3}, \quad \{\mathcal{S}u\}_n = \{\mathcal{D}u\}_n = u_x(x_n, t) + T_{e3},$$

where $|T_{e3}| = \mathcal{O}(\Delta x^r)$ and

$$\mathcal{S} = \frac{1}{\Delta x}\begin{pmatrix} s_{00} & s_{01} & s_{02} & s_{03} & \cdots & & \\ 0 & 1 & 0 & & & & \\ & 0 & 1 & 0 & & & \\ & & \ddots & \ddots & \ddots & & \\ & & & 0 & 1 & 0 & \\ & & & & 0 & 1 & 0 \\ & & \cdots & s_{nn-3} & s_{nn-2} & s_{nn-1} & s_{nn} \end{pmatrix}.$$

The second derivative defined in (28) and (29) satisfies a modified SBP rule We have

$$(\mathbf{U}, \mathcal{D}^2 V)_{\mathcal{P}} = \mathbf{U}_n\{\mathcal{D}\mathbf{V}\}_n - \mathbf{U}_0\{\mathcal{D}\mathbf{V}\}_0 - (\mathcal{S}\mathbf{U})^T M(\mathcal{S}\mathbf{V}).$$

The notation $|T_{e1}|, |T_{e2}| = \mathcal{O}(\Delta x^i, \Delta x^b)$ and $|T_{e3}| = \mathcal{O}(\Delta x^r)$ means that the approximation of the differential operator is accurate to order i in the interior of the domain, to order b at the boundary and that the approximation of the boundary conditions is accurate to order r. This nomenclature is valid for any of the SBP schemes mentioned in the introduction, including HOFDM and spectral collocation. The relation between the different orders of accuracy, i.e., i, b, r is discussed in section (4) below, where formal proofs of accuracy are given for HOFDM.

3.3 The semi-discrete single domain problem

The following semi-discrete derivations and proofs are closely related to proofs of wellposedness at the continuous level. For completeness, a complete derivation of wellposedness is presented in Appendix (B) for both a single and a two domain problem. A derivation of the semi-discrete equation is now presented.

Imagine that we are solving the constant coefficient, linear Burgers' equation

$$\begin{array}{rcccll} c_t \,+\, a\, c_x & = & \epsilon c_{xx} \,+\, F(x,t) & & ,t \geq 0 & ,-1 \leq x \leq 1, \\ c(x,0) & = & f(x) & & ,t = 0 & ,-1 \leq x \leq 1, \\ \gamma c(-1,t) - \epsilon c_x(-1,t) & = & g_{-1}(t) & = \quad L_{-1}(c) & ,t \geq 0 & ,x = -1, \\ \zeta c(+1,t) + \epsilon c_x(+1,t) & = & g_{+1}(t) & = \quad L_{+1}(c) & ,t \geq 0 & ,x = +1, \end{array} \tag{30}$$

with constants a and ϵ $(0 \,<\, \epsilon)$. The boundary conditions that lead to a wellposed problem satisfy the following constraints [(a detailed discussion of wellposedness is included in Appendix (A)].

$$0 \,\leq\, a \,+\, 2\,\zeta \qquad ;\quad 0 \,\leq\, -a \,+\, 2\,\gamma \quad . \tag{31}$$

Consider the semi-discrete, finite difference representation of the linear Burgers' equation (30) of the form

$$\begin{array}{rcll} C_t \,+\, a\,\mathcal{D}\mathbf{C} & = & \epsilon \mathcal{D}\mathcal{D}\mathbf{C} \,+\, \mathbf{F}(\mathbf{C}) & \\ & - & \mathcal{P}^{-1}\{\sigma_{-1}\,[L^D_{-1}\,(\mathbf{C}) \,-\, g_{-1}]\,\mathbf{e}_{-1}\} & \\ & - & \mathcal{P}^{-1}\{\sigma_{+1}\,[L^D_{+1}\,(\mathbf{C}) \,-\, g_{+1}]\,\mathbf{e}_{+1}\} & ,t \,\geq\, 0 \quad -1 \,\leq\, x \,\leq\, +1 \\ \mathbf{C}(x_i,0) & = & \mathbf{f}(x_i) & ,t \,=\, 0 \quad -1 \,\leq\, x \,\leq\, +1\,. \end{array} \tag{32}$$

The discrete boundary operators are defined by

$$L^D_{-1}(\mathbf{C}) \,=\, (\gamma C - \,\epsilon\,\mathcal{D}\mathbf{C})|_{-1} \;;\; L^D_{+1}(\mathbf{C}) \,=\, (\zeta C + \,\epsilon\,\mathcal{D}\mathbf{C})|_{+1}, \tag{33}$$

while the penalty vectors are defined by $\mathbf{e}_{-1} \,=\, [1,0,...,0,0]^T$ and $\mathbf{e}_{+1} \,=\, [0,0,...,0,1]^T$.

We have introduced a uniform mesh $-1 \,\leq\, x_i \,\leq\, +1$ with $x_0 = -1, x_n = +1$ and $x_i = -1 + i\Delta x$, and the boundary conditions are treated weakly via a penalty technique (see reference [10]).

Theorem 1 *The approximation (32) of the problem (30) is strongly stable if the boundary conditions satisfy the constraints given in equation (31), and the numerical boundary conditions given in equation (32,33) satisfy the following inequalities:*

$$\begin{array}{rcccl} 1 + \frac{2\alpha\gamma}{\epsilon} \,-\, \sqrt{(\frac{2\alpha\gamma}{\epsilon})^2 \,+\, \frac{2\alpha}{\epsilon}(2\,\gamma \,-\, a)} & \leq & \sigma_{-1} & \leq & 1 + \frac{2\alpha\gamma}{\epsilon} \,+\, \sqrt{(\frac{2\alpha\gamma}{\epsilon})^2 \,+\, \frac{2\alpha}{\epsilon}(2\,\gamma \,-\, a)} \\ 1 + \frac{2\alpha\zeta}{\epsilon} \,-\, \sqrt{(\frac{2\alpha\zeta}{\epsilon})^2 \,+\, \frac{2\alpha}{\epsilon}(2\,\zeta \,+\, a)} & \leq & \sigma_{+1} & \leq & 1 + \frac{2\alpha\zeta}{\epsilon} \,+\, \sqrt{(\frac{2\alpha\zeta}{\epsilon})^2 \,+\, \frac{2\alpha}{\epsilon}(2\,\zeta \,+\, a)} \end{array} \tag{34}$$

with

$$\alpha \quad = \quad \frac{1}{\mathbf{e_{i\_}}^T\,\mathcal{P}^{-1}\,\mathbf{e_{i\_}}}$$

Proof : The energy method applied to equation (32) leads to

$$\begin{array}{rcl} \frac{d}{dt}\|C\|^2_{\mathcal{P}} \,+\, a\,\mathbf{C}^T[\mathcal{P}\mathcal{D} \,+\, \mathcal{D}^T\mathcal{P}]\mathbf{C} & = & 2\,\epsilon\,\mathbf{C}^T[\mathcal{P}\mathcal{D}\mathcal{D} + \mathcal{D}^T\mathcal{D}^T\mathcal{P}]\mathbf{C} \,+\, 2\,\|\mathbf{C},\mathbf{F}\|_{\mathcal{P}} \\ & - & 2\,\sigma_{-1}\,C_{-1}\,[L^D_{-1}(\mathbf{C}) \,-\, g_{-1}] \\ & - & 2\,\sigma_{+1}\,C_{+1}\,[L^D_{+1}(\mathbf{C}) \,-\, g_{+1}]. \end{array} \tag{35}$$

The definitions of the first derivative operators $\mathcal{D} = \mathcal{P}^{-1}\mathcal{Q}$, presented in equations (25) - (27) lead to

$$\begin{array}{rcl} \mathbf{C}^T[\mathcal{P}\mathcal{D} \,+\, \mathcal{D}^T\mathcal{P}]\mathbf{C} & = & \mathbf{C}^T\mathcal{B}\mathbf{C} \\ \mathbf{C}^T[\mathcal{P}\mathcal{D}\mathcal{D} + \mathcal{D}^T\mathcal{D}^T\mathcal{P}]\mathbf{C} & = & \mathbf{C}^T\mathcal{B}\mathcal{D}\mathbf{C} - \mathbf{C}^T\mathcal{D}^T\mathcal{P}\mathcal{D}\mathbf{C} \end{array} \tag{36}$$

Introducing equations (36) and (33) into (35) yields

$$\begin{array}{rcl} \frac{d}{dt}\|\mathbf{C}\|^2_{\mathcal{P}} & = & -2\,\epsilon\,(\mathcal{D}\mathbf{C})^T\mathcal{P}\mathcal{D}\mathbf{C} + 2\|\mathbf{C},\mathbf{F}\|_{\mathcal{P}} \\ & & +[-a\mathbf{C}^T\mathcal{B}\mathbf{C} + 2\,\epsilon\,\mathbf{C}^T\mathcal{D}\mathbf{C}]|_{x=-1}^{x=+1} \\ & & -2\,\sigma_{-1}\,C_{-1}\,[(\gamma C - \,\epsilon\,\mathcal{D}\mathbf{C})|_{-1} \,-\, g_{-1}] \\ & & -2\,\sigma_{+1}\,C_{+1}\,[(\zeta C + \,\epsilon\,\mathcal{D}\mathbf{C})|_{+1} \,-\, g_{+1}] \end{array} \tag{37}$$

Substituting the relations

$$\begin{array}{rcccl} 2\,\|\mathbf{C},\mathbf{F}\|_{\mathcal{P}} & = & -\,\|\sqrt{\eta}\,\mathbf{C}\,-\,\frac{1}{\sqrt{\eta}}\,\mathbf{F}\|^2_{\mathcal{P}}\,+\,\eta\|\,\mathbf{C}\,\|^2_{\mathcal{P}}\,+\,\frac{1}{\eta}\|\,\mathbf{F}\,\|^2_{\mathcal{P}} & \leq & +\eta\|\,\mathbf{C}\,\|^2_{\mathcal{P}}\,+\,\frac{1}{\eta}\|\,\mathbf{F}\,\|^2_{\mathcal{P}} \\ 2C_{-1}g_{-1} & = & -[\sqrt{\eta_-}C_{-1}-\frac{1}{\sqrt{\eta_-}}g_{-1}]^2+\eta_-\,(C_{-1})^2+\frac{1}{\eta_-}\,(g_{-1})^2 & \leq & \sqrt{\eta_-}(C_{-1})^2+\frac{1}{\sqrt{\eta_-}}(g_{-1})^2 \\ 2C_{+1}g_{+1} & = & -[\sqrt{\eta_+}C_{+1}-\frac{1}{\sqrt{\eta_+}}g_{+1}]^2+\eta_+\,(C_{+1})^2+\frac{1}{\eta_+}\,(g_{+1})^2 & \leq & \sqrt{\eta_+}(C_{+1})^2+\frac{1}{\sqrt{\eta_+}}(g_{+1})^2 \end{array} \tag{38}$$

into equation (37) yields the equation

$$\begin{array}{rcccl} e^{\eta t}\,\frac{\partial}{\partial t}\{e^{-\eta t}\|C\|^2_{\mathcal{P}}\}\,+\,2\,\epsilon\,\|\mathcal{D}\mathbf{C}\|^2_{\bar{\mathcal{P}}} & = & +\,\frac{1}{\eta}\,\|\mathbf{F}\|^2_{\mathcal{P}} & - & \|\sqrt{\eta}\,\mathbf{C}\,-\,\frac{1}{\sqrt{\eta}}\,\mathbf{F}\|^2_{\mathcal{P}} \\ & + & \frac{\sigma_{-1}}{\eta_-}\,(g_{-1})^2 & - & \sigma_{-1}\,[\sqrt{\eta_-}C_{-1}-\frac{1}{\sqrt{\eta_-}}g_{-1}]^2 \\ & + & \frac{\sigma_{+1}}{\eta_+}\,(g_{+1})^2 & - & \sigma_{+1}\,[\sqrt{\eta_+}C_{+1}-\frac{1}{\sqrt{\eta_+}}g_{+1}]^2 \\ & - & \Phi_{-1} & - & \Phi_{+1} \end{array} \tag{39}$$

with

$$\Phi_{-1}=\begin{bmatrix} C_{-1} \\ \mathcal{D}\mathbf{C}|_{-1} \end{bmatrix}^T\begin{bmatrix} -a+\sigma_{-1}(2\gamma-\eta_{-1}) & +\epsilon(1\,-\,\sigma_{-1}) \\ +\epsilon(1\,-\,\sigma_{-1}) & +2\epsilon\alpha \end{bmatrix}\begin{bmatrix} C_{-1} \\ \mathcal{D}\mathbf{C}|_{-1} \end{bmatrix} \tag{40}$$

$$\Phi_{+1}=\begin{bmatrix} C_{+1} \\ \mathcal{D}\mathbf{C}|_{+1} \end{bmatrix}^T\begin{bmatrix} +a+\sigma_{+1}(2\zeta-\eta_{+1}) & -\epsilon(1\,-\,\sigma_{+1}) \\ -\epsilon(1\,-\,\sigma_{+1}) & +2\epsilon\alpha \end{bmatrix}\begin{bmatrix} C_{+1} \\ \mathcal{D}\mathbf{C}|_{+1} \end{bmatrix} \tag{41}$$

It is shown in Appendix (B) that part of the quadratic diffusion term $2\,\epsilon\,\|\mathcal{D}\mathbf{C}\|^2_{\mathcal{P}}$ can be moved to the (RHS) to stabilize the boundary terms Φ_{-1} and Φ_{+1}. Only a small portion can be borrowed, however, without destroying the definiteness of the term. The new diffusion term remains definite in the norm

$$\bar{\mathcal{P}} \quad = \quad \mathcal{P}\,-\,\alpha\,\mathbf{e}_{\mathbf{i}_-}\,{\mathbf{e}_{\mathbf{i}_-}}^T$$

See Appendix (C) for the value of alpha that produces a semi-definite matrix $\bar{\mathcal{P}}$.

To ensure stability the terms Φ_{+1} and Φ_{-1} must be positive definite, and thus lead to stability if the inequalities given by equation (34) in Theorem 1 are satisfied. (Here we assume that the parameters $\eta_{\pm 1}\,=\,0$.) Note that the wellposedness conditions given in equation (31) ensure positivity of the square roots in both expressions.

Grouping like terms results in

$$\frac{\partial}{\partial t}\{e^{-\eta t}\|C\|^2_{\mathcal{P}}\}\,+\,e^{-\eta t}\,\{2\,\epsilon\,\|\mathcal{D}\mathbf{C}\|^2_{\bar{\mathcal{P}}}\,+\,BC_d\} \quad = \quad e^{-\eta t}\,\{Data\,-\,PosDef_d\} \tag{42}$$

with

$$\begin{array}{rcl} BC_d & = & \Phi_{-1}\,+\,\Phi_{+1} \\ Data & = & +\,\frac{1}{\eta}\|F\|^2_{\mathcal{P}}\,+\,\frac{\sigma_{+1}}{\eta_{+1}}{g_{+1}}^2\,+\,\frac{\sigma_{-1}}{\eta_{-1}}{g_{-1}}^2 \\ PosDef_d & = & +\,\|\sqrt{\eta}C-\frac{1}{\sqrt{\eta}}F\|^2_{\mathcal{P}}\,+\,\sigma_{+1}\,(\sqrt{\eta_{+1}}C_{+1}-\frac{1}{\sqrt{\eta_{+1}}}g_{+1})^2\,+\,\sigma_{-1}\,(\sqrt{\eta_{-1}}C_{-1}-\frac{1}{\sqrt{\eta_{-1}}}g_{-1})^2 \end{array} \tag{43}$$

Finally, integrating equation (42) in time leads to

$$\|C(x_i,T)\|^2_{\mathcal{P}}\,+\,\int_0^T e^{-\eta(t-T)}\,\{2\,\epsilon\,\|\mathcal{D}\mathbf{C}\|^2_{\bar{\mathcal{P}}}\,+\,BC_d\}dt \quad = \quad e^{+\eta T}\{\|f(x_i)\|^2_{\mathcal{P}}\,+\,\int_0^T e^{-\eta t}\,[Data\,-\,PosDef_d]dt\} \tag{44}$$

from which follows a strongly stable estimate of the form

$$\|C\|^2_{\mathcal{P}}+\int_0^t\|C\|^2_{\Gamma}dt\leq K_d e^{\eta t}\{\|f\|^2_{\mathcal{P}}+\int_0^t(\|F\|^2_{\mathcal{P}}+\|g\|^2_{\Gamma})dt\}, \tag{45}$$

Hence (32) is a strongly stable approximation. □

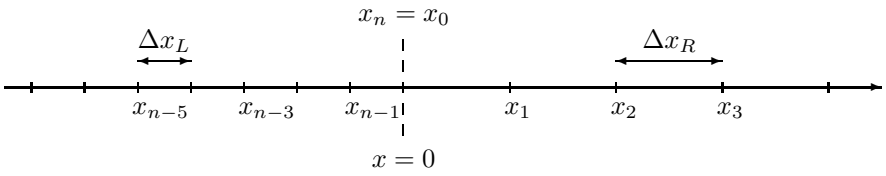

Figure 2: The mesh close to the interface at $x = 0$.

3.4 The semi-discrete two domain problem

3.4.1 A "Primal" discretization technique

We are interested in the stability, accuracy and conservation of the new interface treatments. The previous single-domain result established the conditions required to achieve semi-discrete strong-stability, subject to an arbitrary source term and consistent, wellposed initial and boundary conditions. For clarity of presentation (and without loss of generality), we shall neglect the source term, and the physical boundary conditions from the subsequent two-domain derivations.

A collocation approximation of the coupled problem (168) written in primal form and motivated by the FEM proposed by Baumann and Oden [7] is

$$\begin{array}{rcl}
\mathcal{P}_l\mathbf{U}_t + a\mathcal{P}_l\mathcal{D}_l\mathbf{U} - \epsilon\mathcal{P}_l\mathcal{D}_l\mathcal{D}_l\mathbf{U} &=& l_{00}[U_i - V_i] \quad \mathcal{I}_l\ \mathbf{e}_{\mathbf{i}_-} \quad + \quad l_{01}[(\mathcal{D}_l U)_i - (\mathcal{D}_r V)_i] \quad \mathcal{I}_l\ \mathbf{e}_{\mathbf{i}_-} \\
&+& l_{10}[U_i - V_i] \quad \mathcal{D}_l^T\mathbf{e}_{\mathbf{i}_-} \quad + \quad l_{11}[(\mathcal{D}_l U)_i - (\mathcal{D}_r V)_i] \quad \mathcal{D}_l^T\mathbf{e}_{\mathbf{i}_-} \\
\mathbf{U}(x,0) &=& \mathbf{0}. \\
\mathcal{P}_r\mathbf{V}_t + a\mathcal{P}_r\mathcal{D}_r\mathbf{V} - \epsilon\mathcal{P}_r\mathcal{D}_r\mathcal{D}_r\mathbf{V} &=& r_{00}[V_i - U_i] \quad \mathcal{I}_r\ \mathbf{e}_{\mathbf{i}_+} \quad + \quad r_{01}[(\mathcal{D}_r V)_i - (\mathcal{D}_r U)_i] \quad \mathcal{I}_r\ \mathbf{e}_{\mathbf{i}_+} \\
&+& r_{10}[V_i - U_i] \quad \mathcal{D}_r^T\mathbf{e}_{\mathbf{i}_+} \quad + \quad r_{11}[(\mathcal{D}_r V)_i - (\mathcal{D}_r U)_i] \quad \mathcal{D}_r^T\mathbf{e}_{\mathbf{i}_+} \\
\mathbf{V}(x,0) &=& \mathbf{0}.
\end{array} \tag{46}$$

The variables in the left (subscript l) $[x_0 = -1, x_n = 0]$ and right (subscript r) $[x_0 = 0, x_m = +1]$ domains are $\bar{U}$ and $\bar{V}$, respectively, (see Figure 2).

Definitions of the n_l (n_r) dimensional operator $\mathcal{D}_l$ ($\mathcal{D}_r$) are given by

$$\mathcal{D}_l = \mathcal{P}_l^{-1}\mathcal{Q}_l; \quad -1 \le x \le x_i \quad ; \quad \mathcal{D}_r = \mathcal{P}_r^{-1}\mathcal{Q}_r; \quad x_i \le x \le 1$$

and $\mathbf{e}_{\mathbf{i}_-}$ and $\mathbf{e}_{\mathbf{i}_+}$ are given by $e_{i_-} = [0, 0, ..., 0, 1]^T$ and $e_{i_+} = [1, 0, ..., 0, 0]^T$. Note that the difference operators $\mathcal{D}_l$, and $\mathcal{D}_r$ are in general different in the left and right domains ($\Delta x_L \neq \Delta x_R$ and/or $n_l \neq n_r$).

What remains is to determine the values of the interface parameters l_{00}, l_{01}, l_{10}, l_{11}, and r_{00}, r_{01}, r_{10}, r_{11}, that lead to stability and conservation.

3.4.2 Stability

Remark. Stability of the one domain problem *does not* imply stability of the multiple domain problem. Stability means that the solution can be estimated in terms of the (bounded) boundary data. In a multiple domain problem, the boundary data are made up of the solution(s) in the other domain(s). Boundedness of the data would require an a priori assumption.

Theorem 2 *The approximation (46) of the problem (30) is strongly stable if the eight parameters are related by the two equalities*

$$l_{00} = r_{00} + a \quad ; \quad l_{01} = r_{01} - \epsilon \tag{47}$$

and constrained by the following inequalities

$$2[r_{11} + l_{11}] \quad \le \quad [(\alpha + \beta)\epsilon] \tag{48}$$

$$\frac{\left[\epsilon(-\alpha+\beta)-(r_{11}-l_{11})\right]^2}{\epsilon(\alpha+\beta)-2(r_{11}+l_{11})} \quad \leq \quad [(\alpha+\beta)\epsilon] \tag{49}$$

$$l_{00} \quad \leq \quad \frac{a}{2} \; - \; \frac{(\epsilon+2l_{01}+l_{10}+r_{10})^2}{4[\epsilon(\alpha+\beta)-2(r_{11}+l_{11})]} \; - \; \frac{\{\epsilon+l_{10}-r_{10}+\frac{[\epsilon(-\alpha+\beta)-(r_{11}-l_{11})](\epsilon+2l_{01}+l_{10}+r_{10})}{[\epsilon(\alpha+\beta)-2(r_{11}+l_{11})]}\}^2}{4\{[(\alpha+\beta)\epsilon]-\frac{[\epsilon(-\alpha+\beta)-(r_{11}-l_{11})]^2}{[\epsilon(\alpha+\beta)-2(r_{11}+l_{11})]}\}} \tag{50}$$

where

$$\alpha \; = \; \frac{1}{\mathbf{e_{i_-}}^T \; \mathcal{P}_l^{-1} \; \mathbf{e_{i_-}}} \quad ; \quad \beta \; = \; \frac{1}{\mathbf{e_{i_+}}^T \; \mathcal{P}_r^{-1} \; \mathbf{e_{i_+}}} \tag{51}$$

Proof : Strong stability of (46) follows if the interface treatment at $x = x_i$ is of a dissipative nature. As we have already established the stability of the far-field boundary penalties we need only focus on the interface terms.

The energy method applied to equation (46) (multiplying the discrete equations in the left and right subdomains by $\mathbf{U}^T$ and $\mathbf{V}^T$ respectively), and using the relation $Q \; + \; Q^T \; = \; B$ from the SBP rule (27), yields

$$\begin{array}{rcccccc} \frac{d}{dt}[\; \|\mathbf{U}\|^2_{\mathcal{P}_l} \; + & \|\mathbf{V}\|^2_{\mathcal{P}_r}] & & & & & \\ +\,2\epsilon[\,\|\mathcal{D}_l\mathbf{U}\|^2_{\mathcal{P}_l} \; + \; \|\mathcal{D}_r\mathbf{V}\|^2_{\mathcal{P}_r}] & = & [2\,\epsilon U\mathcal{D}_l U \; - \; a\,U^2]_{-1}^{i_-} & + & [2\,\epsilon V\mathcal{D}_r V \; - \; a\,V^2]_{i_+}^{1} & & \\ & + & 2l_{00} \quad U_i \; [U_i - V_i] & + & 2l_{01} \quad U_i \; [(\mathcal{D}_l U)_i - (\mathcal{D}_r V)_i] & & \\ & + & 2l_{10}(\mathcal{D}_l U)_i[U_i - V_i] & + & 2l_{11}(\mathcal{D}_l U)_i[(\mathcal{D}_l U)_i - (\mathcal{D}_r V)_i] & & \\ & + & 2r_{00} \quad V_i \; [V_i - U_i] & + & 2r_{01} \quad V_i \; [(\mathcal{D}_r V)_i - (\mathcal{D}_l U)_i] & & \\ & + & 2r_{10}(\mathcal{D}_r V)_i[V_i - U_i] & + & 2r_{11}(\mathcal{D}_r V)_i[(\mathcal{D}_r V)_i - (\mathcal{D}_l U)_i] & & \end{array} \tag{52}$$

The stability of equation (52) is ensured if all the terms on the (RHS) are negative. Once again, a small portion of the diffusion terms $\|\mathcal{D}_l\mathbf{U}\|_{\mathcal{P}_l}$ and $\|\mathcal{D}_r\mathbf{V}\|_{\mathcal{P}_r}$ arising at the interface can be moved to the (RHS) to help in the proof of stability. Defining

$$\bar{\mathcal{P}}_l \; = \; \mathcal{P}_l \; - \; \alpha \, \mathbf{e_{i_-}} \, \mathbf{e_{i_-}}^T \quad ; \quad \bar{\mathcal{P}}_r \; = \; \mathcal{P}_r \; - \; \beta \, \mathbf{e_{i_+}} \, \mathbf{e_{i_+}}^T \tag{53}$$

with

$$\alpha \; = \; \frac{1}{\mathbf{e_{i_-}}^T \; \mathcal{P}_l^{-1} \; \mathbf{e_{i_-}}} \quad ; \quad \beta \; = \; \frac{1}{\mathbf{e_{i_+}}^T \; \mathcal{P}_r^{-1} \; \mathbf{e_{i_+}}} \tag{54}$$

and collecting all the interface contributions into one term, (52) becomes

$$\begin{array}{rcl} \frac{d}{dt}\left[\|\mathbf{U}\|^2_{\mathcal{P}_l} \; + \; \|\mathbf{V}\|^2_{\mathcal{P}_r}\right] \; + \; 2\epsilon\left[\|\mathcal{D}_l\mathbf{U}\|^2_{\bar{\mathcal{P}}_l} \; + \; \|\mathcal{D}_r\mathbf{V}\|^2_{\bar{\mathcal{P}}_r}\right] & = & \left[2\,\epsilon U\mathcal{D}_l U \; - \; a\,U^2\right]_{-1} \\ & + & \left[2\,\epsilon V\mathcal{D}_r V \; - \; a\,V^2\right]^1 \; + \; \Upsilon_i \end{array} \tag{55}$$

with the interface term $\Upsilon_i \; = \; [\mathcal{I}_i]^T \; M_i \, \mathcal{I}_i$ defined by

$$\Upsilon_i \quad = \quad \begin{bmatrix} U_i \\ V_i \\ (\mathcal{D}_l U)_i \\ (\mathcal{D}_r V)_i \end{bmatrix}^T \begin{bmatrix} (-a+2l_{00}) & -(l_{00}+r_{00}) & (\epsilon+l_{01}+l_{10}) & -(l_{01}+r_{10}) \\ -(l_{00}+r_{00}) & (+a+2r_{00}) & -(r_{01}+l_{10}) & (-\epsilon+r_{01}+r_{10}) \\ (\epsilon+l_{01}+l_{10}) & -(r_{01}+l_{10}) & -2(\alpha\epsilon+l_{11}) & -(l_{11}+r_{11}) \\ -(l_{01}+r_{10}) & (-\epsilon+r_{01}+r_{10}) & -(l_{11}+r_{11}) & -2(\beta\epsilon+r_{11}) \end{bmatrix} \begin{bmatrix} U_i \\ V_i \\ (\mathcal{D}_l U)_i \\ (\mathcal{D}_r V)_i \end{bmatrix} \tag{56}$$

(Again, see Appendix (C) for an estimate of the magnitude of α.)

The first and second (RHS) terms are negative semi-definite based on single domain arguments, whereas the stability of the interface term Υ_i is guaranteed if the matrix M_i is negative semi-definite:

$$\Upsilon_i \; = \; \mathcal{I}_i^T \; M_i \, \mathcal{I}_i \; \leq \; 0. \tag{57}$$

The definiteness of a symmetric matrix is completely determined by the signs its eigenvalues, specifically if the eigenvalues λ_i of the matrix M_i satisfy $\lambda_i \; \leq \; 0 \;\; ; i \; = \; 1, 4$, then M_i is negative semi-definite.

The stability analysis is simplified if M_i is rotated with a similarity transformation. Define the new vector $\hat{\mathcal{I}}_i = \mathcal{S}\mathcal{I}_i$ such that:

$$\hat{\mathcal{I}}_i = \frac{1}{\sqrt{2}} \begin{bmatrix} U_i + V_i \\ U_i - V_i \\ (\mathcal{D}_l U)_i + (\mathcal{D}_r V)_i \\ (\mathcal{D}_l U)_i - (\mathcal{D}_r V)_i \end{bmatrix} = \frac{1}{\sqrt{2}} \begin{bmatrix} 1 & 1 & 0 & 0 \\ 1 & -1 & 0 & 0 \\ 0 & 0 & 1 & 1 \\ 0 & 0 & 1 & -1 \end{bmatrix} \begin{bmatrix} U_i \\ V_i \\ (\mathcal{D}_l U)_i \\ (\mathcal{D}_r V)_i \end{bmatrix} \tag{58}$$

The rotation matrix $\mathcal{S}$ replaces the stability condition given in equation (57) with the following equivalent condition:

$$\mathcal{I}_i^T M^i \mathcal{I}_i \;=\; \mathcal{I}_i^T \mathcal{S}^T \mathcal{S} M_i \mathcal{S}^T \mathcal{S} \mathcal{I}_i \;=\; \hat{\mathcal{I}}_i^T \hat{M}_i \hat{\mathcal{I}}_i \leq 0; \tag{59}$$

where

$$\hat{M}_i \;=\; \begin{bmatrix} 0 & -a + l_{00} - r_{00} & 0 & \epsilon + l_{01} - r_{01} \\ -a + l_{00} - r_{00} & 2(l_{00} + r_{00}) & \epsilon + l_{10} - r_{10} & l_{01} + l_{10} + r_{01} + r_{10} \\ 0 & \epsilon + l_{10} - r_{10} & -((\alpha+\beta)\epsilon) & (-\alpha+\beta)\epsilon + l_{11} - r_{11} \\ \epsilon + l_{01} - r_{01} & l_{01} + l_{10} + r_{01} + r_{10} & (-\alpha+\beta)\epsilon + l_{11} - r_{11} & -((\alpha+\beta)\epsilon) + 2(l_{11} + r_{11}) \end{bmatrix} \tag{60}$$

Every submatrix within $\hat{M}_i$ must be negative semi-definite to ensure the semi-definiteness of $\hat{M}_i$. Specifically, the zero at the (1,1) element of $\hat{M}_i$, forces the first row (and column) to be entirely zero. Thus, the conservation conditions $l_{00} = r_{00} + a$; and $l_{01} = r_{01} - \epsilon$, (equation 47) are necessary conditions for $\mathcal{P}$-norm stability of the interface. Upon substitution, the resultant matrix becomes

$$\hat{M}_i \;=\; \begin{bmatrix} 0 & 0 & 0 & 0 \\ 0 & -2a + 4l_{00} & \epsilon + l_{10} - r_{10} & \epsilon + 2l_{01} + l_{10} + r_{10} \\ 0 & \epsilon + l_{10} - r_{10} & -((\alpha+\beta)\epsilon) & (-\alpha+\beta)\epsilon + l_{11} - r_{11} \\ 0 & \epsilon + 2l_{01} + l_{10} + r_{10} & (-\alpha+\beta)\epsilon + l_{11} - r_{11} & -((\alpha+\beta)\epsilon) + 2(l_{11} + r_{11}) \end{bmatrix} \tag{61}$$

The necessary algebra is greatly simplified if a change of variables is introduced. Defining

$$\begin{aligned} t_1 \;=\; (\epsilon + l_{01} + l_{10}) \quad ; \quad t_2 \;=\; (l_{01} + r_{10}) \\ r_{11} \;=\; \epsilon[(-\alpha + 3\beta)/4 - s_1(\alpha+\beta)] \quad ; \quad l_{11} \;=\; \epsilon[(3\alpha - \beta)/4 - s_2(\alpha+\beta)] \end{aligned} \tag{62}$$

and substituting these new variables into $\hat{M}_i$ yields

$$\hat{M}_i \;=\; \begin{bmatrix} 0 & 0 & 0 & 0 \\ 0 & -2a + 4l_{00} & t_1 - t_2 & t_1 + t_2 \\ 0 & t_1 - t_2 & -[(\alpha+\beta)\epsilon] & [(\alpha+\beta)\epsilon][s_1 - s_2] \\ 0 & t_1 + t_2 & [(\alpha+\beta)\epsilon][s_1 - s_2] & -2[(\alpha+\beta)\epsilon][s_1 + s_2] \end{bmatrix}$$

Sylvester's Theorem can be used to rotate $\hat{M}_i$ into diagonal form without changing the signs of the eigenvalues. Repeated use of the theorem produces the following seven necessary conditions governing negative eigenvalues.

$$-2a + 4l_{00} \;\leq\; 0 \quad ; \quad -[(\alpha+\beta)\epsilon] \;\leq\; 0 \quad ; \quad -2[(\alpha+\beta)\epsilon][s_1 + s_2] \;\leq\; 0$$

$$[-2a + 4l_{00}] \;\leq\; \frac{-(t_1 - t_2)^2}{[(\alpha+\beta)\epsilon]} \quad ; \quad [-2a + 4l_{00}] \;\leq\; \frac{-(t_1 + t_2)^2}{2[(\alpha+\beta)\epsilon][s_1 + s_2]} \quad ; \quad \frac{[s_1 - s_2]^2}{2[s_1 + s_2]} \;\leq\; 1$$

$$-2a + 4l_{00} \quad \leq \quad \frac{-[t_1 + t_2]^2}{2[(\alpha+\beta)\epsilon][s_1 + s_2]} \;-\; \frac{[t_1 - t_2 + \frac{[s_1 - s_2][t_1 + t_2]}{2(s_1 + s_2)}]^2}{(\alpha+\beta)\epsilon[1 - \frac{[s_1 - s_2]^2}{2[s_1 + s_2]}]}$$

Recalling that the variables α, β and ϵ are positive quantities, these seven constraints can be reduced to just three independent inequalities. Thus, the stability of the method is governed by the following three conditions

$$\begin{aligned} 0 \quad &\leq \quad [s_1 + s_2] \\ 0 \quad &\leq \quad 1 \;-\; \frac{[s_1 - s_2]^2}{2[s_1 + s_2]} \\ l_{00} \quad &\leq \quad \frac{a}{2} \;-\; \frac{[t_1 + t_2]^2}{8[(\alpha+\beta)\epsilon][s_1 + s_2]} \;-\; \frac{[t_1 - t_2 + \frac{[s_1 - s_2][t_1 + t_2]}{2(s_1 + s_2)}]^2}{4(\alpha+\beta)\epsilon[1 - \frac{[s_1 - s_2]^2}{2[s_1 + s_2]}]} \end{aligned} \tag{63}$$

Figure 3 shows the admissible parameter space for the variables s_1 and s_2, as determined from the first two inequalities.

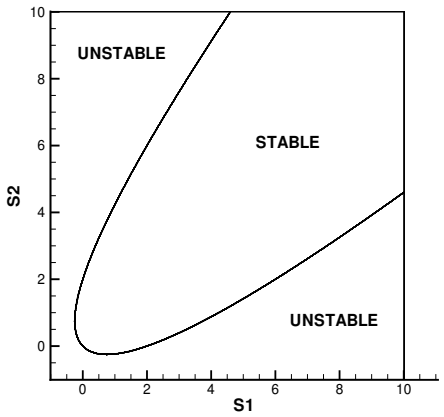

Figure 3: Stability plane for parameters s_1 and s_2.

Written in terms of the original penalty parameters , equation (63) becomes

$$\begin{array}{rcl} [2(r_{11}+l_{11})] & \leq & [(\alpha+\beta)\epsilon] \\ \frac{[\epsilon(-\alpha+\beta)-(r_{11}-l_{11})]^2}{\epsilon(\alpha+\beta)-2(r_{11}+l_{11})} & \leq & [(\alpha+\beta)\epsilon] \\ l_{00} & \leq & \frac{a}{2} - \frac{(\epsilon+2l_{01}+l_{10}+r_{10})^2}{4[\epsilon(\alpha+\beta)-2(r_{11}+l_{11})]} - \frac{\{\epsilon+l_{10}-r_{10}+\frac{[\epsilon(-\alpha+\beta)-(r_{11}-l_{11})](\epsilon+2l_{01}+l_{10}+r_{10})}{[\epsilon(\alpha+\beta)-2(r_{11}+l_{11})]}\}^2}{4\{(\alpha+\beta)\epsilon-\frac{[\epsilon(-\alpha+\beta)-(r_{11}-l_{11})]^2}{[\epsilon(\alpha+\beta)-2(r_{11}+l_{11})]}\}} \end{array} \tag{64}$$

the desired result for the eight parameters that ensures negative semi-definiteness of Υ_i in equation (55).

Finally, integrating equation (55) in time leads to

$$\begin{array}{rcl} \|U(x_l,T)\|^2_{\mathcal{P}_l} + \|V(x_r,T)\|^2_{\mathcal{P}_r} & + & \int_0^T e^{-\eta(t-T)} \{2\,\epsilon\,[\|\mathcal{D}_l\mathbf{U}\|^2_{\bar{\mathcal{P}}_l} + \|\mathcal{D}_r\mathbf{V}\|^2_{\bar{\mathcal{P}}_r}] + BC_d - \Upsilon_i\}dt \\ & = & e^{+\eta T}\{\|f(x_l)\|^2_{\mathcal{P}_l} + \|f(x_r)\|^2_{\mathcal{P}_r} + \int_0^T e^{-\eta t}\,[Data - PosDef_d]dt\} \end{array} \tag{65}$$

Comparing equation (65) with the definition of semi-discrete strong stability [Definition (2)] leads immediately to the desired result. [Consult the single domain case, equations (37) - (44), for the intermediate steps in developing equation (65)]. □

Remark. The stability constraints (48), (49) relate the acceptable values of the parameters l_{11} and r_{11}, relative to the background dissipation inherent in the discretization brought about by the parameters α, β and ϵ.

Remark. Constraint (50) describes the acceptable values of the parameter l_{00}, in terms of l_{01}, l_{10}, l_{11}, r_{10}, and r_{11}. The variables l_{01}, l_{10}, l_{11}, r_{10}, and r_{11} are subject to no explicit stability constraints, but seriously influence the acceptable values of the parameter l_{00} via constraint (48). Stable values of the parameter l_{00} must be strictly less than $a/2$ and become progressively smaller for inappropriate choices of the other five parameters.

Remark. Setting the parameters to the values $l_{11} = r_{11} = 0$ removes from consideration the stability constraints (48), (49), and greatly simplifies constraint (50). This is the original Baumann-Oden formulation.

3.4.3 Pointwise Stability

Equations (44) and (65) describe the temporal evolution of the single- and multi-domain numerical solutions, thereby establishing strong stability of each respective formulation. Groups of numerical solution terms found on the (LHS) of each equation, are dominated by positive and bounded data found on the (RHS). Three distinct groups of terms appear on the (LHS). The groups include the solution terms $\|\mathbf{U}\|^2_{\mathcal{P}_l}$ and $\|\mathbf{V}\|^2_{\mathcal{P}_r}$, the derivative terms $\|\mathcal{D}_l\mathbf{U}\|^2_{\bar{\mathcal{P}}_l}$ and $\|\mathcal{D}_r\mathbf{V}\|^2_{\bar{\mathcal{P}}_r}$, and the boundary/interface terms BC_d and Υ_i. The solution and derivative terms are weakly bounded in $\mathcal{P}$-norms for finite times, while the boundary/interface terms are locally pointwise bounded.

Note that equations (44) and (65) do not establish the pointwise stability of the solution at *interior* gridpoints. To establish interior pointwise boundedness, a discrete Sobolev inequality is required. Appendix (C) provides a proof of

the discrete Sobolev inequality,

$$(U_i)^2 \;\le\; c_1\|\mathbf{U}\|_{\mathcal{P}}^2 \;+\; c_2\|\mathcal{D}\mathbf{U}\|_{\mathcal{P}}^2$$

derived specifically for SBP operators. This inequality, combined with equations (44), or (65), provides the link between $\mathcal{P}$-boundedness of $\mathbf{U}$ and $\mathcal{D}\mathbf{U}$, and pointwise boundedness of the solution over the entire domain, and lead to the following theorem.

Theorem 3 *For any grid function* $\mathbf{U}$ *on* $(0 \le x_j \le l)\,; j = 1, n$*, and a consistent derivative operator* $\mathcal{D}$ *of rank* $n-1$*, then* $\mathcal{P}$*-boundedness of* $\|\mathbf{U}\|_{\mathcal{P}}^2$ *and* $\|\mathcal{D}\mathbf{U}\|_{\mathcal{P}}^2$*, implies a pointwise estimate of the form*

$$\|\mathbf{U}\|_{\infty}^2 \;\le\; (c_{mpm} \;+\; l^{-1})\|\mathbf{U}\|^2 \;+\; {c_{mpm}}^{-1}\|\mathcal{D}\mathbf{U}\|^2 \tag{66}$$

Proof : See Appendix D for the proof of Theorem 3. Extension to two domains is straightforward.

In addition to providing a stronger measure of stability, a pointwise stability estimate can be a necessary condition used in proofs of global accuracy. Indeed, a pointwise estimate is the critical condition used in the work of Svärd and Nordström [38], and in Section **4** of this work, to establish a sharp estimate of global solution accuracy.

3.4.4 Primal Conservation

We are interested in numerical solutions to the 1-D equation in divergence form

$$u_t + f_x = 0, |x| \le 1, t \ge 0 \;\;;\;\; f \;= a\,u \;-\; \epsilon\,u_x \tag{67}$$

where f involves convective and diffusive terms arising from for example the nonlinear Burgers' equation. *Assume* that the discrete solution converges to a function $u(x,t)$. We then ask the question whether this convergent limit function $u(x,t)$ is a weak solution to equation (67) and satisfies

$$\int_{-1}^{1} \Phi(x)u(x)|_0^T dx + \int_0^T \Phi(t)f(t)|_{-1}^{+1} dt = \int_0^T \int_{-1}^{1} [\Phi_t(x,t)u(x,t) + \Phi_x(x,t)f(u(x,t))]dxdt \tag{68}$$

for any smooth function $\Phi(x,t)$.

The definition of conservation for the diffusive terms is somewhat ambiguous. (The original Lax-Wendroff Theorem was presented for the hyperbolic case, not the parabolic case.) For example, using the relation

$$\int_{-1}^{1} \Phi_x(x,t)u_x(x,t)dx \;=\; \int_{-1}^{1} \Phi_{xx}(x,t)u(x,t)dx \;-\; \Phi_x(x,t)u(x,t)|_{-1}^{+1} \tag{69}$$

equation (68) could be further manipulated into the form

$$\int_{-1}^{1} \Phi(x)u(x)|_0^T dx + = \int_0^T \int_{-1}^{1} [(\Phi_t(x,t) + a\,\Phi_x(x,t) + \epsilon\Phi_{xx})\,u(x,t)]dxdt \tag{70}$$

A variant of the classical Lax-Wendroff Theorem is now presented in the context of the SBP formulation defined in equation (46). Special attention is given to the interface conditions, and the diffusive terms.

Theorem 4 *Two conditions are necessary if approximation (46) is to be conservative (in the* $\mathcal{P}$ *norm) across the interface. They are*

$$l_{00} \;=\; r_{00} \;+\; a, \quad l_{01} \;=\; r_{01} \;-\; \epsilon, \tag{71}$$

Proof : Multiplying (46) with $\mathbf{\Phi}_l^T\mathcal{P}_l$ and $\mathbf{\Phi}_r^T\mathcal{P}_r$, (neglecting the farfield boundary terms) leads to

$$\begin{array}{rcrcl}
\mathbf{\Phi}_l^T\mathcal{P}_l\mathbf{U}_t & + & \mathbf{\Phi}_r^T\mathcal{P}_r\mathbf{V}_t & & \\
+\,a[\mathbf{\Phi}_l^T\mathcal{P}_l\mathcal{D}_l\mathbf{U} & + & \mathbf{\Phi}_r^T\mathcal{P}_r\mathcal{D}_r\mathbf{V}] & & \\
-\,\epsilon[\;\mathbf{\Phi}_l^T\mathcal{P}_l\mathcal{D}_l\mathcal{D}_l\mathbf{U} & + & \mathbf{\Phi}_r^T\mathcal{P}_r\mathcal{D}_r\mathcal{D}_r\mathbf{V}] & = & \begin{array}{rcrcl} l_{00} & \Phi_i\,[U_i - V_i] & + & l_{01} & \Phi_i\,[(\mathcal{D}_l U)_i - (\mathcal{D}_r V)_i] \\ + & l_{10}\;(\Phi')_i[U_i - V_i] & + & l_{11} & (\Phi')_i[(\mathcal{D}_l U)_i - (\mathcal{D}_r V)_i] \\ + & r_{00} & \Phi_i\,[V_i - U_i] & + & r_{01}\;\;\Phi_i\,[(\mathcal{D}_r V)_i - (\mathcal{D}_l U)_i] \\ + & r_{10}\;(\Phi')_i[V_i - U_i] & + & r_{11} & (\Phi')_i[(\mathcal{D}_r V)_i - (\mathcal{D}_l U)_i] \end{array}
\end{array} \tag{72}$$

where Φ_i and $(\Phi')_i$ are the values of the test function and its derivative at the interface location x_i. Both are continuous across the interface.

Rearranging the time terms yields

$$\mathbf{\Phi}_l^T \mathcal{P}_l \mathbf{U}_t + \mathbf{\Phi}_r^T \mathcal{P}_r \mathbf{V}_t = \frac{d}{dt}(\mathbf{\Phi}_l^T \mathcal{P}_l \mathbf{U} + \mathbf{\Phi}_r^T \mathcal{P}_r \mathbf{V}) - [(\Phi_l)_t^T \mathcal{P}_l \mathbf{U} + (\Phi_r)_t^T \mathcal{P}_r \mathbf{V}] \tag{73}$$

Making use of the SBP rules (26 - 27) on the advection terms yields

$$\begin{array}{rcccc} \mathbf{\Phi}_l^T \mathcal{P}_l \mathcal{D}_l \mathbf{U} + \mathbf{\Phi}_r^T \mathcal{P}_r \mathcal{D}_r \mathbf{V} & = & -(\mathbf{\Phi'}_l)^T \mathcal{P}_l \mathbf{U} & - & (\mathbf{\Phi'}_r)^T \mathcal{P}_r \mathbf{V} \\ & + & [\Phi U]|_{-1}^{i_-} & + & [\Phi V]|_{i_-}^{+1} \end{array} \tag{74}$$

Again, note the ambiguity in the meaning of conservation for the diffusive terms. Using the SBP rules (26 - 27) once on the diffusion terms yields,

$$\begin{array}{rcccc} \mathbf{\Phi}_l^T \mathcal{P}_l \mathcal{D}_l \mathcal{D}_l \mathbf{U} \, + \, \mathbf{\Phi}_r^T \mathcal{P}_r \mathcal{D}_r \mathcal{D}_r \mathbf{V} & = & -(\Phi'_l)^T \mathcal{P}_l \mathcal{D}_l U) & - & (\Phi'_r)^T \mathcal{P}_r \mathcal{D}_r V) \\ & + & [\Phi_l(\mathcal{D}_l U)]|_{-1}^{i_-} & + & [\Phi_r(\mathcal{D}_r U)]|_{i_+}^{+1} \end{array} \tag{75}$$

while twice yields

$$\begin{array}{rcccc} \mathbf{\Phi}_l^T \mathcal{P}_l \mathcal{D}_l \mathcal{D}_l \mathbf{U} \, + \, \mathbf{\Phi}_r^T \mathcal{P}_r \mathcal{D}_r \mathcal{D}_r \mathbf{V} & = & (\Phi''_l)^T \mathcal{P}_l U) & + & (\Phi''_r)^T \mathcal{P}_r V) \\ & + & [\Phi_l(\mathcal{D}_l U) - (\Phi'_l) U]|_{-1}^{i_-} & + & [\Phi_r(\mathcal{D}_r U) - (\Phi'_r) V]|_{i_+}^{+1} \end{array} \tag{76}$$

Inserting (73), (74) and (75) into (72), yields the condition

$$\begin{array}{rcl} \frac{d}{dt}(\mathbf{\Phi}_l^T \mathcal{P}_l \mathbf{U} + \mathbf{\Phi}_r^T \mathcal{P}_r \mathbf{V}) & & \\ +[\Phi_l(a - \epsilon \mathcal{D}_l) U] \, |_{-1} \, + \, [\Phi_r(a - \epsilon \mathcal{D}_r) V] \, |^{+1} & = & [(\Phi_l)_t^T \mathcal{P}_l \mathbf{U} \, + \, (\Phi_r)_t^T \mathcal{P}_r \mathbf{V}] \\ & + & (\Phi'_l)^T \mathcal{P}_l (a\mathcal{I}_l - \epsilon \mathcal{D}_l) \mathbf{U} \, + \, (\Phi'_r)^T \mathcal{P}_r (a\mathcal{I}_r - \epsilon \mathcal{D}_r) \mathbf{V} \\ & + & \Phi_i (l_{00} \, - r_{00} \, - \, a)(U_i - V_i) \\ & + & \Phi_i (l_{01} \, - r_{01} \, + \, \epsilon)(\mathcal{D}U_i - \mathcal{D}V_i) \\ & + & (\Phi')_i (l_{10} \, - r_{10})(U_i - V_i) \\ & + & (\Phi')_i (l_{11} \, - r_{11})(\mathcal{D}U_i - \mathcal{D}V_i) \end{array} \tag{77}$$

Integrating equation (77) with respect to time, applying the conservation conditions given by equation (71) and the additional conditions $l_{10} = r_{10}$ and $l_{11} = r_{11}$ produces the equation

$$\begin{array}{rcl} (\mathbf{\Phi}_l^T \mathcal{P}_l \mathbf{U} + \mathbf{\Phi}_r^T \mathcal{P}_r \mathbf{V})|_0^T & & \\ + \int_0^T \{[\Phi_l(a - \epsilon \mathcal{D}_l) U] \, |_{-1} \, + \, [\Phi_r(a - \epsilon \mathcal{D}_r) V] \, |^{+1}\} dt & = & \int_0^T [(\Phi_l)_t^T \mathcal{P}_l \mathbf{U} \, + \, (\Phi_r)_t^T \mathcal{P}_r \mathbf{V}] dt \\ & + & \int_0^T \{(\Phi'_l)^T \mathcal{P}_l (a\mathcal{I}_l - \epsilon \mathcal{D}_l) \mathbf{U} \, + \, (\Phi'_r)^T \mathcal{P}_r (a\mathcal{I}_r - \epsilon \mathcal{D}_r) \mathbf{V}\} dt \end{array} \tag{78}$$

which matches the weak solution given by equation (68) term by term, in the limit of infinite spatial resolution. □

Inserting (73), (74) and (76) into (72), yields the condition

$$\begin{array}{rcl} \frac{d}{dt}(\mathbf{\Phi}_l^T \mathcal{P}_l \mathbf{U} + \mathbf{\Phi}_r^T \mathcal{P}_r \mathbf{V}) & & \\ +[\Phi_l(a - \epsilon \mathcal{D}_l) U] \, |_{-1} \, + \, [\Phi_r(a - \epsilon \mathcal{D}_r) V] \, |^{+1} & = & [(\Phi_l)_t^T \mathcal{P}_l \mathbf{U} \, + \, (\Phi_r)_t^T \mathcal{P}_r \mathbf{V}] \\ & + & (\Phi'_l)^T \mathcal{P}_l (a\mathcal{I}_l) \mathbf{U} \, + \, (\Phi'_r)^T \mathcal{P}_r (a\mathcal{I}_r) \mathbf{V} \\ & + & \epsilon (\Phi''_l)^T \mathcal{P}_l \mathbf{U} \, + \, \epsilon (\Phi''_r)^T \mathcal{P}_r \mathbf{V} \, - \, \epsilon [\Phi'_l U \, |_{-1} \, + \, \Phi'_r V \, |^{+1}] \\ & + & \Phi_i (l_{00} \, - r_{00} \, - \, a)(U_i - V_i) \\ & + & \Phi_i (l_{01} \, - r_{01} \, + \, \epsilon)(\mathcal{D}U_i - \mathcal{D}V_i) \\ & + & (\Phi')_i (l_{10} \, - \, r_{10} \, - \, \epsilon)(U_i - V_i) \\ & + & (\Phi')_i (l_{11} \, - \, r_{11})(\mathcal{D}U_i - \mathcal{D}V_i) \end{array} \tag{79}$$

Integrating equation (79) with respect to time, applying the conservation conditions given by equation (71) and the additional conditions $l_{10} = r_{10} + \epsilon$ and $l_{11} = r_{11}$, we see that expression matches the weak form of the advection diffusion equation in the limit of infinite spatial resolution.

Remark. Note that the auxiliary constraints in equations (78) and (79) depend on the definition chosen for conservation. Still another definition (perhaps a linear combination of the two) would have produced a third set of constraints.

3.4.5 A "flux-form" discretization technique

A finite difference approximation of the coupled problem (168) motivated by the Local Discontinuous Galerkin FEM proposed by Cockburn and Shu and referred to as "LDG" [14] is

$$\begin{array}{rcl}
\mathcal{P}_l\mathbf{U}_t \,+\, a\mathcal{P}_l\mathcal{D}_l\mathbf{U} \,-\, \epsilon\mathcal{P}_l\mathcal{D}_l\phi &=& L_{00}[U_i - V_i]\ \mathbf{e_{i_-}} \;+\; L_{01}[(\phi)_i - (\psi)_i]\ \mathbf{e_{i_-}} \\
\epsilon\mathcal{P}_l\,(\phi \,-\, \mathcal{D}_l\mathbf{U}) &=& L_{10}[U_i - V_i]\ \mathbf{e_{i_-}} \;+\; L_{01}[(\phi)_i - (\psi)_i]\ \mathbf{e_{i_-}} \\
\mathbf{U}(x,0) &=& \mathbf{0}. \\
\mathcal{P}_r\mathbf{V}_t \,+\, a\mathcal{P}_r\mathcal{D}_r\mathbf{V} \,-\, \epsilon\mathcal{P}_r\mathcal{D}_r\psi &=& R_{00}[V_i - U_i]\ \mathbf{e_{i_+}} \;+\; R_{01}[(\psi)_i - (\phi)_i]\ \mathbf{e_{i_+}} \\
\epsilon\mathcal{P}_r\,(\psi \,-\, \mathcal{D}_r\mathbf{V}) &=& R_{10}[V_i - U_i]\ \mathbf{e_{i_+}} \;+\; R_{11}[(\psi)_i - (\phi)_i]\ \mathbf{e_{i_+}} \\
\mathbf{V}(x,0) &=& \mathbf{0}.
\end{array} \tag{80}$$

Theorem 5 *The approximation (80) of the problem (168) is strongly stable if the eight parameters are related by the two equalities*

$$L_{00} \,=\, R_{00} \,+\, a \quad ; \quad L_{01} \,=\, R_{01} \,-\, \epsilon \tag{81}$$

and constrained by the following inequalities

$$2[R_{11} + L_{11}] \quad \leq \quad [(\alpha+\beta)\epsilon] \tag{82}$$

$$\frac{[\epsilon(-\alpha+\beta) - (R_{11} - L_{11})]^2}{\epsilon(\alpha+\beta) - 2(R_{11} + L_{11})} \quad \leq \quad [(\alpha+\beta)\epsilon] \tag{83}$$

$$L_{00} \quad \leq \quad \tfrac{a}{2} \,-\, \frac{(\epsilon+2L_{01}+L_{10}+R_{10})^2}{4[\epsilon(\alpha+\beta)-2(R_{11}+L_{11})]} \,-\, \frac{\{\epsilon+L_{10}-R_{10}+\frac{[\epsilon(-\alpha+\beta)-(R_{11}-L_{11})](\epsilon+2L_{01}+L_{10}+R_{10})}{[\epsilon(\alpha+\beta)-2(R_{11}+L_{11})]}\}^2}{4\{(\alpha+\beta)\epsilon-\frac{[\epsilon(-\alpha+\beta)-(R_{11}-L_{11})]^2}{[\epsilon(\alpha+\beta)-2(R_{11}+L_{11})]}\}} \tag{84}$$

where (as with the primal form)

$$\alpha \,=\, \frac{1}{\mathbf{e_{i_-}}^T\ \mathcal{P}_l^{-1}\ \mathbf{e_{i_-}}} \quad ; \quad \beta \,=\, \frac{1}{\mathbf{e_{i_+}}^T\ \mathcal{P}_r^{-1}\ \mathbf{e_{i_+}}}$$

Furthermore, the stability constraints for the LDG scheme are identical to those of the primal scheme although stability is proven in different variables.

Proof : Strong stability of (80) follows if the interface treatment at $x = x_i$ is of a dissipative nature. As we have already established the stability of the farfield boundary penalties we need only focus on the interface terms.

The energy method applied to equation (80) is derived by multiplying the first and second discrete equations in the left subdomain by $\mathbf{U}^T$ and ϕ^T, respectively, and the first and second discrete equations in the right subdomain by $\mathbf{V}^T$ and ψ^T, respectively, and using the relation $Q \,+\, Q^T \,=\, B$ from the SBP rule (27), yields

$$\begin{array}{rcl}
\frac{d}{dt}[\ \|\mathbf{U}\|^2_{\mathcal{P}_l} \,+\, \|\mathbf{V}\|^2_{\mathcal{P}_r}] & & \\
+\,2\epsilon[\ \|\phi\|^2_{\mathcal{P}_l} \,+\, \|\psi\|^2_{\mathcal{P}_r}] &=& [2\,\epsilon U\phi \,-\, a\,U^2]^{i_-}_{-1} \;+\; [2\,\epsilon V\psi \,-\, a\,V^2]^1_{i_+} \\
&+& 2L_{00}\ U_i\,[U_i - V_i] \;+\; 2L_{01}\ U_i\,[(\phi)_i - (\psi)_i] \\
&+& 2L_{10}(\phi)_i[U_i - V_i] \;+\; 2L_{11}(\phi)_i[(\phi)_i - (\psi)_i] \\
&+& 2R_{00}\ V_i\,[V_i - U_i] \;+\; 2R_{01}\ V_i\,[(\psi)_i - (\phi)_i] \\
&+& 2R_{10}(\psi)_i[V_i - U_i] \;+\; 2R_{11}(\psi)_i[(\psi)_i - (\phi)_i]
\end{array} \tag{85}$$

The stability of equation (52) is ensured if all the terms on the (RHS) are negative.

Collecting all the interface contributions into one term, (85) becomes

$$\begin{array}{rcl}
\frac{d}{dt}\left[\|\mathbf{U}\|^2_{\mathcal{P}_l} \,+\, \|\mathbf{V}\|^2_{\mathcal{P}_r}\right] \,+\, 2\epsilon\left[\|\phi\|^2_{\bar{\mathcal{P}}_l} \,+\, \|\psi\|^2_{\bar{\mathcal{P}}_r}\right] &=& \left[2\,\epsilon U\phi \,-\, a\,U^2\right]_{-1} \\
&+& \left[2\,\epsilon V\psi \,-\, a\,V^2\right]^1 \,+\, \Upsilon_i
\end{array} \tag{86}$$

with the interface term $\Upsilon_i \,=\, \mathcal{T}_i^T\, M_i\, \mathcal{T}_i$ defined by

$$\Upsilon_i \;=\; \begin{bmatrix} U_i \\ V_i \\ (\phi)_i \\ (\psi)_i \end{bmatrix}^T \begin{bmatrix} (-a+2L_{00}) & -(L_{00}+R_{00}) & (\epsilon+L_{01}+L_{10}) & -(L_{01}+R_{10}) \\ -(L_{00}+R_{00}) & (+a+2R_{00}) & -(R_{01}+\text{Ł}_{10}) & (-\epsilon+R_{01}+R_{10}) \\ (\epsilon+L_{01}+L_{10}) & -(R_{01}+\text{Ł}_{10}) & -2(\alpha\epsilon+L_{11}) & -(L_{11}+R_{11}) \\ -(L_{01}+R_{10}) & (-\epsilon+R_{01}+R_{10}) & -(L_{11}+R_{11}) & -2(\beta\epsilon+R_{11}) \end{bmatrix} \begin{bmatrix} U_i \\ V_i \\ (\phi)_i \\ (\psi)_i \end{bmatrix} \tag{87}$$

Comparing equation (87) with (56), we see that the stability matrix M_i for the LDG formulation is **identical** to that obtained with the primal formulation. Applying similarity rotations produces an LDG conservation condition

$$L_{00} \;=\; R_{00} \;+\; a \quad ; \quad L_{01} \;=\; R_{01} \;-\; \epsilon, \tag{88}$$

Manipulating the matrix M_i, (exactly as in the primal formulation), yields the stability inequalities

$$\begin{array}{rcl} 0 & \leq & [S_1+S_2] \\ 0 & \leq & 1 \;-\; \frac{[S_1-S_2]^2}{2[S_1+S_2]} \\ L_{00} & \leq & \frac{a}{2} \;-\; \frac{[T_1+T_2]^2}{8[(\alpha+\beta)\epsilon][S_1+S_2]} \;-\; \frac{[T_1-T_2+\frac{[S_1-S_2][T_1+T_2]}{2(S_1+S_2)}]^2}{4(\alpha+\beta)\epsilon[1-\frac{[S_1-S_2]^2}{2[S_1+S_2]}]} \end{array} \tag{89}$$

Figure 3 again shows the admissible parameter space for the LDG variables S_1 and S_2. Thus, the LDG and primal stability conditions are identical. Transforming equation (89) back to the original variables $L_{00}-R_{11}$ yields the desired result for the eight parameters that ensures negative semi-definiteness of Υ_i in equation (86).

Finally, integrating equation (86) in time leads to

$$\begin{array}{rcl} \|U(x_l,T)\|^2_{\mathcal{P}_l} \;+\; \|V(x_r,T)\|^2_{\mathcal{P}_r} & + & \int_0^T e^{-\eta(t-T)} \{2\,\epsilon\,[\|\mathbf{\Phi}\|^2_{\bar{\mathcal{P}}_l} \;+\; \|\mathbf{\Psi}\|^2_{\bar{\mathcal{P}}_r}] \;+\; BC_d \;-\; \Upsilon_i\} dt \\ & = & e^{+\eta T}\{\|f(x_l)\|^2_{\mathcal{P}_l} \;+\; \|f(x_r)\|^2_{\mathcal{P}_r} \;+\; \int_0^T e^{-\eta t}\,[Data \;-\; PosDef_d] dt\} \end{array} \tag{90}$$

Comparing equation (90) with the definition of semi-discrete strong stability [Definition (2)] leads immediately to the desired result. □

Remark. Although the stability boundaries for the eight interface parameters are identical for the primal and LDG schemes, as are the norms used in both cases, the two methods are stable in different diffusive variables.

Remark. As with the primal formulation, the stability constraints (82,83) strongly constrain the acceptable values of the parameters L_{11} and R_{11}, as compared to the background dissipation inherent in the discretization. The constraint (84) describes the acceptable values of the parameter L_{00}, in terms of L_{01}, L_{10}, L_{11}, R_{10}, and R_{11}. The variables L_{01}, L_{10}, L_{11}, R_{10}, and R_{11} are subject to no explicit stability constraints, but seriously influence the acceptable values of the parameter L_{00} via constraint (84).

Remark. As with the primal formulation, a proof of pointwise stability is achieved using a Sobolev inequality. We state without proof, the following theorem.

Theorem 6 *For any grid function* $\mathbf{U}$ *on* $(0 \leq x_j \leq l)\,; j = 1, n$*, and a consistent derivative operator* $\mathcal{D}$ *of rank* $n-1$*, then* $\mathcal{P}$*-boundedness of* $\|\mathbf{U}\|^2_{\mathcal{P}}$ *and* $\|\mathbf{\Phi}\|^2_{\mathcal{P}}$*, implies a pointwise estimate of the form*

$$\|\mathbf{U}\|^2_{\infty} \;\leq\; (c_{mpm} \;+\; l^{-1})\|\mathbf{U}\|^2 \;+\; {c_{mpm}}^{-1}\|\mathbf{\Phi}\|^2 \tag{91}$$

Proof : See Appendix D for the proof of theorem 6. Extension to two domains is straightforward.

3.4.6 LDG Conservation

Again, we are interested in accurate numerical solutions to 1-D divergence equations of a form consistent with that of equation (67). We then ask the question whether the convergent limit function $u(x,t)$ is a weak solution to equation (67) and satisfies equation (68). The convective terms at the interface in the LDG formulation are penalized the same as in the primal formulation. It is reasonable to expect the necessary conservation conditions to be the same in the two formulations. The diffusive interface terms are very different between the two formulations. We now prove the conservation theorem in the LDG formulations.

Theorem 7 *Two conditions are necessary if approximation (80) is to be conservative (in the $\mathcal{P}$ norm) across the interface. They are*

$$L_{00} \;=\; R_{00} \;+\; a, \quad L_{01} \;=\; R_{01} \;-\; \epsilon, \tag{92}$$

Proof : Multiplying (80) with $\mathbf{\Phi}_l^T\mathcal{P}_l$ and $\mathbf{\Phi}_r^T\mathcal{P}_r$, (neglecting the physical boundary terms) and rearranging terms [using the SBP rules (26 - 27)] leads to

$$\begin{array}{rcccc} \mathbf{\Phi}_l^T\mathcal{P}_l\mathcal{D}_l\phi \;+\; \mathbf{\Phi}_r^T\mathcal{P}_r\mathcal{D}_r\psi & = & -(\Phi_l')^T\mathcal{P}_l\phi) & - & (\Phi_r')^T\mathcal{P}_r\psi) \\ & & + \quad [\Phi_l(\phi)]|_{-1}^{i_-} & + & [\Phi_r(\psi)]|_{i_+}^{+1} \end{array} \tag{93}$$

Φ_i is the value of the test function at the interface location x_i, and it is continuous across the interface.

Manipulating (73), (74) and (93) yields the condition

$$\begin{array}{rcl} \frac{d}{dt}(\mathbf{\Phi}_l^T\mathcal{P}_l\mathbf{U} + \mathbf{\Phi}_r^T\mathcal{P}_r\mathbf{V}) & = & [(\Phi_l)_t^T\mathcal{P}_l\mathbf{U} \;+\; (\Phi_r)_t^T\mathcal{P}_r\mathbf{V}] \\ & + & (\Phi'_l)^T\mathcal{P}_l[(a\mathbf{U} - \epsilon\phi) \;-\; \epsilon\,\mathbf{U}] \;+\; (\Phi'_r)^T\mathcal{P}_r[(a\mathbf{V} - \epsilon\psi) \;-\; \epsilon\,\mathbf{V}] \\ & + & \Phi_l[(-aU + \epsilon\phi) - \epsilon U]\,|_{-1} \;+\; \Phi_r[(-aV + \epsilon\psi) - \epsilon V]\,|_{+1} \\ & + & \Phi_i(L_{00} \;- R_{00} \;-\; a \;+\; \epsilon \;+\; L_{10} \;-\; R_{10})(U_i - V_i) \\ & + & \Phi_i(L_{01} \;- R_{01} \;+\; \epsilon \qquad + \; L_{11} \;-\; R_{11})(\phi_i - \psi_i) \end{array} \tag{94}$$

Integrating equation (94) with respect to time, applying the conservation conditions given by equation (92) and the additional conditions $L_{10} = R_{10} - \epsilon$ and $L_{11} = R_{11}$ produces the equation

$$\begin{array}{rcl} (\mathbf{\Phi}_l^T\mathcal{P}_l\mathbf{U} + \mathbf{\Phi}_r^T\mathcal{P}_r\mathbf{V})|_0^T & & \\ + \int_0^T\{[\Phi_l(a - \epsilon\mathcal{D}_l)U]\,|_{-1} \;+\; [\Phi_r(a - \epsilon\mathcal{D}_r)V]\,|^{+1}\}dt & = & \int_0^T[(\Phi_l)_t^T\mathcal{P}_l\mathbf{U} \;+\; (\Phi_r)_t^T\mathcal{P}_r\mathbf{V}]dt \\ & + & \int_0^T\{(\Phi'_l)^T\mathcal{P}_l(a\mathcal{I}_l - \epsilon\mathcal{D}_l)\mathbf{U} \;+\; (\Phi'_r)^T\mathcal{P}_r(a\mathcal{I}_r - \epsilon\mathcal{D}_r)\mathbf{V}\}dt \end{array} \tag{95}$$

which matches the weak solution given by equation (68) term by term, in the limit of infinite spatial resolution. □

Remark. Only one set of constraint equations results from the conservation condition in the flux formulation. Further, the constraints are different than those obtained by either definition of conservation in the primal form.

3.5 Relating the Primal and Flux Formulations

One can imagine the possible existence of other formulations in addition to the primal and flux collocation formulations. On the other hand, one might also imagine that both are equivalent (as shown in FEM by Arnold et al [3]) with an appropriate change of interface variables. We begin by showing that the LDG formulation can be implemented in terms of the primal scheme if specific values of the interface parameters are used.

Theorem 8 *The LDG interface parameters L_{00} - R_{11} are related to the primal interface parameters l_{00} - r_{11} by the following relations:*

$$\begin{array}{rcccccccc} l_{00} & = & L_{00} & + & L_{01}c_1 & + & \frac{L_{10}}{\alpha} & + & \frac{L_{11}c_1}{\alpha} \\ l_{01} & = & 0 & + & L_{01}c_2 & + & 0 & + & \frac{L_{11}c_2}{\alpha} \\ l_{10} & = & 0 & + & 0 & - & L_{10} & - & L_{11}c_1 \\ l_{11} & = & 0 & + & 0 & + & 0 & - & L_{11}c_2 \\ r_{00} & = & R_{00} & + & R_{01}c_1 & - & \frac{R_{10}}{\beta} & - & \frac{R_{11}c_1}{\beta} \\ r_{01} & = & 0 & + & R_{01}c_2 & + & 0 & - & \frac{R_{11}c_2}{\beta} \\ r_{10} & = & 0 & + & 0 & - & R_{10} & - & R_{11}c_1 \\ r_{11} & = & 0 & + & 0 & + & 0 & - & R_{11}c_2 \end{array} \tag{96}$$

with

$$c_1 \;=\; \frac{\frac{1}{\epsilon}(\frac{L_{10}}{\alpha} + \frac{R_{10}}{\beta})}{1 - \frac{1}{\epsilon}(\frac{L_{11}}{\alpha} + \frac{R_{11}}{\beta})} \quad ; \quad c_2 \;=\; \frac{1}{1 - \frac{1}{\epsilon}(\frac{L_{11}}{\alpha} + \frac{R_{11}}{\beta})} \tag{97}$$

Proof : The LDG two-domain formulation is given in equation (80). Solving equation (80) for ϕ and ψ yields the expressions

$$\begin{array}{rcl} \phi & = & \mathcal{D}_l\mathbf{U} + \frac{1}{\epsilon}\mathcal{P}_l^{-1}\{L_{10}[U_i - V_i]\ \mathbf{e_{i_-}} + L_{11}[(\phi)_i - (\psi)_i]\ \mathbf{e_{i_-}}\} \\ \psi & = & \mathcal{D}_r\mathbf{V} + \frac{1}{\epsilon}\mathcal{P}_r^{-1}\{R_{10}[V_i - U_i]\ \mathbf{e_{i_+}} + R_{11}[(\psi)_i - (\phi)_i]\ \mathbf{e_{i_+}}\} \end{array} \tag{98}$$

while, solving equation (98) for the interface values yields the expressions

$$\begin{array}{rcl} \phi_i = \mathbf{e_{i_-}}^T\phi & = & (\mathcal{D}_l\mathbf{U})|_i + \frac{1}{\epsilon\alpha}\{L_{10}[U_i - V_i] + L_{11}[(\phi)_i - (\psi)_i]\} \\ \psi_i = \mathbf{e_{i_+}}^T\psi & = & (\mathcal{D}_r\mathbf{V})|_i + \frac{1}{\epsilon\beta}\{R_{10}[V_i - U_i] + R_{11}[(\psi)_i - (\phi)_i]\} \end{array} \tag{99}$$

with the difference being

$$\phi_i - \psi_i = (\mathcal{D}_l\mathbf{U})|_i - (\mathcal{D}_r\mathbf{V})|_i + \tfrac{1}{\epsilon}(\tfrac{L_{10}}{\alpha} + \tfrac{R_{10}}{\beta})[U_i - V_i] + \tfrac{1}{\epsilon}(\tfrac{L_{11}}{\alpha} + \tfrac{R_{11}}{\beta})[\phi_i - \psi_i] \tag{100}$$

Rewriting equation (100) in terms of the difference $\phi_i - \psi_i$ yields

$$\begin{array}{rcl} \phi_i - \psi_i = c_1[U_i - V_i] & + & c_2\left[(\mathcal{D}_l\mathbf{U})|_i - (\mathcal{D}_r\mathbf{V})|_i\right] \\ c_1 = \frac{\frac{1}{\epsilon}(\frac{L_{10}}{\alpha} + \frac{R_{10}}{\beta})}{1 - \frac{1}{\epsilon}(\frac{L_{11}}{\alpha} + \frac{R_{11}}{\beta})} & ; & c_2 = \frac{1}{1 - \frac{1}{\epsilon}(\frac{L_{11}}{\alpha} + \frac{R_{11}}{\beta})} \end{array} \tag{101}$$

Substituting equations (98), (99) and (101) back into the original LDG formulation [equation (80)] yields the expression

$$\begin{array}{rcll} \mathcal{P}_l\mathbf{U}_t + a\mathcal{P}_l\mathcal{D}_l\mathbf{U} & = & \epsilon\mathcal{P}_l\mathcal{D}_l\mathcal{D}_l\mathbf{U} & \\ & + & \{L_{00}[U_i - V_i] + L_{01}(c_1[U_i - V_i] + c_2[(\mathcal{D}_l\mathbf{U})|_i - (\mathcal{D}_r\mathbf{V})|_i])\} & \mathcal{I}_l\ \mathbf{e_{i_-}} \\ & + & \{L_{10}[U_i - V_i] + L_{11}(c_1[U_i - V_i] + c_2[(\mathcal{D}_l\mathbf{U})|_i - (\mathcal{D}_r\mathbf{V})|_i])\} & \mathcal{P}_l\mathcal{D}_l\mathcal{P}_l^{-1}\mathbf{e_{i_-}} \\ \mathcal{P}_r\mathbf{V}_t + a\mathcal{P}_r\mathcal{D}_r\mathbf{V} & = & \epsilon\mathcal{P}_r\mathcal{D}_r\mathcal{D}_r\mathbf{V} & \\ & + & \{R_{00}[V_i - U_i] + R_{01}(c_1[V_i - U_i] + c_2[(\mathcal{D}_r\mathbf{V})|_i - (\mathcal{D}_r\mathbf{U})|_i])\} & \mathcal{I}_r\ \mathbf{e_{i_+}} \\ & + & \{R_{10}[V_i - U_i] + R_{11}(c_1[V_i - U_i] + c_2[(\mathcal{D}_r\mathbf{V})|_i - (\mathcal{D}_r\mathbf{U})|_i])\} & \mathcal{P}_r\mathcal{D}_r\mathcal{P}_r^{-1}\mathbf{e_{i_+}} \end{array} \tag{102}$$

Simplifying equation (102) using the relations

$$\begin{array}{rcl} \mathcal{P}_l\mathcal{D}_l\mathcal{P}_l^{-1}\mathbf{e_{i_-}} & = & -\mathcal{D}_l^T\mathbf{e_{i_-}} + \frac{1}{\alpha}\mathbf{e_{i_-}} \\ \mathcal{P}_r\mathcal{D}_r\mathcal{P}_r^{-1}\mathbf{e_{i_+}} & = & -\mathcal{D}_r^T\mathbf{e_{i_-}} - \frac{1}{\beta}\mathbf{e_{i_+}} \end{array}$$

yields

$$\begin{array}{rcl} \mathcal{P}_l\mathbf{U}_t + a\mathcal{P}_l\mathcal{D}_l\mathbf{U} - \epsilon\mathcal{P}_l\mathcal{D}_l\mathcal{D}_l\mathbf{U} & = & \left[\begin{array}{cc} L_{00} & + L_{01}c_1 \\ \frac{L_{10}}{\alpha} & + \frac{L_{11}c_1}{\alpha} \end{array}\right] [U_i - V_i]\ \mathcal{I}_l\ \mathbf{e_{i_-}} \\ & + & \left[\begin{array}{cc} 0 & + L_{01}c_2 \\ 0 & + \frac{L_{11}c_2}{\alpha} \end{array}\right] [(\mathcal{D}_l\mathbf{U})|_i - (\mathcal{D}_r\mathbf{V})|_i]\ \mathcal{I}_l\ \mathbf{e_{i_-}} \\ & + & \left[\begin{array}{cc} 0 & + 0 \\ -L_{10} & - L_{11}c_1 \end{array}\right] [U_i - V_i]\ \mathcal{D}_l^T\mathbf{e_{i_-}} \\ & + & \left[\begin{array}{cc} 0 & + 0 \\ 0 & - L_{11}c_2 \end{array}\right] [(\mathcal{D}_l\mathbf{U})|_i - (\mathcal{D}_r\mathbf{V})|_i]\ \mathcal{D}_l^T\mathbf{e_{i_-}} \\ \mathcal{P}_r\mathbf{V}_t + a\mathcal{P}_r\mathcal{D}_r\mathbf{V} - \epsilon\mathcal{P}_r\mathcal{D}_r\mathcal{D}_r\mathbf{V} & = & \left[\begin{array}{cc} R_{00} & + R_{01}c_1 \\ -\frac{R_{10}}{\beta} & - \frac{R_{11}c_1}{\beta} \end{array}\right] [V_i - U_i]\ \mathcal{I}_r\ \mathbf{e_{i_+}} \\ & + & \left[\begin{array}{cc} 0 & + R_{01}c_2 \\ 0 & - \frac{R_{11}c_2}{\beta} \end{array}\right] [(\mathcal{D}_r\mathbf{V})|_i - (\mathcal{D}_r\mathbf{U})|_i]\ \mathcal{I}_r\ \mathbf{e_{i_+}} \\ & + & \left[\begin{array}{cc} 0 & + 0 \\ -R_{10} & - R_{11}c_1 \end{array}\right] [V_i - U_i]\ \mathcal{D}_r^T\mathbf{e_{i_+}} \\ & + & \left[\begin{array}{cc} 0 & + 0 \\ 0 & - R_{11}c_2 \end{array}\right] [(\mathcal{D}_r\mathbf{V})|_i - (\mathcal{D}_r\mathbf{U})|_i]\ \mathcal{D}_r^T\mathbf{e_{i_+}} \end{array} \tag{103}$$

Comparing equation (103) with the original primal scheme given in equation (46) gives the desired result. □

Remark. Note that the primal coefficients are *not* constants, but rather change with grid resolution. For example, the new parameter

$$l_{00} = L_{00} + L_{01}c_1 + \frac{L_{10}}{\alpha} + \frac{L_{11}c_1}{\alpha}$$

given in equation (96) is inversely proportional to the grid spacing Δx since $\alpha \propto \Delta x$, and becomes larger as the grid is refined.

It is reasonable to ask whether the stability constraints (48) and (49) for the primal method are preserved for methods satisfying the LDG stability constraints (82) and (83).

Theorem 9 *Stability (in the $\mathcal{P}$-norm) in the LDG variables is a sufficient condition for stability (in the $\mathcal{P}$-norm) in the primal variables.*

Proof : We begin by assuming that the LDG variables $L_{00} \rightarrow R_{11}$ are chosen such that the conservation conditions given by equation (88) are satisfied

$$L_{00} = R_{00} + a, \quad L_{01} = R_{01} - \epsilon,$$

that values of the parameters S_1 and S_2 satisfy the constraint equations (89)

$$0 \leq [S_1 + S_2] \quad ; \quad \tfrac{[S_1-S_2]^2}{2[S_1+S_2]} \leq 1$$

and

$$L_{00} \leq \frac{a}{2} - \frac{[T_1+T_2]^2}{8[(\alpha+\beta)\epsilon][S_1+S_2]} - \frac{\left[T_1 - T_2 + \frac{[S_1-S_2][T_1+T_2]}{2(S_1+S_2)}\right]^2}{4(\alpha+\beta)\epsilon[1-\frac{[S_1-S_2]^2}{2[S_1+S_2]}]}$$

Substitution of the transformation relations given by equation (96) into the primal conservations conditions $l_{00} = r_{00} + a$; and $l_{01} = r_{01} - \epsilon$, yields the conservation equations based on the LDG variables;

$$\begin{array}{rcl} l_{00} - r_{00} - a = 0 & \rightarrow & (L_{00} - R_{00} - a) + \frac{4(\alpha R_{10}+\beta L_{10})(L_{01}-R_{01}+\epsilon)}{\epsilon[(\alpha-\beta)^2+4(\alpha+\beta)(\alpha S_1+\beta S_2)]} = 0 \\ l_{01} - r_{01} + \epsilon = 0 & \rightarrow & \frac{4(\alpha\beta)(L_{01}-R_{01}+\epsilon)}{[(\alpha-\beta)^2+4(\alpha+\beta)(\alpha S_1+\beta S_2)]} = 0 \end{array} \tag{104}$$

while substitution of the transformation relations given by equation (96) into the primal and the stability constraints given by equation (63) or equation (64) yields the stability equations based on the LDG variables;

$$\begin{array}{rcl} 0 \leq [s_1+s_2] & \rightarrow & 0 \leq \frac{2[\alpha^2(1+4S_1)-\beta^2(1+4S_2)]^2+64\alpha^2\beta^2[S_1+S_2][1-\frac{(S_1-S_2)^2}{2(S_1+S_2)}]}{[2((\alpha-\beta)^2+4(\alpha+\beta)(\alpha S_1+\beta S_2))]^2} \\ 0 \leq [1-\frac{(s_1-s_2)^2}{2(s_1+s_2)}] & \rightarrow & 0 \leq \frac{32\alpha^2\beta^2[S_1+S_2][1-\frac{(S_1-S_2)^2}{2(S_1+S_2)}]}{[\alpha^2(1+4S_1)-\beta^2(1+4S_2)]^2} \end{array} \tag{105}$$

and

$$\begin{array}{rcl} l_{00} \leq \frac{a}{2} - \frac{[t_1+t_2]^2}{8[(\alpha+\beta)\epsilon][s_1+s_2]} - \frac{[t_1-t_2+\frac{[s_1-s_2][t_1+t_2]}{2(s_1+s_2)}]^2}{4(\alpha+\beta)\epsilon[1-\frac{[s_1-s_2]^2}{2[s_1+s_2]}]} \\ \rightarrow \\ L_{00} \leq \frac{a}{2} - \frac{[T_1+T_2]^2}{8[(\alpha+\beta)\epsilon][S_1+S_2]} - \frac{[T_1-T_2+\frac{[S_1-S_2][T_1+T_2]}{2(S_1+S_2)}]^2}{4(\alpha+\beta)\epsilon[1-\frac{[S_1-S_2]^2}{2[S_1+S_2]}]} \end{array} \tag{106}$$

Thus, if the original scheme written in the LDG variables satisfies the required conservation and stability constraints, then it also satisfies the corresponding conservation and stability constraints written in the primal variables. □

4 Generalized Penalties

Equation (46) presents a new procedure, (Baumann-Oden FEM), for imposing penalties at the interface between two subdomains or elements. The penalties are constructed from precise combinations of "jumps" in the solution and first derivative across the interface. Note, however, that in general, penalties could be constructed from any smooth quantity that spans the interface. Thus, reasonable candidates for penalties include the solution and its first p derivatives.

A semidiscretization of equation (30) that includes penalties on the solution and the first two derivatives written for the two domain problem (in BO form) is

$$\begin{aligned}
\mathcal{P}_l\mathbf{U}_t + a\mathcal{P}_l\mathcal{D}_l\mathbf{U} &= \epsilon\mathcal{P}_l\mathcal{D}_l\mathcal{D}_l\mathcal{D}_l\mathbf{U} \\
&+ \{l_{00}[U_i - V_i] + l_{01}[(\mathcal{D}_l^1 U)_i - (\mathcal{D}_r^1 V)_i] + l_{02}[(\mathcal{D}_l^2 U)_i - (\mathcal{D}_r^2 V)_i]\}\,[\mathcal{I}_l]^T\mathbf{e}_{\mathbf{i}_-} \\
&+ \{l_{10}[U_i - V_i] + l_{11}[(\mathcal{D}_l^1 U)_i - (\mathcal{D}_r^1 V)_i] + l_{12}[(\mathcal{D}_l^2 U)_i - (\mathcal{D}_r^2 V)_i]\}\,[\mathcal{D}_l]^T\mathbf{e}_{\mathbf{i}_-} \\
&+ \{l_{20}[U_i - V_i] + l_{21}[(\mathcal{D}_l^1 U)_i - (\mathcal{D}_r^1 V)_i] + l_{22}[(\mathcal{D}_l^2 U)_i - (\mathcal{D}_r^2 V)_i]\}\,[\mathcal{D}_l^2]^T\mathbf{e}_{\mathbf{i}_-} \\
&- \{\sigma_{-1}(L_{-1}^D(\mathbf{U}))\mathbf{e}_{-1}\} \\
\mathbf{U}(x,0) &= \mathbf{0}. \\
\mathcal{P}_r\mathbf{V}_t + a\mathcal{P}_r\mathcal{D}_r\mathbf{V} &= \epsilon\mathcal{P}_r\mathcal{D}_r\mathcal{D}_r\mathcal{D}_r\mathbf{V} \\
&+ \{r_{00}[V_i - U_i] + r_{01}[(\mathcal{D}_r^1 V)_i - (\mathcal{D}_l^1 U)_i] + r_{02}[(\mathcal{D}_r^2 V)_i - (\mathcal{D}_l^2 U)_i]\}\,[\mathcal{I}_r]^T\mathbf{e}_{\mathbf{i}_+} \\
&+ \{r_{10}[V_i - U_i] + r_{11}[(\mathcal{D}_r^1 V)_i - (\mathcal{D}_l^1 U)_i] + r_{12}[(\mathcal{D}_r^2 V)_i - (\mathcal{D}_l^2 U)_i]\}\,[\mathcal{D}_r]^T\mathbf{e}_{\mathbf{i}_+} \\
&+ \{r_{20}[V_i - U_i] + r_{21}[(\mathcal{D}_r^1 V)_i - (\mathcal{D}_l^1 U)_i] + r_{22}[(\mathcal{D}_r^2 V)_i - (\mathcal{D}_l^2 U)_i]\}\,[\mathcal{D}_r^2]^T\mathbf{e}_{\mathbf{i}_+} \\
&- \{\sigma_{+1}(L_{+1}^D(\mathbf{V}))\mathbf{e}_{+1}\} \\
\mathbf{V}(x,0) &= \mathbf{0}.
\end{aligned} \tag{107}$$

4.1 Stability

Theorem 10 *The approximation (107) of the problem (30) is strongly stable if the eighteen parameters are related by the six equalities*

$$\begin{gathered}
l_{00} \;=\; r_{00} \;+\; a \quad ; \quad l_{01} \;=\; r_{01} \;-\; \epsilon \\
r_{02} \;=\; l_{02} \quad ; \quad r_{20} \;=\; l_{20} \quad ; \quad r_{21} \;=\; l_{21} \quad ; \quad r_{22} \;=\; l_{22}
\end{gathered} \tag{108}$$

and constrained by the following inequalities

$$2[r_{11} + l_{11}] \quad \leq \quad [(\alpha+\beta)\epsilon] \tag{109}$$

$$\frac{[\epsilon(-\alpha+\beta) - (r_{11} - l_{11})]^2}{\epsilon(\alpha+\beta) - 2(r_{11}+l_{11})} \quad \leq \quad [(\alpha+\beta)\epsilon] \tag{110}$$

$$l_{22} \quad \leq \quad -\frac{(+2r_{21}+r_{12}+l_{12})^2}{4[\epsilon(\alpha+\beta)-2(r_{11}+l_{11})]} \;-\; \frac{\{(l_{12}-r_{12})+\frac{[\epsilon(-\alpha+\beta)-(r_{11}-l_{11})](+2r_{21}+r_{12}+l_{12})}{[\epsilon(\alpha+\beta)-2(r_{11}+l_{11})]}\}^2}{4\{[(\alpha+\beta)\epsilon]-\frac{[\epsilon(-\alpha+\beta)-(r_{11}-l_{11})]^2}{[\epsilon(\alpha+\beta)-2(r_{11}+l_{11})]}\}} \tag{111}$$

$$\begin{aligned}
l_{00} \quad \leq \quad & \frac{a}{2} \;-\; \frac{[t_1+t_2]^2}{8[(\alpha+\beta)\epsilon][s_1+s_2]} \;-\; \frac{[t_1-t_2+\frac{[s_1-s_2][t_1+t_2]}{2(s_1+s_2)}]^2}{4(\alpha+\beta)\epsilon[1-\frac{[s_1-s_2]^2}{2[s_1+s_2]}]} \\
& - \frac{\{2\,x_1 + \frac{(t_1+t_2)(y_1+y_2)}{2(\alpha+\beta)\epsilon(s_1+s_2)} + \frac{[t_1-t_2+\frac{(s_1-s_2)(t_1+t_2)}{2(s_1+s_2)}][y_1-y_2+\frac{(s_1-s_2)(y_1+y_2)}{2(s_1+s_2)}]}{4(\alpha+\beta)\epsilon[1-\frac{[s_1-s_2]^2}{2[s_1+s_2]}]}\}^2}{-4\{l_{22} + \frac{[y_1+y_2]^2}{8[(\alpha+\beta)\epsilon][s_1+s_2]} + \frac{[y_1-y_2+\frac{[s_1-s_2][y_1+y_2]}{2(s_1+s_2)}]^2}{4(\alpha+\beta)\epsilon[1-\frac{[s_1-s_2]^2}{2[s_1+s_2]}]}\}}
\end{aligned} \tag{112}$$

with

$$\begin{gathered}
t_1 \;=\; (\epsilon + l_{01} + l_{10}) \quad ; \quad t_2 \;=\; (l_{01} + r_{10}) \\
r_{11} \;=\; \epsilon[(-\alpha+3\beta)/4 - s_1(\alpha+\beta)] \quad ; \quad l_{11} \;=\; \epsilon[(3\alpha-\beta)/4 - s_2(\alpha+\beta)], \\
x_1 \;=\; (r_{20} + l_{02}) \quad ; \quad y_1 \;=\; (l_{12} + r_{21})\,;\; y_2 \;=\; (r_{12} + r_{21})
\end{gathered} \tag{113}$$

and once again

$$\alpha \;=\; \frac{1}{\mathbf{e}_{\mathbf{i}_-}{}^T\;\mathcal{P}_l^{-1}\;\mathbf{e}_{\mathbf{i}_-}} \quad ; \quad \beta \;=\; \frac{1}{\mathbf{e}_{\mathbf{i}_+}{}^T\;\mathcal{P}_r^{-1}\;\mathbf{e}_{\mathbf{i}_+}} \tag{114}$$

Proof : Strong stability of (107) follows if the interface treatment at $x = x_i$ is of a dissipative nature. As we have already established the stability of the farfield boundary penalties we need only focus on the interface terms.

The energy method applied to equation (107) by multiplying the discrete equations in the left and right subdomains by $\mathbf{U}^T$ and $\mathbf{V}^T$ respectively, yield

$$\begin{aligned}
\mathbf{U}^T\mathcal{P}_l\tfrac{d}{dt}\mathbf{U}+\mathbf{V}^T\mathcal{P}_r\tfrac{d}{dt}\mathbf{V} &= -a[\mathbf{U}^T\mathcal{Q}_l\mathbf{U}+\mathbf{V}^T\mathcal{Q}_r\mathbf{V}]+\epsilon[\ \mathbf{U}^T\mathcal{Q}_l\mathcal{D}_l\mathbf{U}+\mathbf{V}^T\mathcal{Q}_r\mathcal{D}_r\mathbf{V}]\\
&+ U_i\{l_{00}[U_i-V_i]+l_{01}[(\mathcal{D}_lU)_i-(\mathcal{D}_rV)_i]+l_{02}[(\mathcal{D}_l^2U)_i-(\mathcal{D}_r^2V)_i]\}\\
&+ (\mathcal{D}_l^1U)_i\{l_{10}[U_i-V_i]+l_{11}[(\mathcal{D}_lU)_i-(\mathcal{D}_rV)_i]+l_{12}[(\mathcal{D}_l^2U)_i-(\mathcal{D}_r^2V)_i]\}\\
&+ (\mathcal{D}_l^2U)_i\{l_{20}[U_i-V_i]+l_{21}[(\mathcal{D}_lU)_i-(\mathcal{D}_rV)_i]+l_{22}[(\mathcal{D}_l^2U)_i-(\mathcal{D}_r^2V)_i]\}\\
&+ V_i\{r_{00}[V_i-U_i]+r_{01}[(\mathcal{D}_rV)_i-(\mathcal{D}_lU)_i]+r_{02}[(\mathcal{D}_r^2V)_i-(\mathcal{D}_l^2U)_i]\}\\
&+ (\mathcal{D}_r^1V)_i\{r_{10}[V_i-U_i]+r_{11}[(\mathcal{D}_rV)_i-(\mathcal{D}_lU)_i]+r_{12}[(\mathcal{D}_r^2V)_i-(\mathcal{D}_l^2U)_i]\}\\
&+ (\mathcal{D}_r^2V)_i\{r_{20}[V_i-U_i]+r_{21}[(\mathcal{D}_rV)_i-(\mathcal{D}_lU)_i]+r_{22}[(\mathcal{D}_r^2V)_i-(\mathcal{D}_l^2U)_i]\}
\end{aligned} \tag{115}$$

Using the relation $Q+Q^T=B$ from the SBP rule (27), borrowing a small portion of the $\|\mathcal{D}_l\mathbf{U}\|_{\mathcal{P}_l}$ and $\|\mathcal{D}_r\mathbf{V}\|_{\mathcal{P}_r}$ terms arising at the interface, and collecting all the interface contributions into one term, equation (115) becomes

$$\begin{aligned}
\tfrac{d}{dt}\left[\|\mathbf{U}\|^2_{\mathcal{P}_l}+\|\mathbf{V}\|^2_{\mathcal{P}_r}\right]+2\epsilon\left[\|\mathcal{D}_l\mathbf{U}\|^2_{\bar{\mathcal{P}}_l}+\|\mathcal{D}_r\mathbf{V}\|^2_{\bar{\mathcal{P}}_r}\right] &= \left[2\,\epsilon U\mathcal{D}_lU-a\,U^2\right]_{-1}\\
&+ \left[2\,\epsilon V\mathcal{D}_rV-a\,V^2\right]^1+\bar{\Upsilon}_i
\end{aligned} \tag{116}$$

with the interface term $\bar{\Upsilon}_i=[\mathcal{J}_i]^T\,\bar{M}_i\,\mathcal{J}_i$ defined by

$$\mathcal{J}_i = \left[U_i,V_i,(\mathcal{D}_lU)_i,(\mathcal{D}_rV)_i,(\mathcal{D}_l^2U)_i,(\mathcal{D}_r^2V)_i\right]^T \tag{117}$$

$$\bar{M}_i = \begin{bmatrix}
(-a+2l_{00}) & -(l_{00}+r_{00}) & (\epsilon+l_{01}+l_{10}) & -(l_{01}+r_{10}) & (l_{02}+l_{20}) & -(l_{02}+r_{20})\\
-(l_{00}+r_{00}) & (+a+2r_{00}) & -(r_{01}+l_{10}) & (-\epsilon+r_{01}+r_{10}) & -(l_{20}+r_{02}) & (r_{02}+r_{20})\\
(\epsilon+l_{01}+l_{10}) & -(r_{01}+l_{10}) & 2(l_{11}-\alpha\epsilon) & -(l_{11}+r_{11}) & (l_{12}+l_{21}) & -(l_{12}+r_{21})\\
-(l_{01}+r_{10}) & (-\epsilon+r_{01}+r_{10}) & -(l_{11}+r_{11}) & 2(r_{11}-\beta\epsilon) & -(l_{21}+r_{12}) & (r_{21}+r_{12})\\
(l_{02}+l_{20}) & -(l_{20}+r_{02}) & (l_{12}+l_{21}) & -(l_{21}+r_{12}) & 2\,l_{22} & -(l_{22}+r_{22})\\
-(l_{02}+r_{20}) & (r_{02}+r_{20}) & -(l_{12}+r_{21}) & (r_{21}+r_{12}) & -(l_{22}+r_{22}) & 2\,r_{22}
\end{bmatrix} \tag{118}$$

Stability of the interface is guaranteed if the matrix $\bar{M}_i$ is negative semi-definite which yields an interface term of the form $\bar{\Upsilon}_i=[\mathcal{J}_i]^T\,\bar{M}_i\,\mathcal{J}_i\le 0$. The definiteness of a symmetric matrix is governed by the sign of its eigenvalues. Thus, Sylvester's Theorem is used to systematically rotate $\bar{M}_i$ into diagonal form while maintaining the signs of its eigenvalues.

Applying similarity rotations, yields the generalized conservation conditions

$$\begin{gathered}
l_{00}=r_{00}+a \quad ; \quad l_{01}=r_{01}-\epsilon\\
r_{02}=l_{02} \ ; \ r_{20}=l_{20} \quad ; \quad r_{21}=l_{21} \ ; \ r_{22}=l_{22}
\end{gathered}$$

and changing variables

$$\begin{aligned}
t_1 &= (\epsilon+l_{01}+l_{10}) \ ; \ t_2=(l_{01}+r_{10})\\
r_{11} &= \epsilon[(-\alpha+3\beta)/4-s_1(\alpha+\beta)] \ ; \ l_{11}=\epsilon[(3\alpha-\beta)/4-s_2(\alpha+\beta)],\\
x_1 &= (r_{20}+l_{02}) \ ; \ y_1=(l_{12}+r_{21})\,;\, y_2=(r_{12}+r_{21})
\end{aligned} \tag{119}$$

yields the reduced matrix

$$\bar{M}_i = \begin{bmatrix}
0 & 0 & 0 & 0 & 0 & 0\\
0 & -2a+4l_{00} & t_1-t_2 & t_1+t_2 & 0 & 2\,x_1\\
0 & t_1-t_2 & -((\alpha+\beta)\epsilon) & (\alpha+\beta)\epsilon(s1-s2) & 0 & y_1-y_2\\
0 & t_1+t_2 & (\alpha+\beta)\epsilon(s1-s2) & -2\,(\alpha+\beta)\epsilon(s1+s2) & 0 & y_1+y_2\\
0 & 0 & 0 & 0 & 0 & 0\\
0 & 2\,x_1 & y_1-y_2 & y_1+y_2 & 0 & 4\,l_{22}
\end{bmatrix} \tag{120}$$

Repeated application of Sylvester's Theorem produces the stability inequalities

$$
\begin{aligned}
0 &\leq [s_1 + s_2] \\
0 &\leq 1 - \tfrac{[s_1 - s_2]^2}{2[s_1 + s_2]} \\
\\
l_{22} &\leq -\tfrac{[y_1+y_2]^2}{8[(\alpha+\beta)\epsilon][s_1+s_2]} - \tfrac{[y_1 - y_2 + \frac{[s_1-s_2][y_1+y_2]}{2(s_1+s_2)}]^2}{4(\alpha+\beta)\epsilon[1-\frac{[s_1-s_2]^2}{2[s_1+s_2]}]} \\
\\
l_{00} &\leq \tfrac{a}{2} - \tfrac{[t_1+t_2]^2}{8[(\alpha+\beta)\epsilon][s_1+s_2]} - \tfrac{[t_1 - t_2 + \frac{[s_1-s_2][t_1+t_2]}{2(s_1+s_2)}]^2}{4(\alpha+\beta)\epsilon[1-\frac{[s_1-s_2]^2}{2[s_1+s_2]}]} \\
\\
&- \frac{\{2\,x_1 + \frac{(t_1+t_2)(y_1+y_2)}{2(\alpha+\beta)\epsilon(s_1+s_2)} + \frac{[t_1 - t_2 + \frac{(s_1-s_2)(t_1+t_2)}{2(s_1+s_2)}][y_1 - y_2 + \frac{(s_1-s_2)(y_1+y_2)}{2(s_1+s_2)}]}{4(\alpha+\beta)\epsilon[1-\frac{[s_1-s_2]^2}{2[s_1+s_2]}]}\}^2}{-4\{l_{22} + \frac{[y_1+y_2]^2}{8[(\alpha+\beta)\epsilon][s_1+s_2]} + \frac{[y_1 - y_2 + \frac{[s_1-s_2][y_1+y_2]}{2(s_1+s_2)}]^2}{4(\alpha+\beta)\epsilon[1-\frac{[s_1-s_2]^2}{2[s_1+s_2]}]}\}}
\end{aligned}
\tag{121}
$$

Changing back to the original variables [via equation (119)] yields the desired result. □

Remark: A general interface procedure would include derivative terms up to p^{th}-order, and would result in the interface parameters $l_{00} \rightarrow l_{pp}$, and $r_{00} \rightarrow r_{pp}$. A stability analysis could be used to identify conservation conditions, as well as the parameter space that guarantees L_2 and pointwise stability.

Remark: A general interface procedure could be constructed based on the "flux-form" of the equation.

5 Formal Accuracy

We derive error estimates for both semi-discrete discretization methods. We begin with the primal form representation [equation (46)], and conclude with the flux form representation [equation (80)]. Extensive analysis of the accuracy of FEM is available in the literature (see for example the work of Arnold et al. [3]). Thus, the focus of attention herein is high-order finite difference methods.

Define the vectors $\mathbf{u} = [u(x_0,t), \cdots, u(x_n,t)]^T$, $\mathbf{u_x} = [u_x(x_0,t), \cdots, u_x(x_n,t)]^T$, and $\mathbf{u_{xx}} = [u_{xx}(x_0,t), \cdots, u_{xx}(x_n,t)]^T$, to be the projected values of the *exact* solution and derivatives, defined in the left domain at gridpoints $\mathbf{x}$. Similarly, define the vectors $\mathbf{v}$, $\mathbf{v_x}$ and $\mathbf{v_{xx}}$ in the right domain. With these definitions, the continuous problem (30) can be represented in vector nomenclature as

$$
\begin{aligned}
\mathbf{u}_t + a\mathbf{u}_x - \epsilon\mathbf{u}_{xx} &= l_{00}[u_i - v_i]\ \ \mathcal{P}_l^{-1}\mathcal{I}_l\ \mathbf{e_{i_-}} + l_{01}[u_x - v_x]_i\ \ \mathcal{P}_l^{-1}\mathcal{I}_l\ \mathbf{e_{i_-}} \\
&+ l_{10}[u_i - v_i]\ \ \mathcal{P}_l^{-1}\mathcal{D}_l^T\mathbf{e_{i_-}} + l_{11}[u_x - v_x]_i\ \ \mathcal{P}_l^{-1}\mathcal{D}_l^T\mathbf{e_{i_-}} \\
\mathbf{u}(x,0) &= \mathbf{0}. \\
\mathbf{v}_t + a\mathbf{v}_x - \epsilon\mathbf{v}_{xx} &= r_{00}[v_i - u_i]\ \ \mathcal{P}_r^{-1}\mathcal{I}_r\ \mathbf{e_{i_+}} + r_{01}[v_x - u_x]_i\ \ \mathcal{P}_r^{-1}\mathcal{I}_r\ \mathbf{e_{i_+}} \\
&+ r_{10}[v_i - u_i]\ \ \mathcal{P}_r^{-1}\mathcal{D}_r^T\mathbf{e_{i_+}} + r_{11}[v_x - u_x]_i\ \ \mathcal{P}_r^{-1}\mathcal{D}_r^T\mathbf{e_{i_+}} \\
\mathbf{v}(x,0) &= \mathbf{0}.
\end{aligned}
\tag{122}
$$

with suitable initial and boundary data, and the source term $F(\mathbf{x},t) = 0$. Note that the interface terms $[u_i - v_i]$ and $[u_x - v_x]_i$ are identically zero for the exact solution, but have been added to the right hand side of equation (122) to facilitate subsequent manipulations.

Substituting the discrete accuracy relations $\mathbf{u}_x = \mathcal{D}_l\mathbf{u} + \mathbf{T_{e1}}_l$ and $\mathbf{u}_{xx} = \mathcal{D}_l\mathcal{D}_l\mathbf{u} + \mathbf{T_{e2}}_l$ [see definitions (25) and

(28)], into equation (122) yields

$$
\begin{array}{rcllcll}
\mathbf{u}_t + a\mathcal{D}_l\mathbf{u} - \epsilon\mathcal{D}_l\mathcal{D}_l\mathbf{u} &=& l_{00}[u_i - v_i] & \mathcal{P}_l^{-1}\,\mathcal{I}_l\ \mathbf{e_{i_-}} &+& l_{01}[(\mathcal{D}_l\mathbf{u})_i - (\mathcal{D}_r\mathbf{v})_i] & \mathcal{P}_l^{-1}\,\mathcal{I}_l\ \mathbf{e_{i_-}} \\
&+& l_{10}[u_i - v_i] & \mathcal{P}_l^{-1}\,\mathcal{D}_l^T\mathbf{e_{i_-}} &+& l_{11}[(\mathcal{D}_r\mathbf{v})_i - (\mathcal{D}_l\mathbf{u})_i] & \mathcal{P}_l^{-1}\,\mathcal{D}_l^T\mathbf{e_{i_-}} \\
&-& a\mathbf{T_{e1}}_l & & +& l_{01}[(\mathbf{T_{e1}}_l)_i - (\mathbf{T_{e1}}_r)_i] & \mathcal{P}_l^{-1}\,\mathcal{I}_l\ \mathbf{e_{i_-}} \\
&+& \epsilon\mathbf{T_{e2}}_l & & +& l_{11}[(\mathbf{T_{e1}}_l)_i - (\mathbf{T_{e1}}_r)_i] & \mathcal{P}_l^{-1}\,\mathcal{D}_l^T\ \mathbf{e_{i_-}} \\
\mathbf{u}(x,0) &=& \mathbf{0}. & & & & \\
\mathbf{v}_t + a\mathcal{D}_r\mathbf{v} - \epsilon\mathcal{D}_r\mathcal{D}_r\mathbf{v} &=& r_{00}[v_i - u_i] & \mathcal{P}_r^{-1}\,\mathcal{I}_r\ \mathbf{e_{i_+}} &+& r_{01}[(\mathcal{D}_r\mathbf{v})_i - (\mathcal{D}_l\mathbf{u})_i] & \mathcal{P}_r^{-1}\,\mathcal{I}_l\ \mathbf{e_{i_-}} \\
&+& r_{10}[v_i - u_i] & \mathcal{P}_r^{-1}\,\mathcal{D}_r^T\mathbf{e_{i_+}} &+& r_{11}[(\mathcal{D}_l\mathbf{u})_i - (\mathcal{D}_r\mathbf{v})_i] & \mathcal{P}_r^{-1}\,\mathcal{D}_l^T\mathbf{e_{i_-}} \\
&-& a\mathbf{T_{e1}}_r & & +& r_{01}[(\mathbf{T_{e1}}_r)_i - (\mathbf{T_{e1}}_l)_i] & \mathcal{P}_r^{-1}\,\mathcal{I}_r\ \mathbf{e_{i_-}} \\
&+& \epsilon\mathbf{T_{e2}}_r & & +& r_{11}[(\mathbf{T_{e1}}_r)_i - (\mathbf{T_{e1}}_l)_i] & \mathcal{P}_r^{-1}\,\mathcal{D}_r^T\ \mathbf{e_{i_-}} \\
\mathbf{v}(x,0) &=& \mathbf{0}. & & & &
\end{array}
\tag{123}
$$

Next, define the semi-discrete error vectors $\mathbf{\Xi_l} = \mathbf{U} - \mathbf{u}$ and $\mathbf{\Xi_r} = \mathbf{V} - \mathbf{v}$ in the left and right domains, respectively. Premultiplying equation (46) by $\mathcal{P}^{-1}$ and subtracting equation (123) produces an evolution equation for the error vectors. Specifically, the collocation error of the coupled problem (168) written in primal form is

$$
\begin{array}{rcllcll}
\frac{\partial\mathbf{\Xi_l}}{\partial t} + a\mathcal{D}_l\mathbf{\Xi_l} - \epsilon\mathcal{D}_l\mathcal{D}_l\mathbf{\Xi_l} &=& l_{00}[\Xi_{li} - \Xi_{ri}] & \mathcal{P}_l^{-1}\,\mathcal{I}_l\ \mathbf{e_{i_-}} &+& l_{01}[(\mathcal{D}_l\Xi_l)_i - (\mathcal{D}_r\Xi_r)_i] & \mathcal{P}_l^{-1}\,\mathcal{I}_l\ \mathbf{e_{i_-}} \\
&+& l_{10}[\Xi_{li} - \Xi_{ri}] & \mathcal{P}_l^{-1}\,\mathcal{D}_l^T\mathbf{e_{i_-}} &+& l_{11}[(\mathcal{D}_l\Xi_l)_i - (\mathcal{D}_r\Xi_r)_i] & \mathcal{P}_l^{-1}\,\mathcal{D}_l^T\mathbf{e_{i_-}} \\
&+& a\mathbf{T_{e1}}_l & & -& l_{01}[(\mathbf{T_{e1}}_l)_i - (\mathbf{T_{e1}}_r)_i] & \mathcal{P}_l^{-1}\,\mathcal{I}_l\ \mathbf{e_{i_-}} \\
&-& \epsilon\mathbf{T_{e2}}_l & & -& l_{11}[(\mathbf{T_{e1}}_l)_i - (\mathbf{T_{e1}}_r)_i] & \mathcal{P}_l^{-1}\,\mathcal{D}_l^T\ \mathbf{e_{i_-}} \\
\mathbf{\Xi_l}(x,0) &=& \mathbf{0}. & & & & \\
\frac{\partial\mathbf{\Xi_r}}{\partial t} + a\mathcal{D}_r\mathbf{\Xi_r} - \epsilon\mathcal{D}_r\mathcal{D}_r\mathbf{\Xi_r} &=& r_{00}[\Xi_{ri} - \Xi_{li}] & \mathcal{P}_r^{-1}\,\mathcal{I}_r\ \mathbf{e_{i_+}} &+& r_{01}[(\mathcal{D}_r\Xi_r)_i - (\mathcal{D}_r\Xi_l)_i] & \mathcal{P}_r^{-1}\,\mathcal{I}_r\ \mathbf{e_{i_+}} \\
&+& r_{10}[\Xi_{ri} - \Xi_{li}] & \mathcal{P}_r^{-1}\,\mathcal{D}_r^T\mathbf{e_{i_+}} &+& r_{11}[(\mathcal{D}_r\Xi_r)_i - (\mathcal{D}_r\Xi_l)_i] & \mathcal{P}_r^{-1}\,\mathcal{D}_r^T\mathbf{e_{i_+}} \\
&+& a\mathbf{T_{e1}}_r & & -& r_{01}[(\mathbf{T_{e1}}_r)_i - (\mathbf{T_{e1}}_l)_i] & \mathcal{P}_r^{-1}\,\mathcal{I}_r\ \mathbf{e_{i_-}} \\
&-& \epsilon\mathbf{T_{e2}}_r & & -& r_{11}[(\mathbf{T_{e1}}_r)_i - (\mathbf{T_{e1}}_l)_i] & \mathcal{P}_r^{-1}\,\mathcal{D}_r^T\ \mathbf{e_{i_-}} \\
\mathbf{\Xi_r}(x,0) &=& \mathbf{0}. & & & &
\end{array}
\tag{124}
$$

Four distinct types of discretization errors appear in equation (124). The first two truncation error vectors: $\mathbf{T_{e1}}$ and $\mathbf{T_{e2}}$, arise from errors associated with the approximation of the first and second derivative terms, respectively. Like conventional HOFDM operators, they are seldom uniformly accurate throughout the domain. Points near boundaries are commonly discretized less accurately than those in the interior. Furthermore, the boundary stencils used in first and second difference operators are frequently of different orders.

The last two error vectors result from the interface penalty terms and have the forms: $[(\mathbf{T_{e1}})_i - (\mathbf{T_{e1}})_i]\,\mathcal{P}^{-1}\,\mathcal{I}\ \mathbf{e_i}$ and $[(\mathbf{T_{e1}})_i - (\mathbf{T_{e1}})_i]\,\mathcal{P}^{-1}\,\mathcal{D}^T\ \mathbf{e_i}$. Note that the accuracy of these vectors is influenced both by the truncation error of the interface derivative operators, $(\mathbf{T_{e1}}_r)_i$, and by the size of the penalty scaling terms. To assess the size of the scaling terms, first note that the differentiation operator and its transpose, [$\mathcal{D}$ and $\mathcal{D}^T$] scale as $\mathcal{O}(\Delta x)^{-1}$. Further, since $\mathcal{Q}$ is unitless, and $\mathcal{D} = \mathcal{P}^{-1}\mathcal{Q}$, the inverse norm operator $\mathcal{P}^{-1}$ scales as $\mathcal{O}(\Delta x)^{-1}$. Thus, the penalty error vectors scale as $\mathcal{O}(\Delta x)^{r-1}$ and $\mathcal{O}(\Delta x)^{r-2}$, respectively, where r is the local accuracy of the interface derivative operator.

In summary, error vectors in both domains have leading order truncation terms that scale as

$$
\begin{array}{rcl}
\mathbf{T_{e1}} &=& [\mathcal{O}(\Delta x^{r1}) \ ,\cdots,\mathcal{O}(\Delta x^{r1}) \ ,\mathcal{O}(\Delta x^{2p}),\cdots,\mathcal{O}(\Delta x^{2p}),\mathcal{O}(\Delta x^{r1}) \ ,\cdots,\mathcal{O}(\Delta x^{r1}) \ ]^T \\
\mathbf{T_{e2}} &=& [\mathcal{O}(\Delta x^{r2}) \ ,\cdots,\mathcal{O}(\Delta x^{r2}) \ ,\mathcal{O}(\Delta x^{2p}),\cdots,\mathcal{O}(\Delta x^{2p}),\mathcal{O}(\Delta x^{r2}) \ ,\cdots,\mathcal{O}(\Delta x^{r2}) \ ]^T \\
(\mathbf{T_{e1}})_i\,\mathcal{P}^{-1}\,\mathcal{I}^T\ \mathbf{e_i} &=& [\mathcal{O}(\Delta x^{r1-1}),\cdots,\mathcal{O}(\Delta x^{r1-1}),\quad 0\quad ,\cdots,\quad 0\quad ,\mathcal{O}(\Delta x^{r1-1}),\cdots,\mathcal{O}(\Delta x^{r1-1})]^T \\
(\mathbf{T_{e1}})_i\,\mathcal{P}^{-1}\,\mathcal{D}^T\ \mathbf{e_i} &=& [\mathcal{O}(\Delta x^{r1-2}),\cdots,\mathcal{O}(\Delta x^{r1-2}),\quad 0\quad ,\cdots,\quad 0\quad ,\mathcal{O}(\Delta x^{r1-2}),\cdots,\mathcal{O}(\Delta x^{r1-2})]^T
\end{array}
\tag{125}
$$

where the $r1$ and $r2$ exponents denote the boundary stencil order of accuracy in the first- and second-derivative operators, respectively. (Here, we assume the interior stencils to be the same order of accuracy for both the first- and second-derivative operators.)

Local lower order error terms do not necessarily decrease the global formal accuracy. The impact of lower-order terms on global discretization accuracy is a long-standing area of research that dates back to the pioneering work of Gustafsson [18]. There it was established that hyperbolic operators could accommodate local terms one order lower than design order, while still maintaining formal accuracy. Recent work of Svärd and Nordström [38] has extended this result to include the impact of low-order stencils for parabolic problems. Their work on global accuracy is encapsulated in the following theorem.

Theorem 11 *If (46) is a* **pointwise stable** *discretization of the continuous problem (30) for $\Delta x \leq \Delta x_0$, then with interior operators $\mathcal{D}$ and $\mathcal{DD}$ satisfying discretization orders of $2p-2 \leq r1, r2 \leq 2p$ at the boundary, and interface penalty terms satisfying discretization orders of $2p-2 \leq r1-2 \leq 2p$, then the global order of accuracy of approximation (46) is $2p$.*

Proof : See Svärd and Nordström [38], Theorems 2.6 and 2.8, pp. 335-337 for the original theorems and proofs.

Now consider a realistic combination of operators and study the effects of each error term on global accuracy. Assume that the derivative operator $\mathcal{D}$ is defined as in equation (125) with $r1 = 2p-1$. Furthermore, assume that the second derivative operator is formed as the action of two first derivative operators $\mathcal{DD}$. Finally, assume that the derivative used in the penalty (obtained from the derivative operator $\mathcal{D}$) is $\mathcal{O}(\Delta x^{2p-1})$, and is used in all penalty terms where necessary. In this scenario, the derivative operators $\mathcal{D}$ and $\mathcal{DD}$ maintain the design accuracy $2p$ of the method, as well as do the penalty terms producing errors of the form $(\mathbf{T_{e1}})_i \mathcal{P}^{-1}$. The remaining penalty terms producing errors of the form $\mathcal{D}^T \ \mathbf{e_i}$ decrease the formal accuracy to $2p-1$, at least in principle.

Remark. Adding penalties of the form $(\mathbf{T_{e1}})_i \mathcal{P}^{-1} \mathcal{D}^T \mathbf{e_i}$ is ill advised on a theoretical basis, although experiments presented later show that these estimates are not always sharp. Furthermore, these experiments will show these terms to be computationally impractical.

Moving now to the flux formulation [equation (80)], define the vectors $\mathbf{u} = [u(x_0,t), \cdots, u(x_n,t)]^T$, and $\bar{\phi} = [u_x(x_0,t), \cdots, u_x(x_n,t)]^T$, to be the projected values of the *exact* solution and derivative, defined in the left domain at gridpoints $\mathbf{x}$. Similarly, define the vectors $\mathbf{v}$, and $\bar{\psi}$ in the right domain. With these definitions, the continuous problem (30) can be represented in vector nomenclature as

$$\begin{array}{rcl}
\mathbf{u}_t + a\mathbf{u}_x - \epsilon\bar{\phi}_x &=& L_{00}[u_i - v_i] \ \mathcal{P}_l^{-1}\mathbf{e_{i_-}} + L_{01}[\bar{\phi} - \bar{\psi}]_i \ \mathcal{P}_l^{-1}\mathbf{e_{i_-}} \\
\epsilon\,(\bar{\phi} - \mathbf{u}_x) &=& L_{10}[u_i - v_i] \ \mathcal{P}_l^{-1}\mathbf{e_{i_-}} + L_{11}[\bar{\phi} - \bar{\psi}]_i \ \mathcal{P}_l^{-1}\mathbf{e_{i_-}} \\
\mathbf{u}(x,0) &=& \mathbf{0}. \\
\mathbf{v}_t + a\mathbf{v}_x - \epsilon\bar{\psi}_x &=& R_{00}[v_i - u_i] \ \mathcal{P}_r^{-1}\mathbf{e_{i_+}} + R_{01}[\bar{\psi} - \bar{\phi}]_i \ \mathcal{P}_r^{-1}\mathbf{e_{i_+}} \\
\epsilon\,(\bar{\psi} - \mathbf{v}_x) &=& R_{10}[v_i - u_i] \ \mathcal{P}_r^{-1}\mathbf{e_{i_+}} + R_{11}[\bar{\psi} - \bar{\phi}]_i \ \mathcal{P}_r^{-1}\mathbf{e_{i_+}} \\
\mathbf{v}(x,0) &=& \mathbf{0}.
\end{array} \tag{126}$$

with suitable initial and boundary data, and the source term $F(\mathbf{x},t) = 0$. Note that the interface terms $[u_i - v_i]$ and $[\bar{\phi} - \bar{\psi}]_i$ are identically zero for the exact solution, but have been added to the right hand side of equation (126) for added clarity.

Substituting the discrete accuracy relations $\mathbf{u}_x = \mathcal{D}_l\mathbf{u} + \mathbf{T_{e1l}}$, $\mathbf{v}_x = \mathcal{D}_l\mathbf{v} + \mathbf{T_{e1r}}$, $\bar{\phi}_x = \mathcal{D}_l\bar{\phi} + \mathbf{T}_\phi$, and $\bar{\psi}_x = \mathcal{D}_r\bar{\psi} + \mathbf{T}_\psi$ into equation (126), subtracting the result from $\mathcal{P} \times$ equation (80), and defining the semi-discrete errors $\mathbf{\Xi_l} = \mathbf{U} - \mathbf{u}$, $\mathbf{\Xi_r} = \mathbf{V} - \mathbf{v}$, and $\mathbf{\Theta_l} = \phi - \bar{\phi}$, $\mathbf{\Theta_r} = \psi - \bar{\psi}$, in the left and right domains, respectively, produces an evolution equation for the error. Specifically, the collocation error of the coupled problem (168) written in flux form is

$$\begin{array}{rcl}
\frac{\partial \mathbf{\Xi_l}}{\partial t} + a\mathcal{D}_l\mathbf{\Xi_l} - \epsilon\mathcal{D}_l\mathbf{\Theta_l} &=& L_{00}[\Xi_{li} - \Xi_{ri}] \ \mathcal{P}_l^{-1}\mathbf{e_{i_-}} + L_{01}[\Theta_{li} - \Theta_{ri}] \ \mathcal{P}_l^{-1}\mathbf{e_{i_-}} \\
&+& a\mathbf{T_{e1l}} - \epsilon\mathbf{T}_\phi \\
\epsilon(\mathbf{\Theta_l} - \mathcal{D}_l\mathbf{\Xi_l}) &=& L_{10}[\Xi_{li} - \Xi_{ri}] \ \mathcal{P}_l^{-1}\mathbf{e_{i_-}} + L_{11}[\Theta_{li} - \Theta_{ri}] \ \mathcal{P}_l^{-1}\mathbf{e_{i_-}} \\
&-& \epsilon\mathbf{T_{e1l}} \\
\mathbf{\Xi_l}(x,0) &=& \mathbf{0}. \\
\frac{\partial \mathbf{\Xi_r}}{\partial t} + a\mathcal{I}_r\mathbf{\Xi_r} - \epsilon\mathcal{D}_r\mathbf{\Theta_r} &=& R_{00}[\Xi_{ri} - \Xi_{li}] \ \mathcal{P}_r^{-1}\mathbf{e_{i_+}} + R_{01}[\Theta_{ri} - \Theta_{li}] \ \mathcal{P}_r^{-1}\mathbf{e_{i_+}} \\
&+& a\mathbf{T_{e1r}} - \epsilon\mathbf{T}_\psi \\
\epsilon(\mathbf{\Theta_r} - \mathcal{D}_r\mathbf{\Xi_r}) &=& R_{10}[\Xi_{ri} - \Xi_{li}] \ \mathcal{P}_r^{-1}\mathbf{e_{i_+}} + R_{11}[\Theta_{ri} - \Theta_{li}] \ \mathcal{P}_r^{-1}\mathbf{e_{i_+}} \\
&-& \epsilon\mathbf{T_{e1r}} \\
\mathbf{\Xi_r}(x,0) &=& \mathbf{0}.
\end{array} \tag{127}$$

Equation (127) is not in the form of a semi-discrete PDE. Thus, the accuracy of the flux form solution can not be inferred directly from Theorem (11). To assess the accuracy, equation (127) must be transformed from flux to primal form [For details on how to relate the two forms, see proof of Theorem (8)].

Solving equation (127) for $\mathbf{\Theta_l}$ and $\mathbf{\Theta_r}$ yields the expressions

$$\begin{array}{rcl}
\mathbf{\Theta_l} &=& \mathcal{D}_l\mathbf{\Xi_l} - \mathbf{T_{e1}}_l + \frac{1}{\epsilon}\mathcal{P}_l^{-1}\{L_{10}[(\Xi_l)_i - (\Xi_l)_i] \ \mathbf{e_{i_-}} + L_{11}[(\Theta_l)_i - (\Theta_r)_i] \ \mathbf{e_{i_-}}\} \\
\mathbf{\Theta_r} &=& \mathcal{D}_r\mathbf{\Xi_r} - \mathbf{T_{e1}}_r + \frac{1}{\epsilon}\mathcal{P}_r^{-1}\{R_{10}[(\Xi_l)_i - (\Xi_l)_i] \ \mathbf{e_{i_+}} + R_{11}[(\Theta_r)_i - (\Theta_l)_i] \ \mathbf{e_{i_+}}\}
\end{array} \tag{128}$$

Rewriting equation (127) in terms of the difference $(\Theta_l)_i - (\Theta_r)_i$ yields

$$(\Theta_l)_i - (\Theta_r)_i = c_1[(\Xi_l)_i - (\Xi_r)_i] + c_2\,[(\mathcal{D}_l\boldsymbol{\Xi_l})|_i - (\mathcal{D}_r\boldsymbol{\Xi_r})|_i] - c_2[(\mathbf{T_{e1}}_l)|_i - (\mathbf{T_{e1}}_r)|_i] \tag{129}$$

with the constants c_1 and c_2 defined in equation (101). Substituting equations (128) and (129) back into (127) yields the error evolution equation of the LDG flux form in terms of primal form variables.

$$\begin{aligned}
\boldsymbol{\Xi_l}_t + a\mathcal{D}_l\boldsymbol{\Xi_l} &= \epsilon\mathcal{D}_l\mathcal{D}_l\boldsymbol{\Xi_l} \\
&+ \{L_{00}[(\Xi_l)_i - (\Xi_r)_i] + L_{01}(c_1[(\Xi_l)_i - (\Xi_r)_i] + c_2[(\mathcal{D}_l\boldsymbol{\Xi_l})|_i - (\mathcal{D}_r\boldsymbol{\Xi_r})|_i])\} \quad \mathcal{P}_l^{-1}\mathbf{e_{i_-}} \\
&+ \{L_{10}[(\Xi_l)_i - (\Xi_r)_i] + L_{11}(c_1[(\Xi_l)_i - (\Xi_r)_i] + c_2[(\mathcal{D}_l\boldsymbol{\Xi_l})|_i - (\mathcal{D}_r\boldsymbol{\Xi_r})|_i])\} \quad \mathcal{D}_l\mathcal{P}_l^{-1}\mathbf{e_{i_-}} \\
&+ \mathbf{T_{e1}}_l - \epsilon(\mathcal{D}_l\mathbf{T_{e1}}_l + \mathbf{T}_\phi) \\
&- L_{01}c_2[(\mathbf{T_{e1}}_l)|_i - (\mathbf{T_{e1}}_r)|_i]\mathcal{P}_l^{-1}\mathbf{e_{i_-}} + L_{11}[(\mathbf{T_{e1}}_l)|_i - (\mathbf{T_{e1}}_r)|_i]\mathcal{D}_l\mathcal{P}_l^{-1}\mathbf{e_{i_-}} \\
\boldsymbol{\Xi_r}_t + a\mathcal{D}_r\boldsymbol{\Xi_r} &= \epsilon\mathcal{D}_r\mathcal{D}_r\boldsymbol{\Xi_r} \\
&+ \{R_{00}[(\Xi_r)_i - (\Xi_l)_i] + R_{01}(c_1[(\Xi_r)_i - (\Xi_l)_i] + c_2[(\mathcal{D}_r\boldsymbol{\Xi_r})|_i - (\mathcal{D}_r\boldsymbol{\Xi_l})|_i])\} \quad \mathcal{P}_r^{-1}\mathbf{e_{i_+}} \\
&+ \{R_{10}[(\Xi_r)_i - (\Xi_l)_i] + R_{11}(c_1[(\Xi_r)_i - (\Xi_l)_i] + c_2[(\mathcal{D}_r\boldsymbol{\Xi_r})|_i - (\mathcal{D}_r\boldsymbol{\Xi_l})|_i])\} \quad \mathcal{D}_r\mathcal{P}_r^{-1}\mathbf{e_{i_+}} \\
&+ \mathbf{T_{e1}}_r - \epsilon(\mathcal{D}_r\mathbf{T_{e1}}_r + \mathbf{T}_\psi) \\
&- R_{01}c_2[(\mathbf{T_{e1}}_r)|_i - (\mathbf{T_{e1}}_l)|_i]\mathcal{P}_r^{-1}\mathbf{e_{i_+}} + R_{11}[(\mathbf{T_{e1}}_r)|_i - (\mathbf{T_{e1}}_l)|_i]\mathcal{D}_r\mathcal{P}_r^{-1}\mathbf{e_{i_+}}
\end{aligned} \tag{130}$$

Four distinct types of discretization error appear in equation (130). The first derivative truncation error vector: $\mathbf{T_{e1}}$ matches that found in equation (124). The second derivative truncation vectors ($\mathcal{D}\mathbf{T_{e1}} + \mathbf{T}_\psi$) are dissimilar to those found in (124), but will have similar leading order truncation terms. The final two truncation vectors result from the imposition of penalties and have the same form as those found in the primal form (124). Thus, based on this analysis as well as the truncation analysis performed on the primal formulation, both should have the same asymptotic behavior with respect to grid refinement.

6 Identification of schemes

Specific values are assigned for the eight parameters used in the primal [equation (46)] and flux [equation (80)] formulations. Three popular schemes are identified, including two DGFEM and one strong form HOFDM. Each is shown to satisfy their respective stability constraints.

6.1 Carpenter, Nordström, Gottlieb [13]

We begin with the scheme proposed by Carpenter et. al (CNG) [13] which is a special case of the primal formulation presented in equation (46). This scheme was originally derived in strong form in the context of HOFDM. This scheme [See reference [13], equation (7).] can be reproduced by assigning the following specific values to the penalty parameters;

$$l_{10} = l_{11} = r_{10} = r_{11} = 0 \;\;;\;\; l_{00} = \sigma_1\,;\;\; l_{01} = \epsilon\sigma_2\,;\;\; r_{00} = \sigma_3\,;\;\; r_{01} = \epsilon\sigma_4\,; \tag{131}$$

Substituting (131) into equations (47, $\cdots$, 50) yields the conditions

$$\sigma_1 = \sigma_3 + a \;\;;\;\; [\sigma_2 = \sigma_4 - 1]\;\epsilon \tag{132}$$

$$0 \le [(\alpha+\beta)\epsilon] \;\;;\;\; [\epsilon(-\alpha+\beta)]^2 \le [(\alpha+\beta)\epsilon]^2 \;\;;\;\; \sigma_1 \le \frac{a}{2} - \epsilon[\frac{{\sigma_2}^2}{4\beta} + \frac{{\sigma_4}^2}{4\alpha}] \tag{133}$$

Further, the stability conditions obtained in equation (132) and (133) are identical to those found in the original CNG work [e.g. equation (8) in reference [13]].

6.2 Baumann, Oden [7]

The scheme proposed by Baumann and Oden [7] is a special case of the primal formulation presented in equation (46). This scheme was originally developed in the weak form in the context of DGFEM. Shu presents in reference [35], an illustrative comparison between this scheme and the LDG scheme for the strictly parabolic case. Therein the

Baumann-Oden scheme is presented in equations (5.1) and (5.2) and can be reproduced from equation (46) with the values

$$l_{00} = r_{00} = l_{11} = r_{11} = 0 \quad ; \quad l_{01} = -\frac{\epsilon}{2}; \quad l_{10} = -\frac{\epsilon}{2}; \quad r_{01} = +\frac{\epsilon}{2}; \quad r_{10} = +\frac{\epsilon}{2} \tag{134}$$

Taking the liberty to extend Shu's definition to include the possibility of convection terms, we define the Baumann-Oden scheme by assigning the following values to the coefficients in equation (46):

$$l_{00} = r_{00} + a\,; \quad l_{11} = r_{11} = 0 \; ; \quad l_{01} = +(\beta - \frac{\epsilon}{2}); \; l_{10} = -(\beta + \frac{\epsilon}{2}); \; r_{01} = +(\beta + \frac{\epsilon}{2}); \; r_{10} = -(\beta - \frac{\epsilon}{2}) \tag{135}$$

Substituting (135) into equations (47, $\cdots$, 50) yields the conditions

$$0 \le [(\alpha+\beta)\epsilon] \quad ; \quad [\epsilon(-\alpha+\beta)]^2 \le [(\alpha+\beta)\epsilon]^2 \quad ; \quad l_{00} \le \frac{a}{2} \tag{136}$$

6.3 Local Discontinuous Galerkin [14]

The scheme proposed by Cockburn and Shu [14] is special case of the flux formulation presented in equation (80). Once again, Shu presents in reference [35], the LDG scheme written strictly for the parabolic case. Therein the LDG scheme is presented in equations (4.1), (4.2), and (4.3) and can be reproduced from equation 80 with the values

$$L_{00} = R_{00} = L_{11} = R_{11} = 0 \quad ; \quad L_{01} = -\frac{\epsilon}{2}; \quad L_{10} = -\frac{\epsilon}{2}; \quad R_{01} = +\frac{\epsilon}{2}; \quad R_{10} = +\frac{\epsilon}{2} \tag{137}$$

Taking the liberty to extend Shu's definition to include the possibility of convection terms, we define the collocation LDG scheme by assigning the following values to the coefficients in equation (80):

$$L_{00} = R_{00} + a\,; \quad L_{11} = R_{11} = 0 \; ; \quad L_{01} = +(\beta - \frac{\epsilon}{2}); \; L_{10} = -(\beta + \frac{\epsilon}{2}); \; R_{01} = +(\beta + \frac{\epsilon}{2}); \; R_{10} = -(\beta - \frac{\epsilon}{2}) \tag{138}$$

Substituting (138) into equations (47, $\cdots$, 50) yields the conditions

$$0 \le [(\alpha+\beta)\epsilon] \quad ; \quad [\epsilon(-\alpha+\beta)]^2 \le [(\alpha+\beta)\epsilon]^2 \quad ; \quad L_{00} \le \frac{a}{2} \tag{139}$$

7 Numerical experiments

7.1 Test Problems

7.1.1 The One-Way Wave Equation

The linear one-way wave equation is used to study the stability and accuracy of the new formulations in the absence of diffusion terms. The functional form is

$$U_t + aU_x = 0 \quad |x| \le 1 \quad , 0 \le t \le 0.1 \tag{140}$$

with the exact solution

$$U(x,t) = \cos[-2\,\pi\,(x - t)] \tag{141}$$

The initial and boundary data coincide with the exact solution for all time.

The wave equation is used to establish a baseline accuracy for each method, before moving on to the parabolic equation. This step is essential to establish the effects of the newly added terms that penalize the diffusive terms. Specifically, the new additional terms could destroy the accuracy of the advection term, not just diffusion. Comparing the two results allows us to determine the source of error.

This study of the first order wave equation raises a subtle point regarding imposition of discrete interface conditions; specifically, that *derivative* fluxes can be penalized between elements, despite the fact that wellposedness requires only *one* interface condition. Thus, the diffusive interface penalty can be thought of as an alternative discrete stencil, one that enforces stronger first derivative continuity across the interface. An a priori stability estimate and accurate interface data guarantee the validity of these penalties.

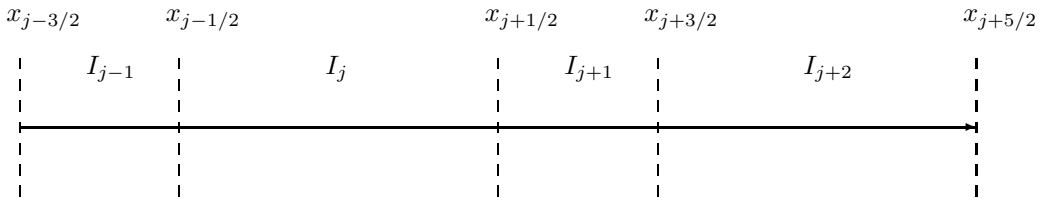

Figure 4: Schematic depicting two periods of the recursive element pattern used in the nonuniform grid accuracy studies.

7.1.2 Linear Burgers' Equations

The linear Burgers' equation tests a combination of the advection and diffusion terms. Five distinct values of the diffusion parameter ϵ are used to deduce the effects of the penalty as the problem becomes diffusion dominated. The functional form is

$$U_t \, + \, a \, U_x \, = \, \epsilon U_{xx} \quad |x| \leq 1 \quad , 0 \, \leq \, t \, \leq \, 0.1 \tag{142}$$

with the exact solution

$$U(x,t) \, = \, \exp[-\epsilon \, b^2 \, t] \, \cos[-2 \, \pi \, (x \, - \, t)] \tag{143}$$

with initial and boundary data that coincides with that of the exact solution. The equation parameters used are $a \, = \, 2$ and $b \, = \, 2 \, \pi$ in all cases. Five values of the parameter ϵ are used: $\epsilon \, = \, 1 \, , \frac{2}{5}, \; 0.1 \; \frac{2}{50}$, and 0.01.

7.2 Test Schemes

Two finite difference and four spectral operators are tested using the linear wave and linear Burgers' equation. The finite difference operators are the 4^{th} and 6^{th} order central difference operators using SBP closures at the boundaries. The boundary closure formulas are those reported in reference [10]. The spectral operators are conventional collocation operators defined using the Gauss-Lobatto-Chebyshev nodal points. Polynomial orders in the range $2 \, \leq \, p \, \leq \, 5$ are used (corresponding to elements having three to six nodal points). The penalties are implemented such that the scheme is equivalent to a Legendre collocation scheme (see Carpenter and Gottlieb [12]). The time advancement scheme used in all cases is the five-stage fourth-order Runge-Kutta (RK) scheme [9]. The timestep is chosen such that the temporal error estimate is independent of further timestep reduction. The magnitude of the temporal error is approximately 10^{-12}, and is obtained by comparing the fourth-order solution with an embedded third-order solution. Thus, the spatial error is the dominant component of error in the simulations.

7.3 Test Matrix

An extensive test matrix is used to distinguish different properties of the new formulations. The matrix includes 1) four geometry definitions, and 2) multiple values of three distinct interface penalty parameters. The geometric definitions included all permutations of uniform and nonuniform element distributions on both periodic and nonperiodic intervals, specifically; 1) uniform-periodic, 2) nonuniform-periodic, 3) uniform-nonperiodic, and 4) nonuniform-nonperiodic. The nonuniform grids are generated using elements that alternate in size with a ratio of $2 : 1$. Figure 4 shows a schematic depicting two periods of the $2 : 1$ nonuniform grid used in the study.

An a priori study was performed, comparing the accuracy of the methods on each of the four different geometries. The results from one of these studies are included in Appendix (E). The most challenging test cases (hyperbolic or parabolic) were those that were run on the nonuniform grid, with nonperiodic boundary conditions. Thus, the nonuniform grid with nonperiodic boundary conditions is used almost exclusively in this work.

The interface penalties are parametrized using three independent variables as (here written for the primal formulation),

$$l_{00} \, = \, \frac{a}{2}(1 \, - \, \alpha); \quad r_{00} \, = \, \frac{a}{2}(-1 \, - \, \alpha); \quad \alpha \, \geq \, 0 \tag{144}$$

$$l_{01} = +(\beta - \frac{\epsilon}{2}); \quad l_{10} = -(\beta + \frac{\epsilon}{2}); \quad r_{01} = +(\beta + \frac{\epsilon}{2}); \quad r_{10} = -(\beta - \frac{\epsilon}{2}) \tag{145}$$

$$l_{11} = r_{11} = \gamma; \quad \gamma \geq 0 \tag{146}$$

The parameter α adjusts the contribution of the Dirichlet penalty between the left and right states. The special value $\alpha = 0$ admits no dissipation at the interface, thus producing a skew-symmetric matrix in the $\mathcal{P}$-norm. The value $\alpha = 1$ produces a fully upwind flux. Two values of the parameter α are tested: $\alpha = 0$ and $\alpha = 1$.

The parameters β and γ adjust the penalty on the derivative fluxes. For β the relationship between the values of l_{01}, l_{10}, r_{01}, and r_{10}, greatly simplifies the energy estimate by producing the conditions $t_1 = t_2 = 0$ in the estimate. This combination of parameters produces no contribution to the energy estimate. [See equation (62).] Note that the value of β can be chosen independent from ϵ, and can be nonzero for values of $\epsilon = 0$. Two values of the parameter β are tested: $\beta = 0$ and $\beta = \frac{1}{4}$. The parameter γ adjusts the contribution from the derivative fluxes and produces contributions to the energy estimate that are strictly dissipative. Four values of γ are tested: $\gamma = 0$, $\gamma = 10^{-4}$, $\gamma = 10^{-3}$ and $\gamma = 10^{-2}$.

All studies include a comparison of the convergence rate of each scheme. A grid refinement exercise involving approximately 40 grid densities is performed for each set of parameters. The convergence rate is determined by fitting a "least-squares" curve through the error data.

7.4 Results

7.4.1 Finite Difference: Wave and Burgers' Equation

Figure 5 compares the convergence behavior of the 4^{th}- and 6^{th}-order finite difference schemes. The model problem used is the linear one-way wave equation. Shown are the results obtained on a nonuniform grid with nonperiodic boundary conditions. Block-norm boundary closures are used that are 3^{rd}- and 5^{th}-order accurate [10], respectively. Seven sets of interface parameters are compared, and in all cases, design order convergence is observed (4^{th}- and 6^{th}-order, respectively). Note that imposing the penalty on the derivative-transpose terms (l_{11}, and r_{11}) does not decrease the formal accuracy of the schemes.

Figure 6 compares the convergence behavior of the the 4^{th} and 6^{th}-order schemes on the linear Burgers' equation. Both the flux (LDG) and the primal (B-O) forms of the penalty are presented in this study. Note that the parameter β is not scaled with the parameter ϵ. In all cases, design order is achieved, implying that increased levels of interface coupling has little impact on formal solution accuracy. Two other values of the physical viscosity ϵ were also simulated (but not shown) to assess the impact of the interface penalties. Similar trends were observed at other values of ϵ.

An anomalous behavior is observed in the convergence of the 4^{th}-order simulations. While the slope remains close to 4, a deflection in convergence behavior is observed at an error of approximately 10^{-8}. The exact cause of this behavior is not known.

All simulations were performed with an explicit RK scheme, and the efficiency of the runs is strongly influenced by spurious eigenvalues generated by the interface coupling terms. For the parameters tested, little sensitivity is observed for the α parameter. A significant decrease in the max-CFL is observed when large values of the β parameter are used. Even small values of the γ parameter rendered the explicit method almost useless because of the magnitude of spurious eigenvalues produced. An implicit method would most certainly be needed if the γ parameter is used extensively to stabilize the interfaces!

Finally, both uniform and nonuniform grids were used in this study, as were periodic and nonperiodic geometries. Neither permutation changed in any way the general convergence behavior of the schemes presented in figures 5 - 6.

7.4.2 Spectral Collocation: One-Way Wave Equation

The same α, β, γ parameter studies performed for the finite difference cases are repeated using the spectral collocation methods. Polynomial orders ranging from $p = 2$ to $p = 5$ are compared on a nonuniform grid with nonperiodic boundaries. In addition to graphical comparisons, a numerically determined convergence rate is used for direct tabular

comparisons. Three different measures of error are used in the tabular comparisons: 1) the L_2-norm of the solution error, 2) the L_∞-norm, and 3) the integral norm, formed using the integration matrix $\mathcal{P}$.

Table 2, shows the convergence results for four permutations of α and β, and polynomial orders $p = 2$ - $p = 5$, at values of γ in the range $[0.0 \leq \gamma \leq 0.025]$. Three distinct convergence rates emerge in this study. We begin by comparing the cases run with $\gamma = 0$. The case $\alpha = 1$, $\beta = 0$ converges at the optimal rate of $p+1$ for all polynomial orders. Changing the value to $\beta = \frac{1}{4}$ reduces the formal convergence rate to p. Next, imposing a nonzero value of the parameter γ decreases the convergence rate of the optimal case ($\alpha = 1$,$\beta = 0$) to what appears to be $p + \frac{1}{2}$. Strangely enough, imposing nonzero values for γ increases the accuracy of the suboptimal cases for which $\beta = \frac{1}{4}$.

Once again, all these studies were run with an explicit RK scheme that is subject to a finite maximum stability condition. The interface penalties have a profound influence on the placement of the maximum eigenvalues, and therefore the maximum allowable timestep $[(\Delta t)_{max}]$. The parameter β decreased the $(\Delta t)_{max}$ significantly for $\mathcal{O}(1)$ values. The parameter γ rendered the explicit time advancement scheme almost useless, by reducing the $(\Delta t)_{max}$ by several orders of magnitude.

7.4.3 Spectral Collocation: Linear Burgers' Equation

Two studies are performed on the linear Burgers' equation: one using the primal formulation (e.g. Baumann-Oden), and one using the flux formulation (e.g. LDG). We begin with a study comparing the influence of the equation parameter ϵ on the convergence rate of the Baumann-Oden scheme.

Table 3 compares the convergence of the B-O scheme for values of the physical parameter $\epsilon = 1.00$, 0.10 , 0.01. (The L_2-norm of the derivative error is included in the results along with the L_2-norm, the L_∞-norm, and the $\mathcal{P}$ integral norm.) The cases with diffusive parameter $\epsilon = 1.0$, are dominated by the parabolic nature of the equations, while as ϵ becomes smaller, the character of the equation becomes increasingly "hyperbolic".

Suboptimal convergence is generally observed for all polynomial orders and schemes. The exceptional cases are when the Dirichlet boundary and interface terms are fully upwinded ($\alpha = 1$) and the Neumann derivative terms are averaged ($\beta = 0$). For this set of parameters, polynomials of odd order ($p =: 3, 5$) converge at an optimal rate of $p + 1$ for the solution and p for the derivative. This result is consistent with that shown by Shu [35] for the strictly parabolic case using DGFEM. As ϵ decreases from the baseline $\epsilon = 1$, the convergence rate increases (unexpectedly), for all schemes and all polynomial orders with the exception of those that are already optimal.

The convergence behavior of the B-O formulation is unpredictable. In contrast, when the linear Burgers' equation is simulated with the LDG scheme, optimal convergence is achieved for every combination of physical/numerical parameters. Table 4 shows the convergence behavior of the LDG scheme for the same four parameter settings, and four polynomial orders. The LDG scheme converges for the solution at a rate of $p+1$, while the derivative converges at a rate p for all polynomial orders p. Little influence is observed when the values of the parameters α or β are adjusted. These results for the LDG scheme are in slight disagreement with those presented by Shu [35] for the DGFEM and a strictly parabolic equation. There it is shown that optimal convergence is only achieved for the specific values of the parameter $\beta = \pm\frac{1}{2}$.

The *formal* accuracy of the LDG scheme is clearly superior to that of the B-O formulation. Figures 7, 8, 9, and 10 compare the *absolute* accuracy of both formulations, all permutations of α and β, and the physical viscosity $\epsilon = 1$. The LDG formulation significantly outperforms the B-O scheme for even order polynomials, but is less advantageous for odd order polynomials (for which the B-O scheme is optimally convergent). Both the B-O and LDG classes of schemes, exhibit little sensitivity to the parameters $\alpha = 0, 1$ and $\beta = 0/4, 1/4$. This result is surprising for the B-O schemes, considering that some are suboptimal for various parameter combinations. Note, however, that absolute accuracy depends on both the order of and size of the truncation terms. Many of the lower-order combinations have smaller truncation terms, which results in *better* accuracy at coarse tolerances.

Figure 11 combines all the polynomial orders in to one plot. For clarity, only the cases with interface parameters $\alpha = 1$ and $\beta = 0$, are presented. Recall that this parameter combination results in an upwind Dirichlet flux and a centered Neumann flux at the interfaces, and resulted in optimal convergence for odd-orders with the B-O scheme. The LDG scheme is significantly more accurate than the B-O scheme for even order polynomials, while they are nearly indistinguishable for odd order polynomials. Note that the convergence behavior of the LDG formulation is dual valued for even order polynomials. Specifically, the simulations with an even number of elements superconverges initially, while those with an odd number of elements converge as expected.

8 Discussion

The present work unifies existing FEM methods into a common strong form framework, and then generalizes that framework by including additional interface penalty terms. The result is a "plethora" of adjustable parameters that generate schemes with remarkably diverse numerical properties. We have provided some broad generalities regarding the choice of parameters, e.g. the accuracy virtues of the LDG flux formulation. Many readers will want concise guidance regarding optimal parameter choices. Given the subjective nature of *optimality*, however, we have intentionally avoided advocating specific parameter values. The following examples illustrate the reasons for our choice. First, a practitioner using an implicit temporal algorithm could utilize all first derivative terms, as well as second derivative penalty terms to enrich interface continuity. This is in contrast to the general conclusions of the present study, i.e. that second derivative terms are never advisable if explicit temporal algorithms are used. Second, specific choices of penalty parameters in the flux formulation result in nearest neighbor stencil compactness, a property that some (but not all) practitioners find desirable. Third, nonlinearity is the ultimate test of scheme accuracy and robustness. Excluding portions of the parameter space based on the present studies in the absence of limiters is premature.

The present derivations and analysis, focus entirely on the scalar, constant coefficient, advection-diffusion equation. This lack of generality is an obvious shortcoming for most practitioners, given their desire to solve systems of nonlinear equations. Straightforward generalization to systems of equations is possible for the penalty terms that originate in the multi-domain work of Carpenter, Nordström, Gottlieb[13]. (See the work of Nordström, and Carpenter [30] for details.) Generalization (FEM reverse engineering) of the penalty terms involving $\mathcal{D}^T$ to systems of equations is the focus of ongoing work.

9 Conclusions

Summation-by-parts (SBP) operators are discrete derivative operators that mimic the integration-by-parts property of the continuous operator. A diverse set of discretization operators can be cast in the SBP convention, including high-order finite difference, (central, upwind, compact, DRP) and spectral collocation operators. Summation-by-parts operators share a close resemblance with finite element methods. In fact, for certain polynomial methods, the (strong form: collocation) SBP operators can be shown to be equivalent to (weak form: integral) FEM methods. The great similarity between the SBP and FEM operators [especially Discontinuous Galerkin FEM (DGFEM)], leads to a fertile exchange of ideas between the two approaches.

Two new collocation approaches are developed to couple multiple SBP domains. The two approaches are essentially the strong form equivalent of the *primal form* method developed by Baumann and Oden, [7], and the *flux form* LDG methods developed by Cockburn and Shu [14]. Both techniques are shown to be L_2 and pointwise stable, and conservative, while (if applied carefully) maintaining the original design accuracy of the adjoining domains. The new approaches generalize the original multi-domain penalty technique of Carpenter et al.[13].

The Baumann and Oden collocation approach is extended to allow construction of interface penalties involving second derivatives. Several free parameters are available in the new approach, that can be adjusted to ensure L_2 and pointwise stability of the interface and two adjoining subdomains. The general structure of the new approach enables (in principle) penalties of derivatives higher than second to be constructed. Similar ideas can be used to construct generalized penalties based on the LDG collocation approach.

Most penalty combinations are theoretically advantageous because they enhance the interface "continuity". There are, however potential costs. Penalizing data that is of inadequate accuracy can degrade the formal global accuracy of the method. Penalties built from second and higher derivatives are ill advised for this reason. A further potential cost is the degree to which some penalties increase the condition number of the resulting discretization matrix, making them unacceptably expensive for explicit time advancement. Extensive numerical experiments on the advection and the advection diffusion (linear Burgers') equation verify the theoretical predictions, although in some cases the theoretical predictions are not sharp.

A FEM Stability

Although arbitrary interface closures are admissible for equations (9) or (10), not all choices result in stable or accurate formulations. An interface parametrization and derivation of the L_2 stability of the LDG method is now presented. As we shall see (section III), this stability analysis closely resembles that used to define admissible strong form discretizations.

The LDG energy is obtained from equation (3) by choosing the test functions to be $v = u$ and $w = q$, resulting in

$$\begin{array}{rcrcl} \int_\Omega u_t\, u\, dx & = & -\int_\Omega q\, u_x dx & + & \sum_\Gamma [[\hat{q}u]] \\ \int_\Omega q\, q\, dx & = & -\int_\Omega u\, q_x dx & + & \sum_\Gamma [[\hat{u}q]] \end{array} \tag{147}$$

Adding the two "energies" yields after manipulation the equation

$$\tfrac{1}{2}\tfrac{d}{dt}\int_\Omega u^2 dx \quad + \quad \int_\Omega q^2 dx \quad = \quad \sum_\Gamma [[\hat{q}u + \hat{u}q - qu]] \tag{148}$$

To this point, the functional form of the interface variables $\hat{u}$ and $\hat{q}$, remains undefined. Their choice, however, greatly influences the properties of the resultant scheme. In general, one would like to choose these fluxes such that the global scheme is stable, conservative and exhibits optimal accuracy.

The fluxes $\hat{u}$ and $\hat{q}$ are generally defined to be *conservative* if they are single-valued on all interfaces Γ. Conservative fluxes that telescope across domain interfaces, eliminate many interface terms in proofs of stability and accuracy. For example, inserting $v = 1$ and $w = 1$ into equation (6) produces the trivial condition $\int_\Omega u_t dx = \int_\Omega q = 0$, for conservative fluxes.

Interface accuracy can only be maintained if the interface fluxes are constructed from accurate interface data. Since all solutions are double valued on the interfaces, natural candidates are averages and differences of the interface variables. This in mind, one might choose a conservative interface flux of the form

$$\begin{array}{rcrcrcl} \hat{u} & = & \{u\} & + & C_1 [[u]] & + & C_2 [[q]] \\ \hat{q} & = & \{q\} & + & C_3 [[u]] & + & C_4 [[q]] \end{array} \tag{149}$$

Substituting these fluxes into the energy estimate given in equation (148), using the relation $[[\zeta\eta]] = \{\zeta\}[[\eta]] + [[\zeta]]\{\eta\}$, and the conservation conditions $[[\hat{u}]] = [[\hat{q}]] = 0$ produces

$$\frac{1}{2}\frac{d}{dt}\int_\Omega u^2 dx + \int_\Omega q^2 dx = \sum_\Gamma \left(C_1 [[u]] + C_2 [[q]]\right)[[u]] + \left(C_3 [[u]] + C_4 [[q]]\right)[[q]] \tag{150}$$

The (RHS) equation (150) is negative (implying stability) if all the conditions

$$C_1 \le 0, \quad C_4 \le 0, \quad [C_1 C_4 - \frac{1}{4}(C_2 + C_3)^2] \ge 0 \tag{151}$$

are satisfied. The precise values of $C_1, \cdots, C_4$ are not important for this discussion, just the functional form of the fluxes.

The primal formulation given by equation (9) produces a slightly different energy estimate, because stability is proved in different variables. Choosing the test function to be $v = u$ in equation (9) produces the energy equation

$$\tfrac{1}{2}\tfrac{d}{dt}\int_\Omega u^2 dx \quad + \quad \int_\Omega u_x^2 dx \quad = \quad \sum_\Gamma [[\hat{u_x}u + \hat{u}u_x - uu_x]] \ . \tag{152}$$

Once again, one might choose a conservative interface flux of the form

$$\begin{array}{rcrcrcl} \hat{u} & = & \{u\} & + & c_1 [[u]] & + & c_2 [[u_x]] \\ \hat{u_x} & = & \{u_x\} & + & c_3 [[u]] & + & c_4 [[u_x]] \end{array} \tag{153}$$

Substituting these primal fluxes into equation (152) produces

$$\frac{1}{2}\frac{d}{dt}\int_\Omega u^2 dx + \int_\Omega u_x^2 = \sum_\Gamma \left(c_1 [[u]] + c_2 [[u_x]]\right)[[u]] + \left(c_3 [[u]] + c_4 [[u_x]]\right)[[u_x]] \tag{154}$$

The methods are stable if the stability conditions

$$c_1 \le 0, \quad c_4 \le 0, \quad [c_1 c_4 - \frac{1}{4}(c_2 + c_3)^2] \ge 0 \tag{155}$$

are satisfied.

Remark. The stability conditions of the two energy estimates are identical with the exception that different diffusive variables appear in the proofs.

Remark. The admissible parameters for the interface fluxes u and q (or u_x) cannot be chosen independently.

Remark. A reasonable (and somewhat more clever) person might choose a conservative interface flux of the form

$$\begin{array}{rcccccccc} \hat{u} & = & \{u\} & + & c_1 [[u]] & + & c_{2a} [[q]] & + & c_{2b} [[u_x]] \\ \hat{u_x} & = & \{u_x\} & + & c_3 [[u]] & + & c_{4a} [[q]] & + & c_{4b} [[u_x]]. \end{array} \tag{156}$$

Numerous methods, similar in type to the LDG and IPFEM methods have recently been developed. They differ primarily in the functional form of the interface fluxes. Arnold et al. [2, 3] presented a framework that unifies nearly all the DG schemes that appear in the literature. A subset of the many schemes presented in Arnold et al. [3] is included in Table 1.

Method	$\hat{u}$	$\hat{q}$
Bassi-Rebay [5]	$\{u\}$	$\{q\}$
Brezzi et al [8]	$\{u\}$	$\{q\} - \alpha_r[[u]]$
LDG [14]	$\{u\} - \beta[[u]]$	$\{q\} - \alpha_j[[u]] + \beta[[u]]$
IP [16]	$\{u\}$	$\{u_x\} - \alpha_j[[u]]$
Bassi et al. [6]	$\{u\}$	$\{u_x\} - \alpha_r[[u]]$
Baumann-Oden [7]	$\{u\} + n \cdot [[u]]$	$\{u_x\}$
NIPG [34]	$\{u\} + n \cdot [[u]]$	$\{u_x\} - \alpha_j[[u]]$

Table 1: Numerical fluxes for various DG schemes.

Note that the methods fall into two distinct categories based on how they form the interface flux $\hat{q}$; the first three penalize the flux variable q , while the last four penalize the derivative of the solution u_x.

B The continuous problem

In this paper we will consider interface conditions between subdomains. However, interface conditions are closely related to boundary conditions; therefore, we start with the single domain problem.

B.1 The continuous single domain problem

We begin with a discussion of the wellposedness of the linear advection-diffusion problem (Burgers' equation), and present a simple proof.

For brevity, we reintroduce the linear Burgers' equation [originally presented in equation (30)], as

$$\begin{array}{rcccccl} c_t + a\, c_x & = & \epsilon c_{xx} + F(x,t) & & & , t \ge 0 & , -1 \le x \le 1, \\ c(x,0) & = & f(x) & & & , t = 0 & , -1 \le x \le 1, \\ \gamma c(-1,t) - \epsilon c_x(-1,t) & = & g_{-1}(t) & = & L_{-1}(c) & , t \ge 0 & , x = -1, \\ \zeta c(+1,t) + \epsilon c_x(+1,t) & = & g_{+1}(t) & = & L_{+1}(c) & , t \ge 0 & , x = +1, \end{array} \tag{157}$$

with constants a and ϵ ($0 < \epsilon$). Arbitrary values of the parameters γ and ζ cannot be used, but they can be determined from the proof of wellposedness.

Theorem 1 *Burgers' equation (157) is strongly wellposed with boundary conditions satisfying the conditions*

$$0 \le a + 2\zeta \quad ; \quad 0 \le -a + 2\gamma$$

Proof : An energy estimate for equation equation (157) is obtained by multiplying by c and integrating over the domain $-1 \leq x \leq 1$ and takes the form

$$\frac{\partial}{\partial t}\|c\|_\Omega^2 \;=\; -\,2\epsilon\|c_x\|_\Omega^2 \;+\; 2\|cF\|_\Omega \;+\; [-ac^2 + 2\epsilon c c_x]_{x=-1}^{x=+1} \tag{158}$$

Solving the boundary conditions in equation (30) for ϵc_x yields the relations

$$\epsilon c_x|_{-1} \;=\; (-g_{-1} + \gamma c_{-1}) \quad ; \quad \epsilon c_x|^{+1} \;=\; (+g_{+1} - \zeta c_{+1}) \tag{159}$$

which upon substitution into equation (158) yields

$$\begin{array}{rcl} \frac{\partial}{\partial t}\|c\|_\Omega^2 \;=\; -\,2\epsilon\|c_x\|_\Omega^2 \;+\; 2\|cF\|_\Omega & + & 2c_{+1}g_{+1} \;-\; (2\zeta + a){c_{+1}}^2 \\ & + & 2c_{-1}g_{-1} \;-\; (2\gamma - a){c_{-1}}^2 \end{array} \tag{160}$$

Expressions of the form

$$2\,A\,B \;=\; -(\sqrt{\xi}A - \frac{1}{\sqrt{\xi}}B)^2 \;+\; \xi A^2 \;+\; \frac{1}{\xi}B^2 \quad ; \quad 0 \;<\; \xi \tag{161}$$

can be used to reduce equation (160) to the form

$$\begin{array}{rcccccc} \frac{\partial}{\partial t}\|c\|_\Omega^2 \;+\; 2\epsilon\|c_x\|_\Omega^2 & = & \xi\|c\|_\Omega^2 & - & (2\zeta \;+\; a \;+\; \xi_{+1}){c_{+1}}^2 & - & (2\gamma \;-\; a \;+\; \xi_{-1}){c_{-1}}^2 \\ & + & \frac{1}{\xi}\|F\|_\Omega^2 & + & \frac{1}{\xi_{+1}}{g_{+1}}^2 & + & \frac{1}{\xi_{-1}}{g_{-1}}^2 \\ & - & \|\sqrt{\xi}c - \frac{1}{\sqrt{\xi}}F\|_\Omega^2 & - & (\sqrt{\xi_{+1}}c_{+1} - \frac{1}{\sqrt{\xi_{+1}}}g_{+1})^2 & - & (\sqrt{\xi_{-1}}c_{-1} - \frac{1}{\sqrt{\xi_{-1}}}g_{-1})^2 \end{array} \tag{162}$$

Grouping like terms results in

$$\frac{\partial}{\partial t}\{e^{-\xi t}\|c\|_\Omega^2\} \;+\; e^{-\xi t}\,\{2\,\epsilon\,\|c_x\|_\Omega^2 \;+\; BC\} \quad = \quad e^{-\xi t}\,[Data \;-\; PosDef] \tag{163}$$

with

$$\begin{array}{rcl} BC & = & +\,(2\zeta \;+\; a \;+\; \xi_{+1}){c_{+1}}^2 \;+\; (2\gamma \;-\; a \;+\; \xi_{-1}){c_{-1}}^2 \\ Data & = & +\,\frac{1}{\xi}\|F\|_\Omega^2 \;+\; \frac{1}{\xi_{+1}}{g_{+1}}^2 \;+\; \frac{1}{\xi_{-1}}{g_{-1}}^2 \\ PosDef & = & +\,\|\sqrt{\xi}c - \frac{1}{\sqrt{\xi}}F\|_\Omega^2 \;+\; (\sqrt{\xi_{+1}}c_{+1} - \frac{1}{\sqrt{\xi_{+1}}}g_{+1})^2 \;+\; (\sqrt{\xi_{-1}}c_{-1} - \frac{1}{\sqrt{\xi_{-1}}}g_{-1})^2 \end{array} \tag{164}$$

The wellposedness conditions for the boundary data, are determined by the requirement that the BC term be positive definite. The fact that ξ_{-1} and ξ_{+1} are arbitrary positive constants, imposes the following constraints on the boundary data

$$0 \;\leq\; a \;+\; 2\,\zeta \qquad ; \quad 0 \;\leq\; -a \;+\; 2\,\gamma \quad . \tag{165}$$

The *Data* term is problem specific, while the *PosDef* term is positive definite by construction. Integrating equation (164) in time and imposing initial conditions yields

$$\|c(x,T)\|_\Omega^2 \;+\; \int_0^T e^{-\xi(t-T)}\,\{2\,\epsilon\,\|c_x\|_\Omega^2 \;+\; BC\}dt \quad = \quad e^{+\xi T}\{\|f(x)\|_\Omega^2 \;+\; \int_0^T e^{-\xi t}\,[Data \;-\; PosDef]dt\} \tag{166}$$

from which a strongly stable estimate of the form

$$\|c\|_\Omega^2 + \int_0^t \|c\|_\Gamma^2 dt \leq K_c e^{\xi_c t}\{\|f\|_\Omega^2 + \int_0^t (\|F\|_\Omega^2 + \|g\|_\Gamma^2)dt\}, \tag{167}$$

immediately follows. □

Remark. A sharper proof is given in great detail in the work of Hesthaven and Gottlieb [20] and will not be repeated here.

B.2 The continuous multiple domain problem

In this section we split the domain $[-1,1]$ into $[-1,0]$ and $[0,1]$ and focus on the interface problem at $x=0$. The two coupled problems are

$$\begin{array}{rcllll}
u_t + a u_x &=& \epsilon u_{xx} + F_l(x,t) & , t \geq 0 & , -1 \leq x \leq 0, \\
u &=& f_l(x) & , t = 0 & , -1 \leq x \leq 0, \\
\gamma\, u(-1,t) - \epsilon\, u_x(-1,t) &=& g_{-1}(t) \quad = \quad L_{-1}(u) & , t \geq 0 & , x = -1, \\
L_0(u - v) &=& 0 & , t \geq 0 & , x = 0, \\
v_t + a v_x &=& \epsilon v_{xx} + F_r(x,t) & , t \geq 0 & , 0 \leq x \leq +1, \\
v &=& f_r(x) & , t = 0 & , 0 \leq x \leq +1, \\
L_0(v - u) &=& 0 & , t \geq 0 & , x = 0, \\
\zeta\, v(+1,t) + \epsilon\, v_x(+1,t) &=& g_{+1}(t) \quad = \quad L_{+1}(v) & , t \geq 0 & , x = +1,
\end{array} \tag{168}$$

respectively. The variables in the left $[-1,0]$ and right $[0,+1]$ domains are u and v, respectively. The coupling between the two domains in equation (168) is given by the operator $L(x=0)$.

B.2.1 Wellposedness

Subtracting (30) from (168) and assuming linearity of L_0, produces the equation

$$\begin{array}{rcllll}
(\delta u)_t + a(\delta u)_x &=& \epsilon(\delta u)_{xx} & , t \geq 0 & , -1 \leq x \leq 0, \\
(\delta u) &=& 0 & , t = 0 & , -1 \leq x \leq 0, \\
\gamma\, (\delta u)(-1,t) - \epsilon(\delta u)_x(-1,t) &=& 0 \quad = \quad L_{-1}((\delta u)) & , t \geq 0 & , x = -1, \\
L_0((\delta u) - (\delta v)) &=& 0 & , t \geq 0 & , x = 0, \\
(\delta v)_t + a(\delta v)_x &=& \epsilon(\delta v)_{xx} & , t \geq 0 & , 0 \leq x \leq +1, \\
(\delta v) &=& 0 & , t = 0 & , 0 \leq x \leq +1, \\
L_0((\delta v) - (\delta u)) &=& 0 & , t \geq 0 & , x = 0, \\
\zeta\, (\delta v)(+1,t) + \epsilon(\delta v)_x(+1,t) &=& 0 \quad = \quad L_{+1}((\delta v)) & , t \geq 0 & , x = +1,
\end{array} \tag{169}$$

where $(\delta u) = u - c$ and $(\delta v) = v - c$ describe the evolution of the differences between the one and two domain solutions. The solutions to equation (169) depends on their boundary conditions imposed at the interface point $x = 0$. It must be shown that imposition of this boundary condition does not affect the wellposedness.

Theorem 2 *If Theorem 1 is used to provide exterior boundary conditions, and the interface conditions*

$$\begin{pmatrix} u_i - v_i \\ [u_x - v_x]|_i \end{pmatrix} \quad = \quad \begin{pmatrix} (\delta u)_i - (\delta v)_i \\ [(\delta u)_x - (\delta v)_x]|_i \end{pmatrix} \quad = \quad 0,$$

are used, then the semi-discrete approximation on two domains (168) is strongly wellposed.

Proof : The energy method applied to equation (169) leads to

$$\begin{array}{rcl}
\frac{\partial}{\partial t}\{\|(\delta u)\|_\Omega^2 \,+\, \|(\delta v)\|_\Omega^2\} &=& -2\epsilon\|(\delta u)_x\|_\Omega^2 \,+\, [(\delta u)a(\delta u) - 2\epsilon(\delta u)(\delta u)_x]_{x=-1}^{x=0} \\
& & -2\epsilon\|(\delta v)_x\|_\Omega^2 \,+\, [(\delta v)a(\delta v) - 2\epsilon(\delta v)(\delta v)_x]_{x=0}^{x=1}
\end{array} \tag{170}$$

The stability of the single domain problem implies that the boundary terms at $x = \pm 1$ are negative semidefinite with the boundary operators given by Theorem 1. The terms arising at the interface $x = 0$ that contribute to the estimate are

$$\begin{array}{c}
[(\delta u)a(\delta u) - 2\epsilon(\delta u)(\delta u)_x]^{x=0} \,+\, [(\delta v)a(\delta v) - 2\epsilon(\delta v)(\delta v)_x]_{x=0} \\
= \frac{1}{2}\begin{pmatrix} (\delta u)_i + (\delta v)_i \\ (\delta u)_i - (\delta v)_i \\ ((\delta u)_x + (\delta v)_x)|_i \\ ((\delta u)_x - (\delta v)_x)|_i \end{pmatrix}^T \begin{pmatrix} 0 & a & 0 & -\epsilon \\ a & 0 & -\epsilon & 0 \\ 0 & -\epsilon & 0 & 0 \\ -\epsilon & 0 & 0 & 0 \end{pmatrix} \begin{pmatrix} (\delta u)_i + (\delta v)_i \\ (\delta u)_i - (\delta v)_i \\ [(\delta u)_x + (\delta v)_x]|_i \\ [(\delta u)_x - (\delta v)_x]|_i \end{pmatrix}.
\end{array} \tag{171}$$

The eigenvalues of this symmetric matrix are $(\pm a \pm \sqrt{a^2 + 4\epsilon^2})/2$ which includes both positive and negative values. A negative semi-definite contribution for the interface terms can only be achieved by choosing the boundary conditions $(\delta u)_i - (\delta v)_i = 0$ and $[(\delta u)_x - (\delta v)_x]|_i = 0$, the desired result. □

Remark. The two domain problem (168) is strongly wellposed in the sense that the solutions can be estimated in terms of the data in the corresponding one domain problem (30).

C Positive Semi-Definite Norms

A small portion of the diffusion term $\|\mathcal{D}\mathbf{U}\|_{\mathcal{P}}$ arising at the boundary of a domain (element) can be moved to the (RHS) to help in the proof of stability. This "borrowing" must be accomplished without destroying the definiteness of the remaining term $\|\mathcal{D}\mathbf{U}\|_{\bar{\mathcal{P}}}$ where

$$\bar{\mathcal{P}} \;=\; \mathcal{P} \;-\; \alpha\, \mathbf{e_{i_+}}\, \mathbf{e_{i_+}}^T \tag{172}$$

with $e_{i_+} = [1, 0, ..., 0, 0]$. What remains to be shown is the range of α for which the new matrix $\bar{\mathcal{P}}$ is positive semi-definite.

Theorem 3 *Assume that the original matrix $\mathcal{P}$ is symmetric positive definite. A positive constant α can be subtracted from the $\mathcal{P}_{11}$ position, without destroying the definiteness, if the value of the parameter α is in the range*

$$0 \;\le\; \alpha \;\le\; \frac{1}{\mathbf{e_{i_+}}^T\, \mathcal{P}^{-1}\, \mathbf{e_{i_+}}} \tag{173}$$

Proof : The new matrix $\bar{\mathcal{P}}$ is still symmetric, and the definiteness of a symmetric matrices is completely determined by its eigenvalues. Thus, if the eigenvalues λ_j of $\bar{\mathcal{P}}$ satisfy $0 \le \lambda_j$, then the matrix is positive semi-definite (positive definite for the strict inequality). The eigenvalues λ_j are identical to the roots of the characteristic polynomial. Accounting for the special form of the matrix $\bar{\mathcal{P}}$, the characteristic polynomial is:

$$det(\bar{\mathcal{P}} \;-\; \lambda\mathcal{I}) \quad = \quad \begin{vmatrix} p_{11} - \alpha - \lambda & p_{12} & \cdots & p_{1N} \\ p_{12} & p_{22} - \lambda & \cdots & p_{2N} \\ \cdot & \cdot & \cdot & \cdot \\ \cdot & \cdot & \cdot & \cdot \\ \cdot & \cdot & \cdot & \cdot \\ p_{1N} & p_{2N} & \cdots & p_{NN} - \lambda \end{vmatrix} \tag{174}$$

Expanding the determinant yields

$$(-1)^N(\lambda)^N \;+\; (-1)^{N-1} Trace[\bar{\mathcal{P}}](\lambda)^{N-1} \;+\; \cdots \;+\; det(\bar{\mathcal{P}}) \;=\; 0. \tag{175}$$

A zero root for equation (175) can be obtained by requiring the term $det(\bar{\mathcal{P}}) = 0$, a condition that allows a λ to be factored out of the expression. Expanding the expression $det(\bar{\mathcal{P}}) = 0$ produces the following condition

$$det(\bar{\mathcal{P}}) \;=\; det(\mathcal{P}) \;-\; \alpha\, det(M_{11}) \;=\; 0 \tag{176}$$

where M_{11} is the $(n-1) \times (n-1)$ minor of the original matrix P obtained by simultaneously eliminating row and column one. Solving equation (176) for α (and using Cramer's rule for the element $\mathcal{P}_{11}^{-1}$) yields the desired result.

$$\alpha \;=\; \frac{det(\mathcal{P})}{det(M_{11})} \;=\; \frac{1}{\mathcal{P}_{11}^{-1}} \;=\; \frac{1}{\mathbf{e_{i_-}}^T\, \mathcal{P}^{-1}\, \mathbf{e_{i_-}}} \tag{177}$$

□.

Remark. The result of Theorem 3 is trivial in the case of the diagonal norm.

Remark. P The corresponding proof that accounts for borrowing α from both the $\mathcal{P}_{11}$ and $\mathcal{P}_{NN}$ terms has not been constructed.

D Pointwise Boundedness

We begin with the Sobolev inequality by presenting without proof the following continuous and discrete theorems.

Theorem 4 *Let $u \in C^1\,(0 \le x \le l)$. For every $\bar{\epsilon} > 0$*

$$\|u\|_\infty^2 \quad \le \quad (\bar{\epsilon}^{-1} + l^{-1})\|u\|^2 + \bar{\epsilon}\|u_x\|^2 \tag{178}$$

Proof : See Gustafsson, Kreiss, and Oliger, [19], Lemma 9.3.1, page 377-378, for the proof. □

Theorem 5 *For any grid function $\mathbf{U}$ on $(0 \le x \le l)$, and every $\bar{\epsilon} > 0$, we have*

$$\|\mathbf{U}\|_\infty^2 \quad \le \quad (\bar{\epsilon}^{-1} + l^{-1})\|\mathbf{U}\|^2 + \bar{\epsilon}\|\mathcal{D}_1\mathbf{U}\|^2 \tag{179}$$

with the discrete derivative operator $\mathcal{D}_1$ being defined as

$$\mathcal{D}_1 = \frac{1}{\Delta x}\begin{pmatrix} -1 & 1 & 0 & & & \\ & -1 & 1 & 0 & & \\ & & \ddots & \ddots & \ddots & \\ & & & -1 & 1 & 0 \\ & & & & -1 & 1 \end{pmatrix}.$$

Proof : See Gustafsson, Kreiss, and Oliger, [19], Lemma 11.2.1, page 459-460, for the proof. □

Remark. Note that the derivative matrix $\mathcal{D}_1$ is of dimension $(n-1 \times n)$, that each row is linearly independent, and the row-sums are zero. The rank of the matrix is therefore $n-1$, and the null space is the constant vector.

The energy method applied to the linear Burgers' equation [see equation (30)], provides "integral" bounds on the solution, and the discrete first derivative. Specifically, the quantities $\|\mathbf{U}\|_{\mathcal{P}}^2$ and $\|\mathcal{D}\mathbf{U}\|_{\mathcal{P}}^2$ are bounded for finite times. The original discrete Sobolev inequality is proved using the first order derivative operator $\mathcal{D}_1$. Thus, to use this estimate for pointwise boundedness, we first must establish that $\mathcal{P}$-boundedness of $\|\mathbf{U}\|_{\mathcal{P}}^2$ and $\|\mathcal{D}\mathbf{U}\|_{\mathcal{P}}^2$, implies $\mathcal{P}$-boundedness of $\|\mathbf{U}\|_{\mathcal{I}}^2$ and $\|\mathcal{D}_1\mathbf{U}\|_{\mathcal{I}}^2$.

The norms $\mathcal{P}$, and $\mathcal{I}$ are of full rank n. Thus, that $\|\mathbf{U}\|_{\mathcal{P}}^2$ implies $\|\mathbf{U}\|_{\mathcal{I}}^2$ is immediate. Because of the inherent difficulties in dealing with rank deficient matrices, the derivative condition is more subtle.

Theorem 6 *For any grid function $\mathbf{U}$ on $(0 \le x_j \le l)\,; j = 1, n$, and a consistent derivative operator $\mathcal{D}$ of rank $n-1$ (the constant vector is the only null vector), then $\mathcal{P}$-boundedness of $\|\mathcal{D}\mathbf{U}\|_{\mathcal{P}}^2$, implies $\mathcal{P}$-boundedness of $\|\mathcal{D}_1\mathbf{U}\|_{\mathcal{I}}^2$.*

Proof. Any *consistent*, first derivative operator, consisting of n distinct stencils for the n grid points on the interval x_j, can be represented as linear combinations of the $n-1$ rows of the matrix $\mathcal{D}_1$. To illustrate this, imagine row i of $\mathcal{D}$ written as

$$\mathcal{D}|_i \;=\; [0, \cdots, 0, d_{i,i-k_l}, \cdots, d_{i,i+k_r}, 0, \cdots, 0] \;=\; [0, \cdots, 0, m_{i,i-k_l}, \cdots, m_{i,i+k_r-1}, 0, \cdots, 0]\;\mathcal{D}_1 \tag{180}$$

Consistent operators always have zero row-sums ($\sum_j d_{i,j} \;=\; 0$). Thus, although of different dimension, the $n-1$ linearly independent rows of $\mathcal{D}_1$ span any n-space stencil in the matrix $\mathcal{D}$. Represented in matrix nomenclature, this observation is equivalent to

$${}_n[\mathcal{D}]_n \;=\; {}_n[\mathcal{M}]_{n-1}\;\;{}_{n-1}[\mathcal{D}_1]_n \tag{181}$$

where the *pre-* and *post-* subscripts are used to denote the *row* and *column* dimensions of the respective matrices.

Substituting equation (181) into the derivative norm $\|\mathcal{D}\mathbf{U}\|_{\mathcal{P}}^2$ yields

$$\|\mathcal{D}\mathbf{U}\|_{\mathcal{P}}^2 \;=\; \mathbf{U}^T\mathcal{D}^T\mathcal{P}\mathcal{D}\mathbf{U} \;=\; \mathbf{U}^T\mathcal{D}_1^T\mathcal{M}^T\mathcal{P}\mathcal{M}\mathcal{D}_1\mathbf{U} \tag{182}$$

We know that $\|\mathcal{D}\mathbf{U}\|_{\mathcal{P}}^2$ is bounded. If the matrix $\mathcal{M}^T\mathcal{P}\mathcal{M}$ is a proper norm of rank $n-1$, then $\|\mathcal{D}_1\mathbf{U}\|_{\mathcal{I}}^2$ follows immediately from equation (182) by equivalence of norms.

By construction, the square matrix $\mathcal{D}$ is of dimension n and of rank $n-1$, and the matrix $\mathcal{M}$ is at most rank $n-1$. The matrix $\mathcal{D}_1$ is rank $n-1$, which implies from equation (182) that the matrix $\mathcal{M}$ is rank $n-1$. Given the full rank of $\mathcal{P}$, the resultant matrix $\mathcal{M}^T\mathcal{P}\mathcal{M}$ is symmetric positive definite, is of rank $n-1$, and constitutes a proper norm. Thus, $\|\mathcal{D}\mathbf{U}\|_{\mathcal{P}}^2$ immediately implies boundedness of $\|\mathcal{D}_1\mathbf{U}\|_{\mathcal{I}}^2$, or more precisely

$$\|\mathcal{D}\mathbf{U}\|_{\mathcal{P}}^2 \;=\; c_{mpm}(h)\|\mathcal{D}_1\mathbf{U}\|_{\mathcal{I}}^2 \qquad \square \tag{183}$$

Substituting (183) into Theorem (5) and choosing $\bar{\epsilon} = c_{mpm}$ produces the desired pointwise estimate of the solution.

$$\|\mathbf{U}\|_{\infty}^2 \quad \leq \quad (c_{mpm} \,+\, l^{-1})\|\mathbf{U}\|^2 \,+\, {c_{mpm}}^{-1}\|\mathcal{D}\mathbf{U}\|^2 \tag{184}$$

E Comparison of grids and geometries for polynomial collocation methods.

Many accuracy studies comparing high-order methods found in the FEM and HOFDM literature, are performed on uniform grids with periodic boundary conditions. While valid, the results from these studies may not be sufficiently general to accurately represent their behavior on nonuniform and/or nonperiodic grids. For example, the spectral collocation methods used in this study, often produced anomalous superconvergent behavior for uniform and/or periodic grids. Furthermore, the superconvergence is sometimes confined to some variables, while others converge at design order or less. The following studies document this complex convergence behavior for the spectral collocation methods used in this study.

Consider tables 5 and 6 comparing the convergence rates of polynomial orders $p = 2$ to $p = 5$. The interface parameters used in the study are $\alpha = 0$, $\beta = 1$ and $\gamma = 0$. Polynomial orders $p = 2$ and $p = 5$ superconverge at a rate of $p + 2$ for the uniform grid case, but at a rate of $p + 1$ for polynomial orders $p = 3$ and $p = 4$. The nonuniform grid case converges at the suboptimal rate of p for polynomial orders $p = 2$ and $p = 4$, at a rate of $p + 1$ for $p = 3$ and at $p + 2$ for $p = 5$. (In some circumstances, this anomalous behavior can be attributed to fortuitous cancellation of the leading order truncation terms arising in the interface derivatives used to build the penalty. Cancellation occurs when the truncation terms are equal. Thus, it depends on the polynomial order and does not occur on nonuniform grids.) Next consider $\alpha = 0$, and $\beta = 0$ or $\beta = 1$. These two cases compare the nonuniform grid convergence behavior on the periodic and nonperiodic domains. Several of the periodic cases superconverge, while the nonperiodic case experiences suboptimal convergence p for all polynomial orders.

Tables 7, and 8 show the convergence results for the four methods, four domains, and the four polynomial orders. Once again note the anomalous convergence behavior in table 8, exhibited for the uniform grid, nonperiodic case. This time for polynomials of odd order, the $\mathcal{P}$ integral error is superconvergent for values of $\beta = \frac{1}{4}$. Stranger still, is that this superconvergence does not improve the convergence behavior of the solution, which still converges at a suboptimal rate p.

These studies makes it clear that the most demanding (and realistic) tests are those performed using nonperiodic boundary conditions on the nonuniform grid. Thus, in subsequent comparisons of spectral collocations methods, BC's that are nonperiodic, with nonuniform grids will be the primary focus of attention.

References

[1] Abarbanel, S., Chertock, A. E., Strict stability of high-order compact difference schemes: The role of boundary conditions for hyperbolic pde's, I, (and II), *J. Comput. Phy*, Vol. 160, (2000), pp. 42-66.

[2] Arnold, D. N., Brezzi, F., Cockburn, B. and Marini, L. D., Discontinuous Galerkin methods for elliptic problems, *Discontiuous Galerkin Methods. Theory, Computation and Applications*, B. Cockburn, G. E. Karniadakis, and C.-W. Shu, eds., Lecture Notes in Comput. Sci. Engrg. Vol. 11, Springer-Verlag, New York, (2000), pp. 89-101.

[3] Arnold, D. N., Brezzi, F., Cockburn, B. and Marini, L. D., Unified analysis of discontinuous Galerkin methods for elliptic problems, *SIAM J. Numer. Anal.*, Vol. 39, No. 5, (2002), pp. 1749-1779.

[4] Baker, G. A. , Finite element methods for elliptic equations using nonconforming elements, *Math. Comp.*, Vol. 31, (1977), pp. 45-59.

[5] Bassi, F. and Rebay, S., A high-order accurate discontinuous finite element method for the numerical solution of the compressible Navier-Stokes equations, *J. Comp. Phys*, Vol. 131, (1997), pp. 267-279.

[6] Bassi, F., Rebay, S., Mariotte, G., Pedinotti, S., and Savini, M., A high-order accurate discontinuous finite element method for inviscid and viscous turbomachinery flows, Proceeding of 2nd European Conf. on Turbomachinary, Fluid Dynamics and Thermodynamics, R. Decuypere and G. Dibelius, Eds., Technologisch Instituut, Antwerpen, Belgium, (1997), pp. 99-108.

[7] Baumann, C. E., and Oden, J. T., A Discontinuous hp finite element method for the Euler and Navier-Stokes equations *I. J. Numer. Methods Fluids*, Vol. 175, (1999), pp. 331-341.

[8] Brezzi, C. , Manzini, G. Marini, D., Pietra, P. and Russo, A., Discontinuous finite elements for diffusion problems, in Atti Convegno in onore di F. Brioschi (Milan, 1997), Istituto Lombardo, Accademia di Scienze e Lettere, Milan, Italy, (1999), pp. 197-217.

[9] Carpenter, M.H. Kennedy, C.A., Fourth-Order 2N-Storage Runge-Kutta schemes, NASA-TM-109111, April 1994.

[10] Carpenter, M.H, Gottlieb, D. and Abarbanel, S., Time-stable boundary conditions for finite difference schemes solving hyperbolic systems: methodology and application to high-order compact schemes, *J. Comput. Phys.*, Vol. 111, No. 2, 1994.

[11] Carpenter, M.H. and Otto, J., High-order cyclo-difference techniques: an alternative to finite differences, *J. Comput. Phys.*, Vol. 118, pp. 242-260,1995.

[12] Carpenter, M.H., Gottlieb, D., Spectral methods on arbitrary grids, *J. Comput. Phys.*, Vol. 129, (1996), pp. 74-86.

[13] Carpenter, M.H., Nordström, J. and Gottlieb, D., A stable and conservative interface treatment of arbitrary spatial accuracy, *J. Comput. Phys.*, Vol. 148, pp. 341-365, (1999).

[14] Cockburn, B. and Shu, C.-W., The local discontinuous Galerkin method for time-dependent convection-diffusion systems, *SIAM J. Numer. Anal.*, Vol. 35, (1998), pp. 2440-2463.

[15] Don, W.S., Gottlieb, D., The Chebyshev-Legendre method: implementing Legendre methods on Chebyshev points, *SIAM J. Num. Anal*, Vol. 31, No. 6, (Dec., 1994), pp. 1519-1534.

[16] Douglas, J. Jr., and Dupont, T., Interior penalty procedures for elliptic and parabolic Galerkin methods, *Lecture Notes in Phys.*, Vol 58. Springer-Verlag, Berlin, 1976.

[17] Funaro, D., Gottlieb, D., Convergence results for pseudospectral approximations of hyperbolic systems by penalty-type boundary treatment, *Math. Comput.*, Vol. 57, No. 196, (Oct., 1991), pp. 585-596.

[18] Gustafsson, B., The convergence rate for difference approximations to mixed initial boundary value problems, *Math. Comp.* Vol. 29 (1975), pp. 396-406.

[19] Gustafsson, B., Kreiss, H.O. and Oliger, J., Time Dependent Problems and Difference Methods, Pure and Applied Mathematics, John Wiley and sons, 1995.

[20] Hesthaven, J.S. and Gottlieb, D., A stable penalty method for the compressible Navier-Stokes equations: I. open boundary conditions, *SIAM J. Sci. Comput.*, Vol. 17, 3, pp.579-612, 1996.

[21] Hesthaven, J.S., A stable penalty method for the compressible Navier-Stokes equations: II. One-dimensional domain decomposition schemes, *SIAM J. Sci. Comput.*, Vol. 18, 3, 1997.

[22] Hesthaven, J. S., Teng, C. H.., Stable spectral methods on tetrahedral elements, *SIAM J. Sci. Comput.*, Vol. 21, (2000), pp. 2352-2380.

[23] Hesthaven, J. S., Warburton, T., Nodal high-order methods on unstructured grids I. Time-domain solution of Maxwell's equations, *J. Comput. Phys.*, Vol. 181, (2002), pp. 186-221.

[24] Hesthaven, J. S., Warburton, T., Nodal high-order methods on unstructured grids II. nonlinear problems, *J. Comput. Phys.*

[25] Kreiss, H.O. and Oliger, J., Comparison of accurate methods for the integration of hyperbolic equations, *Tellus* XXIV, Vol. 3, 1972.

[26] Kreiss, H.O. and Scherer, G., Finite element and finite difference methods for hyperbolic partial differential equations, *Mathematical Aspects of Finite Elements in Partial Differential Equations*, Academic Press, New York, 1974.

[27] Mattsson, K., Svärd, M., Nordström, J, Stable and accurate artificial dissipation, *J. Sci. Comput.*, Vol. 21, No. 1, (Aug. 2004), pp. 57-79.

[28] Mattsson, K., Nordström, J, Summation by parts operators for finite difference approximations of second derivatives, *J. Comp. Phy.*, Vol. 199, No. 2, (Sept. 2004), pp. 503-540.

[29] Müller, B., Johansson, S., Strictly stable high order difference approximations for computational aeroacoustics, Computational aeroacoustics: from acoustic sources modeling to far-field radiated noise prediction Colloquium EUROMECH 449, December 9-12, 2003, Chamonix, France.

[30] Nordström, J., Carpenter, M. H., Boundary and interface conditions for high-order finite-difference methods Applied to the Euler and Navier-Stokes Equations *J. Comput. Phy.*, Vol. 148, (1999), pp. 621-645.

[31] Nordström, J., Carpenter, M. H., High-order finite-difference methods, multidimensional linear problems, and curvilinear coordinate, *J. Comput. Phy.*, Vol. 173, (2001), pp. 149-174.

[32] Olsson, P., Summation by parts, projections, and stability I, *Math. Comp.*, Vol. 64, pp. 1035-1065, 1995.

[33] Olsson, P., Summation by parts, projections, and stability II, *Math. Comp.*, Vol. 64, pp. 1473-1493, 1995.

[34] Rivière, B., Wheeler, M. F., and Girault, V., Improved energy estimates for interior penalty, constrained and discontinuous Galerkin method for elliptic problems I, *Comput. Geosci.*, Vol. 3, (1999), pp. 337-360.

[35] Shu, C.-W., Different formulations of the discontinuous Galerkin method for the viscous terms, in Proceedings of Conference in Honor of Professor H.-C. Huang on the Occasion of His Retirement, W. M. Xui, Z. C. Shi, M. Mu, and J. Zou, eds., Science Press, New York, Beijing, 2000, pp. 14-45.

[36] Strand, B., Summation by parts for finite difference approximations for d/dx, *J. Comput. Phys.*, Vol. 110, No. 1, pp. 47-67, 1994.

[37] Strand, B., High-order difference approximations for hyperbolic initial boundary value problems, PhD Thesis, Uppsala University, Department of Scientific Computing, (1996).

[38] Svärd, M., and Nordström, J., On the order of accuracy for difference approximations of initial-boundary value problems, *J. Comput. Phys.*, Vol. 218, pp. 333-352, 2006.

[39] Wheeler, M.F., An elliptic collocation-finite element method with interior penalties, *SIAM J. Numer. Anal.*, Vol 15, (1978), pp. 152-161.

Penalty	Inflow-Outflow : Nonuniform											
Parameters	$\gamma = 0.000$				$\gamma = 0.010$				$\gamma = 0.025$			
and Norms	p = 2	p = 3	p = 4	p = 5	p = 2	p = 3	p = 4	p = 5	p = 2	p = 3	p = 4	p = 5
$\alpha = 0; \beta = 0$												
$\|U - u\|_2$	-2.00	-3.01	-4.00	-5.02	-2.06	-2.96	-3.95	-6.87	-2.08	-3.02	-4.99	-7.34
$\|U - u\|_\infty$	-2.01	-2.98	-4.00	-5.09	-1.88	-3.09	-4.28	-7.33	-1.91	-3.20	-4.64	-7.54
$\|U - u\|_{\mathcal{P}}$	-1.93	-3.12	-3.97	-5.15	-3.35	-2.32	-5.10	-5.98	-3.36	-2.66	-4.74	-6.04
$\alpha = 0; \beta = \frac{1}{4}$												
$\|U - u\|_2$	-1.97	-3.02	-3.97	-5.00	-2.20	-3.12	-4.11	-4.99	-2.25	-3.11	-4.20	-5.41
$\|U - u\|_\infty$	-1.88	-3.14	-3.99	-5.04	-2.09	-3.11	-4.00	-5.40	-2.30	-3.06	-4.37	-5.30
$\|U - u\|_{\mathcal{P}}$	-1.84	-3.21	-3.93	-5.32	-1.98	-3.23	-4.05	-5.18	-2.31	-3.21	-4.15	-5.20
$\alpha = 1; \beta = 0$												
$\|U - u\|_2$	-3.01	-4.00	-4.93	-6.03	-2.57	-3.58	-4.68	-5.55	-2.57	-3.60	-4.51	-5.49
$\|U - u\|_\infty$	-3.01	-3.95	-4.92	-6.01	-2.35	-3.91	-4.70	-5.45	-2.35	-4.06	-4.63	-5.22
$\|U - u\|_{\mathcal{P}}$	-4.04	-4.01	-6.01	-5.95	-3.04	-4.21	-6.84	-6.36	-3.04	-4.22	-5.38	-6.43
$\alpha = 1; \beta = \frac{1}{4}$												
$\|U - u\|_2$	-1.96	-3.02	-3.98	-4.99	-2.19	-3.12	-4.10	-4.99	-2.25	-3.10	-4.20	-5.43
$\|U - u\|_\infty$	-1.90	-3.03	-3.99	-5.04	-2.08	-3.11	-3.99	-5.39	-2.18	-3.05	-4.31	-5.28
$\|U - u\|_{\mathcal{P}}$	-1.84	-3.20	-3.93	-5.32	-1.97	-3.23	-4.04	-5.18	-2.20	-3.21	-4.11	-5.22

Table 2: Convergence Study of the Linear Wave Equation comparing the effects of γ ($\gamma = 0$).

Penalty	Inflow-Outflow, Nonuniform Domain											
Parameters	$\epsilon = 1.00$				$\epsilon = 0.10$				$\epsilon = 0.01$			
and Norms	p = 2	p = 3	p = 4	p = 5	p = 2	p = 3	p = 4	p = 5	p = 2	p = 3	p = 4	p = 5
$\alpha = 0; \beta = 0$												
$\|U - u\|_2$	-1.98	-4.01	-4.00	-5.84	-1.96	-3.98	-4.04	-6.01	-2.39	-3.74	-4.95	-5.92
$\|U - u\|_\infty$	-1.97	-4.01	-4.01	-5.85	-2.01	-3.98	-4.09	-6.01	-2.90	-3.69	-5.20	-5.88
$\|\mathcal{D}U - u_x\|_2$	-1.99	-3.00	-4.00	-4.99	-1.99	-3.00	-3.99	-4.99	-1.94	-3.10	-4.14	-5.15
$\|U - u\|_\mathcal{P}$	-1.99	-4.03	-4.01	-5.91	-1.94	-3.99	-3.97	-6.00	-1.70	-3.70	-4.13	-5.80
$\alpha = 0; \beta = \frac{1}{4}$												
$\|U - u\|_2$	-2.01	-3.02	-4.02	-5.12	-2.98	-3.36	-4.85	-5.56	-3.38	-4.38	-5.20	-6.40
$\|U - u\|_\infty$	-2.01	-3.02	-4.02	-5.08	-2.75	-4.09	-4.99	-5.96	-2.95	-4.47	-4.81	-6.54
$\|\mathcal{D}U - u_x\|_2$	-2.02	-3.00	-4.01	-4.99	-2.04	-3.02	-4.00	-5.00	-2.44	-3.33	-4.22	-5.26
$\|U - u\|_\mathcal{P}$	-2.03	-5.01	-4.04	-6.42	-2.03	-4.36	-3.78	-6.17	-1.63	-4.27	-4.49	-6.37
$\alpha = 1; \beta = 0$												
$\|U - u\|_2$	-1.96	-4.00	-4.00	-5.83	-1.80	-3.90	-4.00	-5.96	-2.30	-3.47	-4.70	-5.69
$\|U - u\|_\infty$	-1.96	-4.00	-4.00	-5.84	-1.85	-3.90	-4.06	-5.95	-2.74	-3.41	-4.87	-5.64
$\|\mathcal{D}U - u_x\|_2$	-1.98	-3.00	-4.00	-4.99	-1.94	-2.98	-3.99	-4.98	-1.93	-3.07	-4.12	-5.15
$\|U - u\|_\mathcal{P}$	-1.97	-4.02	-4.01	-5.91	-1.78	-3.92	-3.94	-5.95	-1.69	-3.61	-3.88	-5.62
$\alpha = 1; \beta = \frac{1}{4}$												
$\|U - u\|_2$	-2.00	-3.00	-4.01	-5.09	-2.97	-3.36	-4.85	-5.55	-3.37	-4.38	-5.20	-6.40
$\|U - u\|_\infty$	-2.00	-3.01	-4.00	-5.04	-2.73	-4.08	-4.99	-5.96	-2.95	-4.47	-4.81	-6.54
$\|\mathcal{D}U - u_x\|_2$	-2.01	-3.00	-4.00	-4.99	-2.04	-3.02	-4.00	-5.00	-2.44	-3.33	-4.22	-5.26
$\|U - u\|_\mathcal{P}$	-2.02	-5.01	-4.00	-6.41	-2.01	-4.35	-3.78	-6.17	-1.59	-4.27	-4.49	-6.37

Table 3: Convergence Study: Effects of ϵ in the linear Burgers' equation, using the primal (B-O) formulation.

Penalty	Inflow-Outflow, Nonuniform Domain											
Parameters	$\epsilon = 1.00$				$\epsilon = 0.10$				$\epsilon = 0.01$			
and Norms	p = 2	p = 3	p = 4	p = 5	p = 2	p = 3	p = 4	p = 5	p = 2	p = 3	p = 4	p = 5
$\alpha = 0; \beta = 0$												
$\|U - u\|_2$	-2.97	-4.07	-4.96	-5.84	-2.88	-3.89	-4.94	-5.92	-3.42	-4.24	-5.37	-6.10
$\|U - u\|_\infty$	-2.96	-3.99	-4.99	-5.85	-2.59	-3.85	-4.75	-5.87	-3.43	-4.12	-5.22	-5.86
$\|\mathcal{D}U - u_x\|_2$	-2.01	-3.03	-4.02	-5.08	-2.02	-3.03	-4.03	-5.08	-2.28	-3.41	-4.35	-5.45
$\|U - u\|_\mathcal{P}$	-2.81	-3.81	-5.86	-7.28	-1.89	-3.94	-3.72	-5.91	-2.44	-3.91	-3.19	-6.00
$\alpha = 0; \beta = \frac{1}{4}$												
$\|U - u\|_2$	-2.90	-3.96	-4.91	-5.82	-3.01	-4.04	-4.98	-6.00	-3.72	-4.39	-5.56	-6.30
$\|U - u\|_\infty$	-2.91	-3.92	-5.02	-5.90	-3.43	-4.04	-4.99	-6.02	-3.41	-4.42	-5.54	-6.28
$\|\mathcal{D}U - u_x\|_2$	-2.00	-3.00	-3.98	-5.00	-1.99	-2.99	-3.98	-5.02	-2.59	-3.39	-4.44	-5.45
$\|U - u\|_\mathcal{P}$	-2.61	-3.84	-5.62	-6.50	-0.33	-4.21	-4.57	-6.08	-2.42	-4.25	-4.10	-6.51
$\alpha = 1; \beta = 0$												
$\|U - u\|_2$	-2.95	-4.06	-4.95	-5.84	-2.81	-3.82	-4.91	-5.88	-3.18	-3.99	-5.10	-5.67
$\|U - u\|_\infty$	-2.93	-3.98	-4.98	-5.84	-2.46	-3.78	-4.69	-5.83	-3.33	-3.89	-4.98	-5.67
$\|\mathcal{D}U - u_x\|_2$	-2.01	-3.03	-4.02	-5.08	-2.01	-3.02	-4.01	-5.05	-2.01	-3.12	-4.09	-5.13
$\|U - u\|_\mathcal{P}$	-2.79	-3.79	-5.86	-7.30	-1.98	-3.88	-3.72	-5.87	-2.78	-3.70	-3.51	-5.78
$\alpha = 1; \beta = \frac{1}{4}$												
$\|U - u\|_2$	-2.90	-3.94	-4.90	-5.80	-3.00	-4.04	-4.98	-6.00	-3.72	-4.39	-5.56	-6.30
$\|U - u\|_\infty$	-2.92	-3.90	-5.02	-5.88	-3.41	-4.03	-4.98	-6.02	-3.41	-4.42	-5.54	-6.28
$\|\mathcal{D}U - u_x\|_2$	-1.99	-2.99	-3.98	-5.00	-1.99	-2.99	-3.98	-5.02	-2.59	-3.39	-4.44	-5.45
$\|U - u\|_\mathcal{P}$	-2.59	-3.79	-5.63	-6.52	2.18	-4.20	-4.56	-6.07	-2.41	-4.25	-4.10	-6.50

Table 4: Convergence Study: Effects of ϵ in the linear Burgers' equation, using the flux (LDG) formulation.

Penalty	Periodic Domain							
Parameters	Uniform Grid				Nonuniform Grid			
and Norms	p = 2	p = 3	p = 4	p = 5	p = 2	p = 3	p = 4	p = 5
$\alpha = 0; \beta = 0$								
$\|U - u\|_2$	-2.54	-5.00	-4.98	-7.02	-2.00	-4.80	-3.97	-6.88
$\|U - u\|_\infty$	-2.42	-5.02	-4.78	-7.16	-2.01	-4.45	-3.99	-6.73
$\|U - u\|_\mathcal{P}$	-4.00	-4.00	-5.99	-5.96	-4.00	-4.00	-5.99	-5.98
$\alpha = 0; \beta = \frac{1}{4}$								
$\|U - u\|_2$	-4.05	-4.00	-4.96	-7.07	-1.97	-4.30	-3.93	-7.00
$\|U - u\|_\infty$	-3.99	-4.03	-5.30	-6.67	-1.95	-4.20	-3.96	-6.70
$\|U - u\|_\mathcal{P}$	-3.99	-4.00	-5.99	-6.02	-4.00	-4.00	-5.99	-5.98
$\alpha = 1; \beta = 0$								
$\|U - u\|_2$	-3.00	-4.01	-5.07	-6.00	-3.01	-4.00	-4.98	-6.04
$\|U - u\|_\infty$	-3.00	-4.01	-5.06	-5.99	-3.01	-3.98	-4.94	-6.03
$\|U - u\|_\mathcal{P}$	-4.03	-4.00	-5.99	-5.95	-4.03	-4.00	-6.00	-5.97
$\alpha = 1; \beta = \frac{1}{4}$								
$\|U - u\|_2$	-4.00	-4.25	-4.90	-7.05	-1.96	-4.60	-3.98	-6.07
$\|U - u\|_\infty$	-4.00	-4.06	-5.12	-6.67	-1.97	-4.23	-3.96	-6.65
$\|U - u\|_\mathcal{P}$	-4.00	-4.00	-5.99	-6.01	-4.00	-4.00	-6.00	-5.98

Table 5: Convergence Study: Scalar Wave Equation on a uniform grid ($\gamma = 0$).

Penalty	Inflow-Outflow Domain							
Parameters	Uniform Grid				Nonuniform Grid			
and Norms	p = 2	p = 3	p = 4	p = 5	p = 2	p = 3	p = 4	p = 5
$\alpha = 0; \beta = 0$								
$\|U - u\|_2$	-2.95	-2.99	-4.99	-5.01	-2.00	-3.01	-4.00	-5.02
$\|U - u\|_\infty$	-3.03	-3.01	-4.95	-5.04	-2.01	-2.98	-4.00	-5.09
$\|U - u\|_\mathcal{P}$	-3.13	-3.11	-4.95	-5.02	-1.93	-3.12	-3.97	-5.15
$\alpha = 0; \beta = \frac{1}{4}$								
$\|U - u\|_2$	-3.04	-3.03	-4.98	-4.98	-1.97	-3.02	-3.97	-5.00
$\|U - u\|_\infty$	-3.15	-3.03	-5.01	-4.84	-1.88	-3.14	-3.99	-5.04
$\|U - u\|_\mathcal{P}$	-3.09	-3.16	-4.97	-5.11	-1.84	-3.21	-3.93	-5.32
$\alpha = 1; \beta = 0$								
$\|U - u\|_2$	-2.99	-4.01	-4.98	-6.00	-3.01	-4.00	-4.93	-6.03
$\|U - u\|_\infty$	-2.99	-4.01	-4.99	-5.98	-3.01	-3.95	-4.92	-6.01
$\|U - u\|_\mathcal{P}$	-4.02	-4.00	-5.98	-5.92	-4.04	-4.01	-6.01	-5.95
$\alpha = 1; \beta = \frac{1}{4}$								
$\|U - u\|_2$	-3.02	-3.00	-4.98	-4.97	-1.96	-3.02	-3.98	-4.99
$\|U - u\|_\infty$	-3.01	-3.03	-5.00	-4.88	-1.90	-3.03	-3.99	-5.04
$\|U - u\|_\mathcal{P}$	-3.09	-3.11	-4.97	-5.17	-1.84	-3.20	-3.93	-5.32

Table 6: Convergence Study: Scalar Wave Equation on a nonuniform grid ($\gamma = 0$).

Penalty	Periodic Domain							
Parameters	Uniform Grid				Nonuniform Grid			
and Norms	p = 2	p = 3	p = 4	p = 5	p = 2	p = 3	p = 4	p = 5
$\alpha = 0; \beta = 0$								
$\|U - u\|_2$	-1.99	-4.00	-4.02	-6.40	-1.99	-4.00	-4.01	-5.82
$\|U - u\|_\infty$	-1.98	-4.00	-4.02	-6.37	-1.99	-4.00	-4.01	-5.90
$\|\mathcal{D}U - u_x\|_2$	-1.99	-3.00	-4.01	-5.00	-1.99	-3.00	-4.00	-5.00
$\|U - u\|_\mathcal{P}$	-1.98	-4.00	-4.02	-6.43	-1.98	-4.00	-4.01	-5.88
$\alpha = 0; \beta = \frac{1}{4}$								
$\|U - u\|_2$	-2.00	-3.01	-4.03	-5.05	-2.00	-3.00	-4.01	-4.99
$\|U - u\|_\infty$	-2.00	-3.01	-4.03	-5.06	-2.00	-3.01	-4.01	-5.05
$\|\mathcal{D}U - u_x\|_2$	-2.01	-3.00	-4.01	-5.00	-2.01	-3.00	-4.00	-5.00
$\|U - u\|_\mathcal{P}$	-2.00	-4.00	-4.03	-6.54	-2.00	-4.00	-4.01	-5.88
$\alpha = 1; \beta = 0$								
$\|U - u\|_2$	-1.97	-4.00	-4.01	-6.40	-1.97	-4.00	-4.00	-5.81
$\|U - u\|_\infty$	-1.97	-4.00	-4.01	-6.37	-1.97	-4.00	-4.00	-5.89
$\|\mathcal{D}U - u_x\|_2$	-1.97	-3.00	-4.01	-5.00	-1.98	-3.00	-4.00	-4.99
$\|U - u\|_\mathcal{P}$	-1.96	-4.00	-4.01	-6.43	-1.97	-4.00	-4.00	-5.88
$\alpha = 1; \beta = \frac{1}{4}$								
$\|U - u\|_2$	-1.99	-3.00	-4.03	-5.05	-1.99	-3.00	-4.01	-4.99
$\|U - u\|_\infty$	-1.99	-3.01	-4.03	-5.06	-1.98	-3.01	-4.01	-5.04
$\|\mathcal{D}U - u_x\|_2$	-1.99	-3.00	-4.01	-5.00	-2.00	-3.00	-4.00	-4.99
$\|U - u\|_\mathcal{P}$	-1.99	-4.00	-4.03	-6.54	-1.99	-4.00	-4.01	-5.88

Table 7: Convergence Study of the Linear Burgers' equation using the Baumann-Oden scheme on a periodic domain ($\gamma = 0$).

Penalty	NonPeriodic Domain							
Parameters	Uniform Grid				Nonuniform Grid			
and Norms	p = 2	p = 3	p = 4	p = 5	p = 2	p = 3	p = 4	p = 5
$\alpha = 0; \beta = 0$								
$\|U - u\|_2$	-1.97	-4.01	-4.01	-6.18	-1.98	-4.01	-4.00	-5.84
$\|U - u\|_\infty$	-1.97	-4.02	-4.01	-6.20	-1.97	-4.01	-4.01	-5.85
$\|\mathcal{D}U - u_x\|_2$	-1.99	-3.00	-4.01	-5.00	-1.99	-3.00	-4.00	-4.99
$\|U - u\|_\mathcal{P}$	-1.98	-4.02	-4.02	-6.40	-1.99	-4.03	-4.01	-5.91
$\alpha = 0; \beta = \frac{1}{4}$								
$\|U - u\|_2$	-2.01	-2.95	-4.02	-4.99	-2.01	-3.02	-4.02	-5.12
$\|U - u\|_\infty$	-2.00	-3.02	-4.03	-5.07	-2.01	-3.02	-4.02	-5.08
$\|\mathcal{D}U - u_x\|_2$	-2.02	-3.00	-4.01	-5.00	-2.02	-3.00	-4.01	-4.99
$\|U - u\|_\mathcal{P}$	-2.03	-6.02	-4.02	-7.45	-2.03	-5.01	-4.04	-6.42
$\alpha = 1; \beta = 0$								
$\|U - u\|_2$	-1.96	-4.01	-4.01	-6.18	-1.96	-4.00	-4.00	-5.83
$\|U - u\|_\infty$	-1.95	-4.01	-4.01	-6.19	-1.96	-4.00	-4.00	-5.84
$\|\mathcal{D}U - u_x\|_2$	-1.97	-3.00	-4.01	-5.00	-1.98	-3.00	-4.00	-4.99
$\|U - u\|_\mathcal{P}$	-1.96	-4.01	-4.01	-6.40	-1.97	-4.02	-4.01	-5.91
$\alpha = 1; \beta = \frac{1}{4}$								
$\|U - u\|_2$	-1.99	-2.94	-4.02	-4.99	-2.00	-3.00	-4.01	-5.09
$\|U - u\|_\infty$	-1.99	-3.02	-4.03	-5.07	-2.00	-3.01	-4.00	-5.04
$\|\mathcal{D}U - u_x\|_2$	-2.01	-3.00	-4.01	-5.00	-2.01	-3.00	-4.00	-4.99
$\|U - u\|_\mathcal{P}$	-2.01	-6.07	-4.04	-7.46	-2.02	-5.01	-4.00	-6.41

Table 8: Convergence Study of the Linear Burgers' equation using the Baumann-Oden scheme on a nonperiodic domain ($\gamma = 0$).

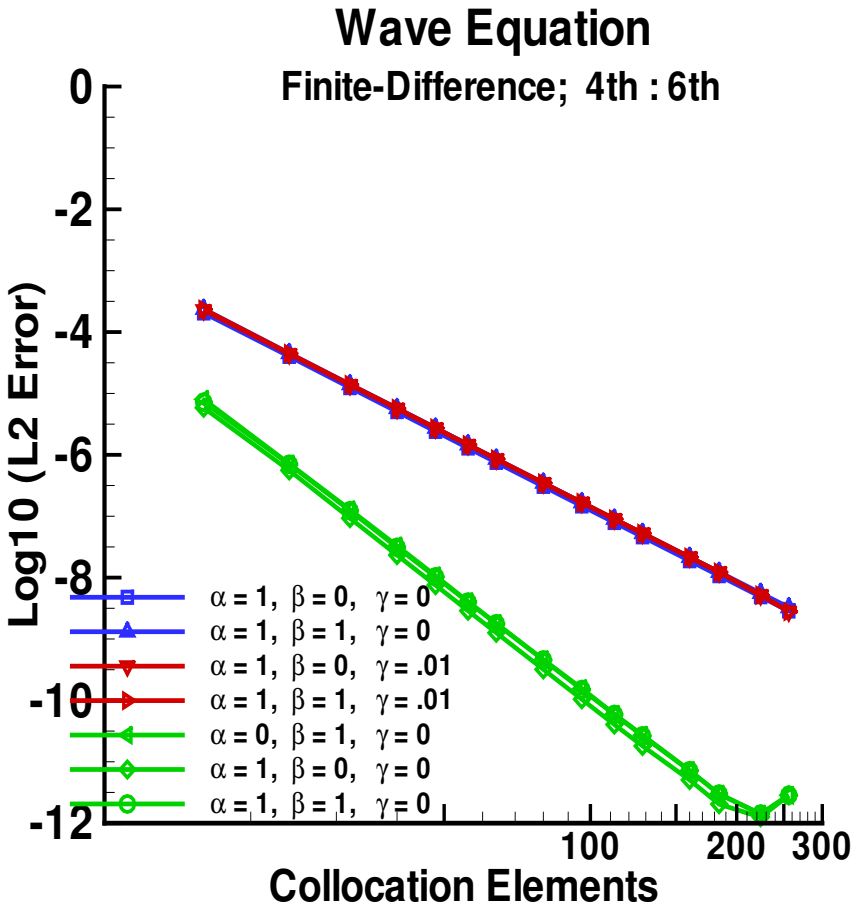

Figure 5: Comparison of 4^{th}- and 6^{th}-order finite difference schemes on wave equation.

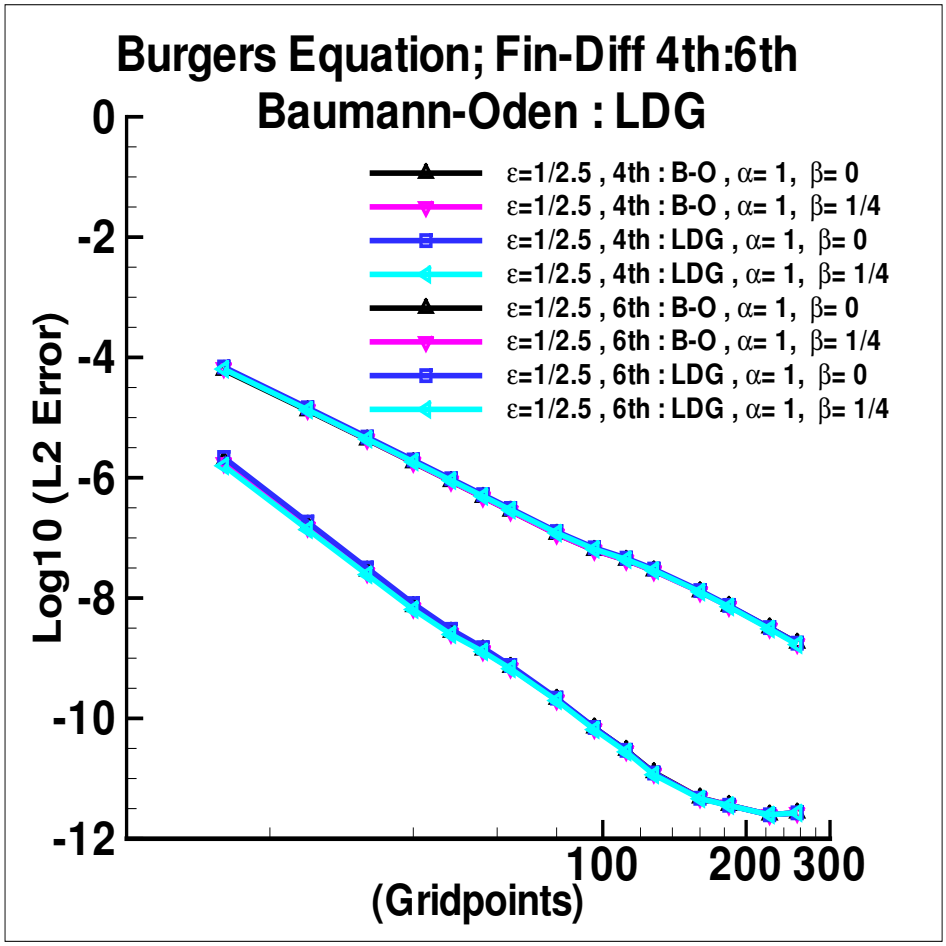

Figure 6: Comparison of 4^{th}- and 6^{th}-order finite difference schemes on Burgers' equation.

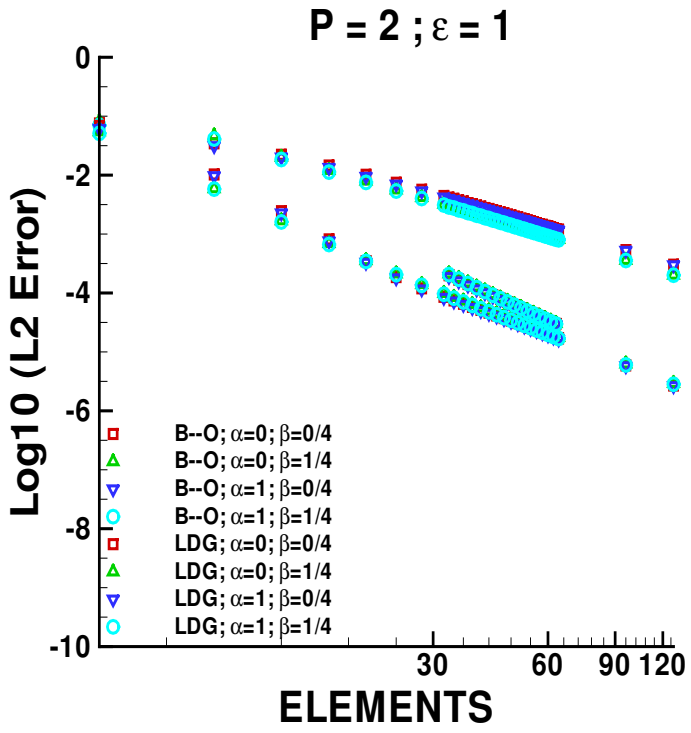

Figure 7: Comparison of Baumann-Oden and LDG schemes for multiple penalty parameters on the linear Burgers' equation: $P = 2$.

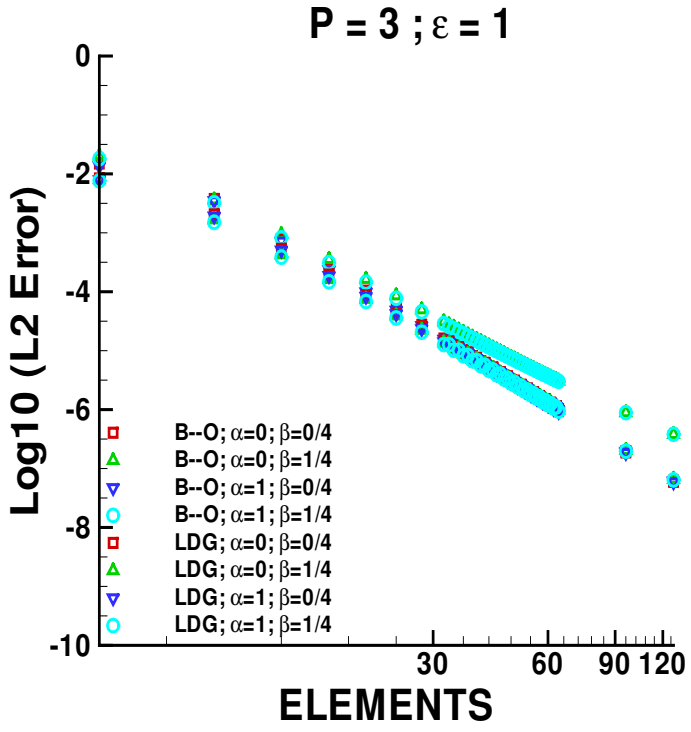

Figure 8: Comparison of Baumann-Oden and LDG schemes for multiple penalty parameters on the linear Burgers' equation: $P = 3$.

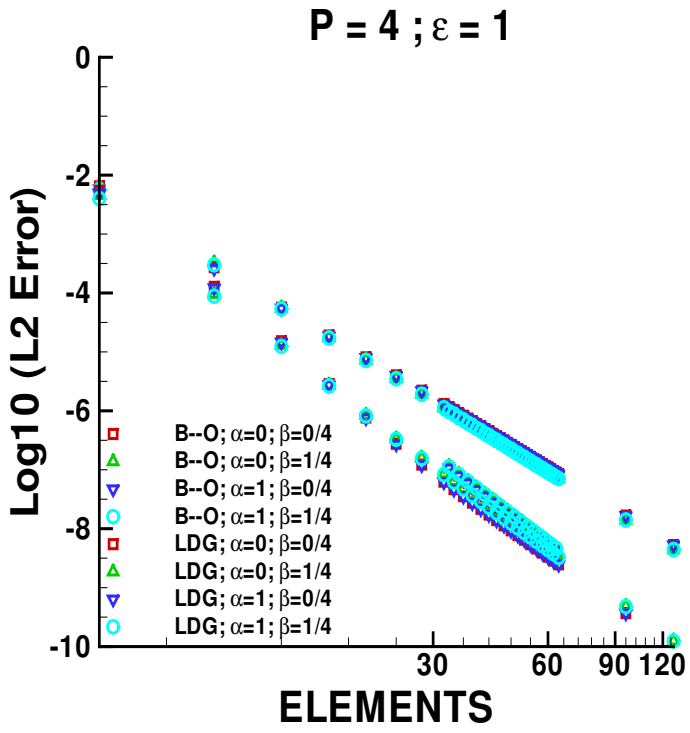

Figure 9: Comparison of Baumann-Oden and LDG schemes for multiple penalty parameters on the linear Burgers' equation: $P = 4$.

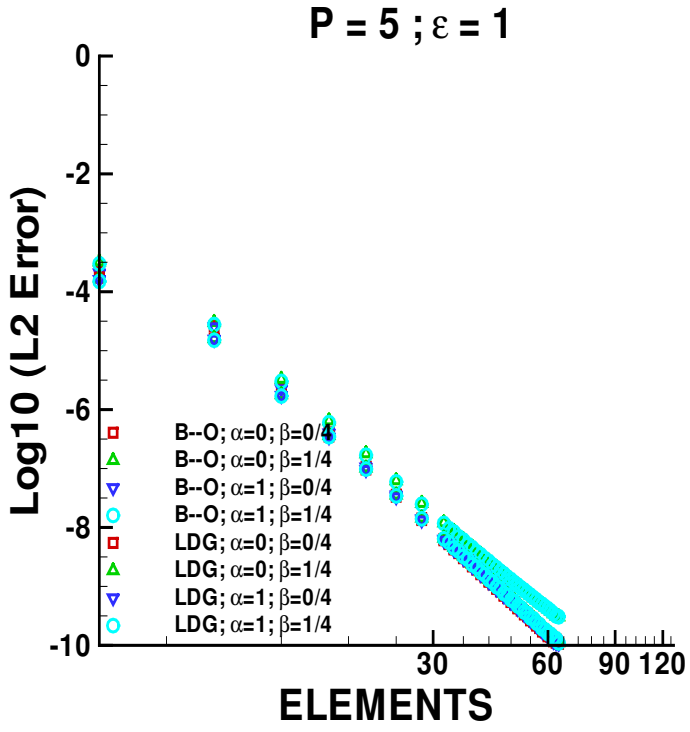

Figure 10: Comparison of Baumann-Oden and LDG schemes for multiple penalty parameters on the linear Burgers' equation: $P = 5$.

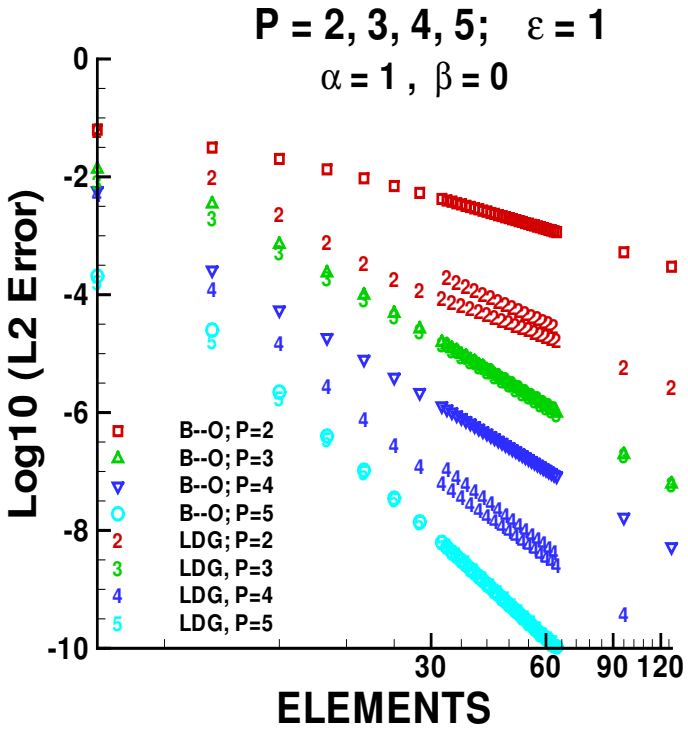

Figure 11: Comparison of Baumann-Oden and LDG schemes for multiple polynomial orders on the linear Burgers' equation: $\alpha = 1,\ \beta = 0$.

REPORT DOCUMENTATION PAGE

Form Approved
OMB No. 0704-0188

1. REPORT DATE *(DD-MM-YYYY)*	2. REPORT TYPE	3. DATES COVERED *(From - To)*
01- 08 - 2007	Technical Memorandum	

4. TITLE AND SUBTITLE
Revisiting and Extending Interface Penalties for Multi-Domain Summation-by-Parts Operators

5a. CONTRACT NUMBER

5b. GRANT NUMBER

5c. PROGRAM ELEMENT NUMBER

6. AUTHOR(S)
Carpenter, Mark H.; Nordstrom, Jan; and Gottlieb, David

5d. PROJECT NUMBER

5e. TASK NUMBER

5f. WORK UNIT NUMBER
23-599489

7. PERFORMING ORGANIZATION NAME(S) AND ADDRESS(ES)
NASA Langley Research Center
Hampton, VA 23681-2199

8. PERFORMING ORGANIZATION REPORT NUMBER
L-19377

9. SPONSORING/MONITORING AGENCY NAME(S) AND ADDRESS(ES)
National Aeronautics and Space Administration
Washington, DC 20546-0001

10. SPONSOR/MONITOR'S ACRONYM(S)
NASA

11. SPONSOR/MONITOR'S REPORT NUMBER(S)
NASA/TM-2007-214892

12. DISTRIBUTION/AVAILABILITY STATEMENT
Unclassified - Unlimited
Subject Category 01
Availability: NASA CASI (301) 621-0390

13. SUPPLEMENTARY NOTES
An electronic version can be found at http://ntrs.nasa.gov

14. ABSTRACT

General interface coupling conditions are presented for multi-domain collocation methods, which satisfy the summation-by-parts (SBP) spatial discretization convention. The combined interior/interface operators are proven to be L2 stable, pointwise stable, and conservative, while maintaining the underlying accuracy of the interior SBP operator. The new interface conditions resemble (and were motivated by) those used in the discontinuous Galerkin finite element community, and maintain many of the same properties. Extensive validation studies are presented using two classes of high-order SBP operators: 1) central finite difference, and 2) Legendre spectral collocation.

15. SUBJECT TERMS
Summation-by-parts (SBP); High-order finite difference; Finite element; DG; Numerical stability; Interface conditions; Conservation

16. SECURITY CLASSIFICATION OF:			17. LIMITATION OF ABSTRACT	18. NUMBER OF PAGES	19a. NAME OF RESPONSIBLE PERSON
a. REPORT	b. ABSTRACT	c. THIS PAGE			STI Help Desk (email: help@sti.nasa.gov)
					19b. TELEPHONE NUMBER *(Include area code)*
U	U	U	UU	57	(301) 621-0390